T.C.

ISTANBUL KÜLTÜR UNIVERSITY

INSTITUTE OF GRADUATE

STUDIES

NONLINEAR STRUCTURAL BEHAVIOR OF RC FRAMES INTEGRATED TO INNER STEEL FRAME BY SHEAR CONNECTORS

Masters of Applied Science Thesis

MIR HADI RASOULI

NADILOUEI

1900004848

Department: Civil Engineering

Program: Structural

Engineering

Supervisor: Prof. Dr. Hüseyin Faruk KARADOĞAN

June 2022

T.C.
ISTANBUL KÜLTÜR UNIVERSITY
INSTITUTE OF GRADUATE STUDIES

NONLINEAR STRUCTURAL BEHAVIOR OF FRAMES INTEGRATED TO INNER FRAME BY SHEAR CONNECTORS

Masters of Applied Science Thesis

MIR HADI RASOULI NADILOUEI

1900004848

Department: Civil Engineering

Program: Structural Engineering

Supervisor and Chairperson:
Prof. Dr. Hüseyin Faruk KARADOĞAN

Members of Examining Committee:
Assist. Prof Dr. Erdal COSKUN

Assist.Prof. Dr. Gökhan YAZICI

June 2022

ACKNOWLEDGEMENT

I want to thank my dear supervisor Prof. Dr Faruk Karadogan for his help and guidance which allowed me to be able to do this study and write this thesis.

I am also very thankful to Istanbul Kültür University (IKU), which allowed me to be a member of their family and allow me to finish my master's degree.

I want to thank my dear professors which I had a chance to have some courses with them during first year of my master's degree program which I have learnt precious knowledge from them.

I also wish to express my appreciation to my family specially my wife for their patient and supporting.

University: **Istanbul Kültür University**

Institute: **Institute of Graduate Studies**

Department: **Civil Engineering**

Program: **Structural Engineering**

Supervisor: **Prof. Dr. Faruk KARADOĞAN**

ABSTRACT

Reinforced concrete frames can be upgraded using steel inner frames connected by different types of shear connectors such as studs, bolts, angles U shape profiles, or steel cushions which are recently appeared in the literature. That is not only important to achieve higher earthquake resisting capacities but also important to retrofit the poorly designed and constructed reinforced concrete structures in earthquake-prone areas. The response of a reinforced concrete structure to an earthquake excitation will be altered by the inner steel frame depending on its lateral rigidity and strength in addition to the type, the rigidity, the strength, energy-absorbing capability, the orientation with respect to peripheral elements, etc. of shear connectors. The effects of all these parameters on the overall behavior of the combined structure consisting of the reinforced concrete frame and steel frame and shear connectors are investigated in this study to better understand the complete redesign process.

The nonlinear behavior of each element is inevitably taken into consideration in this study to see whether it would be possible to reach the limit loads without having had an early failure such as exceeding the local ductility and buckling of steel diagonals which are important to reaching cost-effective retrofitting. A couple of different structural models are defined to observe the possible structural behaviors of combined frames for that purpose and the very well-known computer program SAP2000 was employed for parametrical works.

Special attention has been exercised on the shear connectors in this work. And not only push-over analysis but also step-by-step integration are carried out by choosing several reel earthquakes which are scaled so that code compatible they became.

It can be concluded that the earthquake resistance of an existing structure can be reliably upgraded by steel inner frames in a cost-effective manner and the energy-absorbing capacities are increased by properly used shear connectors.

Keywords: Reinforced Concrete Frame; Steel Inner Frame; Nonlinear Pushover Analysis; Nonlinear Time history Analysis; Shear Connector; Retrofitting;

Üniversite: Istanbul Kültür Üniversitesi

Enstitüsü: Lisansüstü Eğitim Enstitüsü

Anabilim Dalı: Inşaat Mühendisliği

Programı: Yapı (Ingilizce)

Tez Danışmanı: Prof. Dr. Faruk KARADOĞAN

ÖZET

Betonarme çerçeveler, literatürde yeni ortaya çıkan saplamalar, cıvatalar, açılı U şekilli profiller veya çelik yastıklar gibi farklı tipte kesme bağlantı elemanları ile bağlanan çelik iç çerçeveler kullanılarak yükseltilebilir. Bu sadece daha yüksek depreme dayanıklılık kapasiteleri elde etmek için değil, aynı zamanda depreme eğilimli alanlarda kötü tasarlanmış ve inşa edilmiş betonarme yapıların güçlendirilmesi için de önemlidir. Bir betonarme yapının deprem uyarısına tepkisi, tip, rijitlik, dayanım, enerji soğurma kabiliyeti, çevre elemanlara göre yönelime ek olarak yanal rijitliğine ve mukavemetine bağlı olarak iç çelik çerçeve tarafından değiştirilecektir. , vb kesme konektörleri. Tüm bu parametrelerin, betonarme çerçeve ve çelik çerçeve ve kesme bağlantılarından oluşan birleşik yapının genel davranışı üzerindeki etkileri, yeniden tasarım sürecinin tamamını daha iyi anlamak için bu çalışmada incelenmiştir.

Maliyetlere ulaşmak için önemli olan çelik köşegenlerin yerel sünekliklerini ve burkulmalarını aşmak gibi erken bir kırılma olmadan sınır yüklere ulaşmanın mümkün olup olmayacağını görmek için bu çalışmada her bir elemanın doğrusal olmayan davranışı kaçınılmaz olarak dikkate alınmıştır. etkili güçlendirme. Bu amaçla birleştirilmiş çerçevelerin olası yapısal davranışlarını gözlemlemek için birkaç farklı yapısal model tanımlanmıştır ve parametrik çalışmalar için çok iyi bilinen bilgisayar programı SAP2000 kullanılmıştır.

Bu çalışmada kesme bağlantı elemanlarına özel dikkat gösterilmiştir. Ve sadece push-over analizi değil, aynı zamanda kod uyumlu olacak şekilde ölçeklenen birkaç makara deprem seçilerek adım adım entegrasyon da gerçekleştirilir.

Mevcut bir yapının depreme karşı dayanıklılığının, çelik iç çerçeveler ile maliyet etkin bir şekilde güvenilir bir şekilde yükseltilebileceği ve uygun kullanılan kesme bağlantı elemanları ile enerji yutma kapasitelerinin artırılabileceği sonucuna varılabilir.

Anahtar kelimeler: Betonarme Çerçeve; Çelik İç Çerçeve; Doğrusal Olmayan İtme Analizi; Doğrusal Olmayan Zaman Alanı Analizi; Kesme Bağlayıcı; güçlendirme

TABLE OF CONTENTS

LIST OF FIGURES

LIST OF TABLES

LIST OF ABBREVIATIONS

RC : Reinforced concrete

ASCE : American Society of Civil Engineering

MKO : Miyagi Ken Oki japan earthquake **EC8**

: Eurocode 8

UBC : Uniform Building Code

NBCC : National Building Code of Canada

DCH : High Ductility Class

DCM : Medium Ductility Class

DDBD : Direct Displacement Basic Seismic Design

NPO : Nonlinear Pushover Analysis

NTHA : Nonlinear Time History Analysis

KTP : Albanian seismic code

ECT : Turkish Earthquake code

FEMA : Federal Emergency Management Agency

PGA : Peak Ground Acceleration

MDOF: Multi Degree Of freedom

MCE : Maximum Considered Earthquake

LIST OF SYMBOLS

S_S : short period spectral acceleration

S_1 : long period of 1s

Mw : Magnitude

M : Mass of the structure

C : Damping coefficient

K : Stiffness

$\ddot{u}_t$: Total acceleration

$\ddot{u}_r$: Relative acceleration or structural acceleration

$\ddot{u}_g$: Ground motion acceleration

$\dot{u}$: Relative velocity

u : Relative displacement

R : Reduction factor

I : Important factor

DL : Dead load

LL : Live load

E : Earthquake

CHAPTER 1

INTRODUCTION

1.1 General

For one- of-a-kind reasons, like changes in parlous law, emendations withinside the appliance, or quality of operation, it's grown to be important to season up or build an being construction. Recent ruinous earthquakes round the arena have diode to cultures and financial losses worldwide, that has semiconductor widgets to evermore complete constructing canons and new anti-seismic generation being advanced. specifically, growing the parlous practicality of present RC body homes with low or no parlous functionality to cut lower back the fiscal losses and mortal casualties due to earthquakes via important build ways place unit an important ideal [1].

A system of major build ways, like concrete or argentiferous jacket columns, likewise as shear walls, and bottom protection, occasionally supported with the backing of victimization of recent substances like fiber- strengthened polymers (FRP) is deliberate and applied [2 – 5]. specially, pondering the primary charges and also, the ineluctable figure of your term due to creation operations, speedy build ways at the identical time as presently not wet oils like allocating metallic bracing structures or prefab RC panels place unit further engaging [6 – 10].

Presently, the big habituated strengthening ways unit generally on the element stages (e.g., joints, columns, and shafts), like rising part areas [11], adding advanced bars [12], relating argentiferous twine morass [13], and victimization high- octane concrete reserves [14]. doubtless, those ways comprise helpful issues and are tested with the backing of victimization trials quantitatively and followed generally withinside the sensible comes. all of the identical, those tactics units basically concentrated on the structural corridor (i.e., the element- degree overall performance, veritably just like the bearing practicality and stiffness degeneration), whereas as shortly as an earthquake fully happens, systems need to be impelled to square up to the face pressure as a whole on the convenience stages (i.e., the contrivance- degree overall performance, veritably like the roof relegation and injury indicator) [15].

Eleven although element- degree ways contribute to the convenience- degree overall performance to several extents, the choices are not enough best and direct; thus, the retrofitting styles on the contrivance stages unit advanced hastily and are used constantly in earthquake-susceptible regions.

Performance- primarily grounded entirely parlous engineering permits scrutiny of structural overall performance via the crossroad of the implicit wind when the parlous incorporate diapason withinside the pot of spectral acceleration (SA) and spectral relegation (SD). Fig. one indicates the link among the implicit wind of the defective or retrofitted form and so the parlous number diapason, the intention of the crossroad of that represents the overall performance nation at that the shape is subordinated to the required earthquake intensity. utmost of the cited retrofitting ways construct systems that meet the anticipated parlous dreams occasionally with the backing of victimization rising the stiffness and power of the form or vehicle of spare bearing structures, as tested in Fig. 1(a). still, the build approach can indeed discover unplanned issues within the form [16-20].

Some analysis has discovered that also as argentiferous braces in concrete frames can also boost common failure and reason a lower in power as a result. at the identical time as shortly as eccentric braces place unit is supplemental to finish in progressed property, declination of sporting practicality stays discovered [21]. this suggests that the implicit wind of the shape may have an on-ductile failure when that fails to satisfy the parlous dreams (Also tested in Fig. 1(a)). Innovative ways had been added to boost structural overall performance with the backing of victimization growing the damping of the convenience [22 – 24].

1.2 Study background

Numerous studies are done to prognosticate the effectiveness of varied. kinds of damping systems among different recovery strategies for cheapening seismic response [25]. Mutes reduce damage and so the liability of structural collapse by reducing the seismic impact on the structure (shown by the reduction within the seismic demand diapason in Figure 1(b)).

This type of addition strategy is favored for its spatial convenience and short time-out for addition work. Another bettered approach (Figure 1(c)) aims to produce an enhancement within the post-plastic stiffness of the structure which contains an excellent influence on the seismic performance of the structure [26] to serve as a secure reserve for giant earthquakes, thereby reducing the necessity for relegation on a worldwide scale, while avoiding strong hindrance with the vibrational parcels of the primary structure [27].

This result is achieved by constructing mutes with special parcels [28-32] (with lift mutes) or by spaced additions (without lift mutes), like spacers [33,34] or paddings [35,36]. Because of the varied characteristics of varied build strategies, effective assessment procedures are demanded to prognosticate seismic threat and compare the build goods of varied strategies for colorful being

structures.

Representative studies are performed on the conception of real construction cases. specifically, Ghobarah [37] estimated colorful strategies for retrofitting an being low- rise concrete structure, including adding strength, rigidity, stiffness, or a combination of parameters. design number of the column.

The performance of this frame is compared therefore to the fashionable frame by a nonlinear boost analysis. Miano [38] tested the last word build options on the old RC lattice, including FRP enclosures, shear walls, and RC enclosures, and estimated seismic performance using nonlinear static analysis. Beheshti Aval studied the effectiveness of two types of restoration styles, including concentric badge bracing and spherical disunion mute. The performing seismic performance of the considered constructions was bandied by performing an incremental dynamics analysis.

1.3Research problem

Representative studies are performed using real construction cases. specifically, Ghobarah [37] evaluated various strategies for retrofitting an existing low-rise concrete edifice, including increasing strength, ductility, stiffness, or a mix of parameters. Design number of the column. The performance of this

frame was compared therewith to the retrofitted frame by nonlinear thruster analysis. Miano [38] tested the ultimate word retrofit options on the old RC chassis, including FRP enclosures, shear walls, and RC enclosures, and evaluated seismic performance using nonlinear static analysis.

Beheshti Aval studied the effectiveness of two varieties of restoration methods, concentric chevron bracing and cylindrical friction damper. The seismic performance results of the considered structures were discussed by performing an incremental dynamics analysis [39]. Performance-based seismic design (PBSD) provides a simplified solution supported by displacement-based design theory (DBD) developed by Moehle [40], which needs advanced prediction of the state deformation of structures under seismic action. In application, the DBD method starts from the target strain and relies on a project on replacing the model with several degrees of freedom (MDOF) with a system that cherishes one degree of freedom (SDOF) which represents the dominant model. vibrations of a selected pattern. structure [46]. Which, direct DBD (DDBD) [41] and N2DBD [42] are two commonly used methods in concrete

frame structures. the following explains the identical linearization method which may produce an SDOF system and has been included in EC 8 [43].

Analysis of the equivalent SDOF system under seismically excited conditions can help reveal the inelastic seismic performance of the replacement structure and supply recommendations for the choice of design parameters. Several previous studies have investigated that it's possible and practical to guage the seismic performance of a structure from the appropriate back curve of the respective SDOF system [44]. Furthermore, this simplified approach is often incorporated into design processes even taking into consideration the results of flatness and elevation [45].

Additionally, structural improvement analysis supported by this simplified approach has proven to be feasible and practical when applied to plain low-rise and mid-rise buildings [46–47]. But these studies weren't performed within the evaluation of structural reinforcement strategies by different methods.

Previous studies supported nonlinear models of a particular building have the weakness of representing only structures with the identical fundamental period of oscillation. In other words, each structure corresponds to a singular point within the response spectrum. To generalize the results, it's essential to look at the behavior of comparable constructs over the complete range of your time periods which is ready to be considered. additionally, different levels of structural design strength may affect the results. These considerations mean that an oversized amount of analytical work seems infeasible.

1.4 Research aims, objectives, and questions

In this study, we would like to check the general behavior of the system likewise as its individual elements to seek out the efficiency of this leveling system and test the optimal ratio between the stiffness of the 2 concrete frames. and steel, the existence and amount of longitudinal and transverse cutting connectors.

The non-linearity of every element is certainly considered during this study to work out if the last word load may be reached without early problems like local ductility excess and warping of the lines. steel cross, it's important to attain cost-effectiveness. Upgrade. Two different structural models defined to watch the possible structural behaviors of frameworks are

combined for this purpose, and also the well-known malicious program SAP2000 is employed for parametric work.

Paying special attention to shear terminals during this work. And not only thrust analysis but step-by-step integration is finished by selecting multiple scaled coil earthquakes so they're compatible with the code.

It is often concluded that the earthquake resistance of an existing structure will be reliably improved by steel internal frames in an exceedingly cost-effective manner and therefore the energy absorption capacity is increased. because of properly used shear terminals.

1.5 Thesis Scope

The main scope of this study are as follows;

- What should be the rigidity of inner frame in comparison to outer frame?
- Vertical vs lateral shear connectors, which are more effective and in what circumstances?
- Existing of steel diagonals, dimensions and section properties.
- Failure modes of sections.

1.6 Thesis Overview

Chapter 1 presents a general introduction to retrofitting systems of RC frames and goes through some of them implicitly and shows the need to do performance-based analysis of the systems and shows how are study will answer some questions in this field.

Chapter 2 introduces a literature review of previous studies titled retrofitting of RC frames by steel bracings or steel frame. Scientific studies related to this study are presented in this section.

Chapter 3 presents the theoretical background of the study by defining the case study of the RC frame and retrofitting approach and analysis procedures.

Chapter 4 presents the numerical modeling of a case study of the building. The modeling of one bay one story RC frame with an inner steel frame and shear connectors using SAP2000 software [SAP2000, v21]. The first part of this chapter defines the general description of the models by telling building elevations, material properties, a section detailing, and load case definitions. The second part describes analysis procedure for this study by defining some models and doing nonlinear pushover analysis to achieve the optimum configuration of the combined system. At the third part the nonlinear time history analysis are conducted to achieve the energy absorption of the elements and finalize the results of the second step.

Chap 5 presents analysis results and a discussion of the study model. Nonlinear time history analysis comparison of efficiency of the defined systems and energy absorption capacities under various ground motions were presented in terms of tables and graphs.

Chapter 6 highlights the summary, conclusion, and recommendations for future studies.

CHAPTER 2

LITERATURE REVIEW

2.1 General

The extensive literature review has done for this research to obtain a general overview about the topic and find out the needs to do this research and get comprehensive knowledge about the topic.

2.2 Literature Review

Since the 1970s, experimenters in Japan have proposed styles of system- position underpinning by external structural underpinning to reduce damage to being systems and ameliorate integrated seismic performance. Several external substructures are espoused, including external sword frames, ferroconcrete walls, inclined columns, and bracing systems [13]. These sub-structures have the advantage that the addition process is not intruded and can be expended outdoors at the identical time because the inner operation. inclusively of the standard upgrades, concrete frame underpinning contains excellent mechanical parcels and outstanding operating convenience. It developed into a promising kind of system- substructure structure and formed the whole construction process used.

Takeda etal. [17] reviewed build styles in Japan and introduced two kinds of external build approaches to being RCFs, both involving external concrete architecture ways. Meanwhile, two earthquake- resistant structures in Tohoku were studied. Both are retrofitted with external systems and work well PRN. Ishimura etal. [5] delved the results of RCF build using anultra-low strength concrete bracing system, and therefore the event in resistance to seismic forces was verified by two sets of trials.

Kawamoto etal.[21] studied new sword frames with spacers as a seismic build system, and within the strategy, several rudiments associated with connection details were bandied supported the five fitted frames. added. The results show that the anchor bars can significantly affect the bearing capacity and side distortion. Ueki etal. [23] proposed upgrade systems use external fabrics and experimental studies were performed against ten FCRs with analysis concentrated on circular connection goods. The results illustrated the salutary functions of sealants and clarified the advanced effect of external systems to stop being RCFs from fragile destruction. Dubina etal.[26] have performed experimental and numerical studies of the seismic actions of RCF using conventional and external dissipative bracing, and also the affiliated results show good connectivity properties., ideal

rigidity, and better stiffness after underpinning, within the midst of eventual failure of the bracing system in pressure.

Yamada etal.[27] developed the switching mutes to match the rail structure supported tests on the wobbling table, and also the dynamic response and hysteresis angles further vindicated the superior goods of equipping further seismic. Javadi and Yasakawa [28] proposed a mongrel joining fashion to bolster being RCFs employing a sword brace frame, which not only provides the connection function but also improves the mechanical shear and axes of intertwined structures. relative trials are established and also the results indicate that the mongrel bond imparts collective forces to prompt side capabilities.

In recent times, braces with limited relegation (BRB) are used more and more, in situ of conventional braces to comprehend advanced performance pretensions. BRB was first developed in Japan within the primary 1980s and employed in a factual structure in 1990(Fujimoto etal. 1990). These gaskets are designed to limit buckling, give nearly symmetric hysteresis with no visible damage, and achieve a significant proportion of the low cyclic fatigue eventuality of the fabric slip test. introductory material. Applied by build, the combined frame detention is also stable and dependable.

Typical composition consists of a sword core with a face named for the needed strength and a plastic length for the specified elastic drift. This core is enclosed in an axially lined sword tube, which is stuffed with grout and provides side stiffness to regulate the core screwing periphery. The stable and malleable parcels allow this axial elastomer to act as a hysteretic mute to build missing frames. The beginning principles and yield mechanisms of BRBs are well proved (Wakabayashi etal. 1973; Watanabe etal. 1988), and over over to now studies have delved the detailed geste of the components., both analytically and experimentally (Palazzo etal. 2009; Wu etal. two thousand and thirteen).

The commerce of BRBs within the Bulletin of Earthquake Engineering1 subclusters has also been studied considerably (Takeuchi etal. 2014, 2016; Chouand Liu 2012). The time 2003; Kiggins and Uang 2006; Celik and Bruneau 2009; El Bahey and Bruneau 2011; Qu etal. the Year 2012; Freddie etal. the Year 2012; Barbagallo etal. 2019). Experimental studies have handed detailed information on where the BRB is connected to the RC frame using direct connections like preloaded links or erected- in anchors (Dinu etal. 2012; Yooprasertchai and Warnitchai 2008; Mahrenholtz etal. 2015). Other experimental studies have concentrated on balancing or enhancing the BRB frame through sham dynamic testing. Ozcelik and Erdil (2019) tested a BRB- corroborated RC framework during

a very chevron configuration and confirmed the results with temporal analyses. Tsai and associates. (2008) conducted a series of tests on BRB frames with concrete columns (CFTs). In an exceedingly cyclic field trial, Della Corte et al. (2015) implemented a removable all-steel BRB applied in an existing damaged ferroconcrete building. one all told the first practical applications of retrofitting RC frames was reported in 2006 (Takeuchi et al. 2006).

Although limited, numerous recent studies have delved seismic elevation of RC frames with BRBs with different installation options (Pan etal. 2016; Di Sarno and Manfredi 2012). These field studies and executions suggest that there's eventuality for extended use of BRB as a practical build result for low rigidity/ low strength ferroconcrete structures.

To probe the effectiveness of the proposed BRB upgrade scheme and give empirical confirmation, this paper presents a series of large- scale cyclic tests against a BRB- equipped RC lattice.

Majid Zamani etal.(S. Majid Zamani, 2006) conducted an experimental study of a full- size frame that was not slant. They concluded that each possible failure mode may well be converted to in-aeroplane buckling distortions by evolving on thecross-sections of the pillars and their connection to in- aeroplane buckling. They also set up that the inelastic bending of the strut member was the foremost important source of energy dispersion for the Y brace frame (p. Majid Zamani, 2006). Bazzaz etal.(M. Bazzaz etal., 2015) conducted a numerical disquisition on a frame with an off- center bracing system. They introduced a indirect element in an exceedingly bracing system to dissipate energy during cyclic lading. Their results show that the application of ductile rudiments or indirect energy killer to extend rigidity applies not only to out- center brace systems but also to concentric brace systems.

Majid Zamani etal.(2012) conducted another experimental study to check the geste of the brace frame. In their study, four full- scale two- span frames and connection types with different sampling mounts were subordinated toquasi-static repetitious loads. The panels are symmetrically braced for an admixture of tensile and compressive braces at the ultimate cargo stage. Their results show that curve out- of- aeroplane groundwork within the strut can replace double curve in- aeroplane groundwork with corresponding section and connection details. Retrofitting sword braces to being concrete frames can increase the necessity for concrete rudiments like shafts, columns, and foundations by 10Therefore, care must be taken to manage the new demand for members thanks to modernization. the rise in enhanced capability was a side effect of 1 platform (L. Lorenzo De Stefani, 2015).

A study reported by Majid Zamani etal.(S. Majid Zamani, 2011), noted that bracings put much lower perpendicular uplift on foundations compared to X bracings. because of side seismic loads, large uplift forces on foundations are a handicap to X braced frames. Installing bracing in two conterminous kudos of a border an imaged configuration could double the defying switch arm, halting the uplift force. They suggested that in ODBS, a rise within thepost-buckling drift increases the damping rates. At drift rates of over0.02, the damping of Y braced frames was reported to adore that of X braced frames, i.e., ranging between 20 and 25(S. Majid Zamani, 2011).

lately, Sedaghatietal.(P. Sedaghati etal., 2017), report the results of a parametric check conducted on the ODBS response. They set up that the hysteresis cycle pinch effect of a single- connected ODBS ends during a lower hysteresis ring region. This represents lower power consumption. On the contrary hand, an ODBS with rigid connections provides the coming

energy Dispersion capacity due to its lesser hysteresis circle area.

CHAPTER 3

THEORETICAL BACKGROUND

3.1 Introduction

This chapter discusses the theoretical background if the study in both aspects of introducing different types of connectors and analysis cases.

3.2 Composite structural systems

Composite structural systems are employed multitudinous times and are constantly employed in islets and erecting constructions that bear lower material. the benefits of emulsion structure, like a fast construction process, a reduction in vertical bottom spaces, a reduction in overall tone- weight, and cheap structural costs, may help a community to deliver affordable services. A brand shaft concrete dome with shear connections may be a well- known integrated structural element of emulsion constructions (Figure3.1), with high structural performance and profitable feasibility.

Shear connectors are affected link two structural rudiments at an interfacial stratum so as to forestall the vertical splitting of a dome from a brand girder and to permit the graceful transfer of longitudinal shear stresses (6- 9). During an earthquake, shear connectors at the connecting face of the concrete sundeck and brand shaft transport perpendicular inertial stresses during a dome to a side weight defying frame. Shear connections might count the slip of individual corridors generated by perpendicular inertia forces, leading to one T shaft medium fulfilled by an emulsion action. As a result, an emulsion element's stiffness and strength rise.

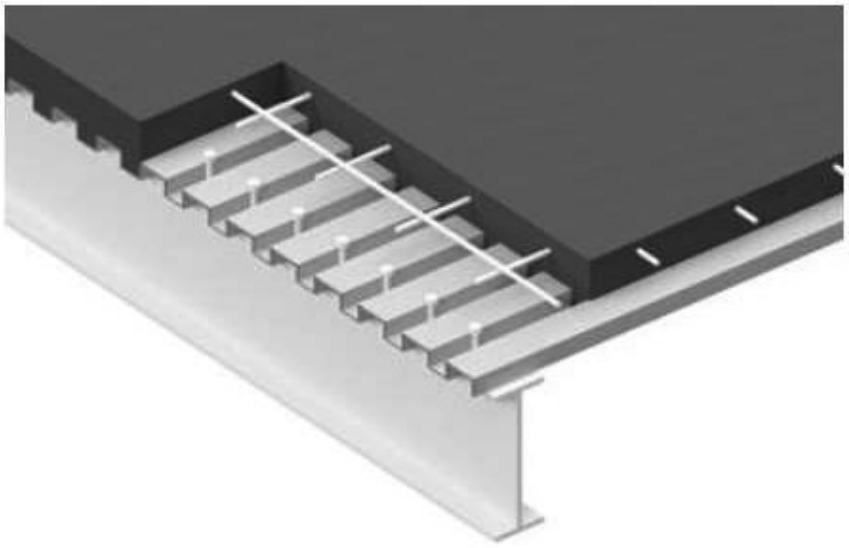

Figure 3.1 Typical arrangement of a composite structure employing shear connectors [5]

3.3 Various shear connectors in composite structures

3.3.1 Headed stud shear connectors

Headed Super studs are the most common shear connectors used in assiduity (Figure3.2); headed super studs include a sword cutter that resists longitudinal shear stresses and an anchored head that prevents arbor perpendicular relegation in compound constructions. In general, special welding outfit is needed to place a headed super stud in a prefabricated sword girder ray. Weld strength should be lesser than super stud strength.

Still, these welds are prone to fatigue when subordinated to repeated ladings. numerous examinations on super stud connections have been conducted over the last seven decades since Viest's development of the headed super stud shear connector.

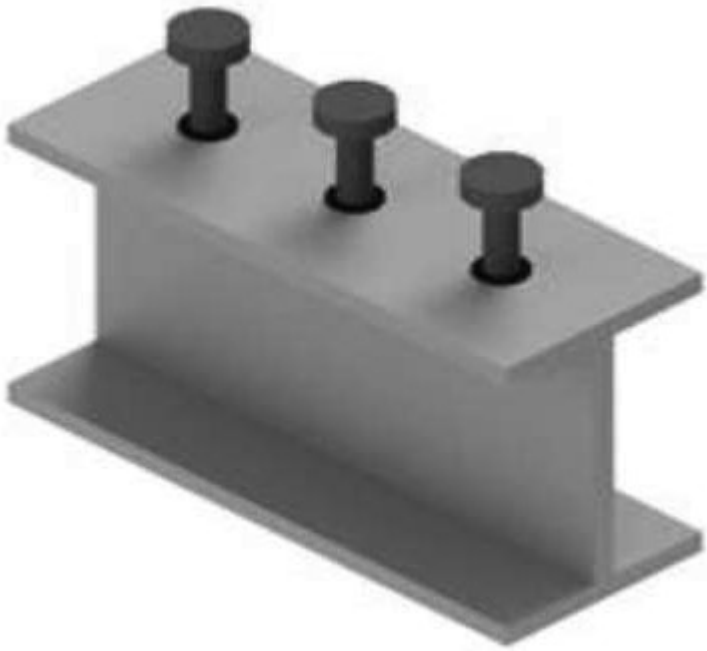

Figure 3.2 Headed stud shear connector [5]

When vanquished to static and cyclic loadings, sources offered four formulae for the nominal shear strength of headed anchors within the solid dome when a emulsion shaft jeopardized the sheer force chargeable for concrete collapse. Spermic etal. tested five distinct groups of 4- headed superstuds using drive- eschewal testing as specified by Eurocode 4 to classify stiffness and shear strength performance differences between the group and standard configurations.

They wanted to cut back the superstud space demanded in precast concrete beams to but the Eurocode 4 standard of 5 times the superstud fringe. Xu and Liu developed a logical model to judge the shear stiffness of rubber- sleeved- headed superstuds at different sleeve heights.

Xu etal. excavated fatigue performance by testing nine rubber- sleeved headed superstuds with varied sleeve heights. they set up that because the sleeve height of the rubber increased, the fatigue strength of the superstud dropped. Ding etal. studied the slip- released behavior of a brand superstud boxed during a fumed plastic block of Ethylene- Vinyl Acetate in a truly drive test. likewise, a finite element (FE) simulation of a shear reference to a polyvinyl resin protective shell caste was done to optimize the connector's slide behavior.

Sjaarda etal. handed a model for predicting the performance of emulsion shafts supported elastic characteristics and nonlinear weight- slip angles of accouterments for a shear connection.

Sun etal[27] . assessed the exhibition of a headed superstud welded to an emulsion sundeck with an

assortment of brand profile decking under cyclic and monotonic burdens. Tests were directed to come to a decision on the effect of decking type, presence, and direction on the welded- headed super super stud's shear capacity. Mirza and Uy employed limited element examination to explore the results of headed super stud connectors in emulsion constructions with the impact of varied strain systems on concrete penciled brand sheeting and robust chunks, presuming that strain systems principally affect strength expectation and burden slip conduct of shear connectors in emulsion designs[32].

Qureshi etal. employed FE examination to explore the shear effect of focal, ideal, and worrisome places of single and twofold super super studs in a veritable box of penciled brand sheeting. Through a fine trial assessment, the impact of profile distance thickness on the plasticity, disappointment modes, and strength of the headed shear connectors employed in emulsion pillars was distinguished. Qureshi etal. saw how shear associations acted in emulsion pillars with various lengths, super super stud samples, and substantial rates[35].

3.3.2 Perfobond ribs shear connectors

Perfobond- roasted (PBL) shear connections were developed for compound designs because to its lesser weariness strength and easier setup than ordinary- headed super studs. PBL connections bear the use of punctured blockish sword plates with round orifices larger than the range ofcross-over support and puncturing rebars. typically, PBL plates are welded at the upper chine of sword supports. Velasco etal. proposed T- caricature perfobond shear connections (Figure3.3 a) for stockpiling alternate regions, corner, and edge section backbones for compound gateway coverings to transport electricity from rebars. Vianna etal. fused two columns of two (Figure3.3 b) or four (Figure3.3 c) orifices in the web plate of T- caricature perfobond shear connections.[18]

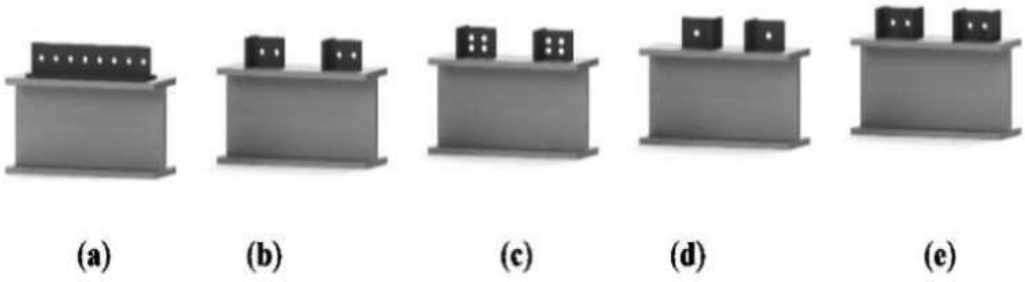

Figure 3.3 Perfobond rib shear connectors[18]

Their drive- eschewal test discoveries demonstrated that the chine game plan of associations with and without cross-over support in caricature openings can give opposition advancements of roughly 150 to 300. Rodrigues and Lam delved the sheer inhibition limit, breakdown mode, and inflexibility of TPBL, T shear connectors, and T- block in fire to decide the shear opposition limit, breakdown mode, and plasticity at encompassing and different expanded up temperatures[9].

Kim etal. created a" Y" shaped PBL shear connection (Figure3.4) and showed its superiority in fatigue and shear resistance by progressive experimental and logical examination under static and cyclic loads Kim et al. Ramasamy and Govindan delved the impacts of triangular holes as perforation on PBL connectors in order to determine strength capability using drive- eschewal testing. To determine the feasibility of defying shear capacity and slip, two kinds of triangle hole facing, facing flange TR1(Figure3.5 a) and facing contrary to flange TR2(Figure3.5 b), perfobond plates were bandied[15].

Zheng etal. studied the performance of indirect and long- hole PBL caricatures using pushout testing, emphasizing the applicability of hole shapes in PBL shear connectors for shear capacity evaluation. Addict and Zhou introduced a new PBL connection, perfobond circle (PBH), which consists of PBL with stirrups placed in the hole for sword- concrete compound bow corridor, videlicet islands. The trial findings revealed that perfobond circle has better mechanical parcels and a advanced shearing capability than PBL connections. Zhang etal.'s theoretical and experimental exploration on PBL connections in groups for the internal force transfer medium indicated unstable force distribution in the elastic stage and indeed plastic distortion. Yu et al estimated the performance of PBL connectors enclosed in recycled aggregate concrete crossbeams for connection strength assessment[17].

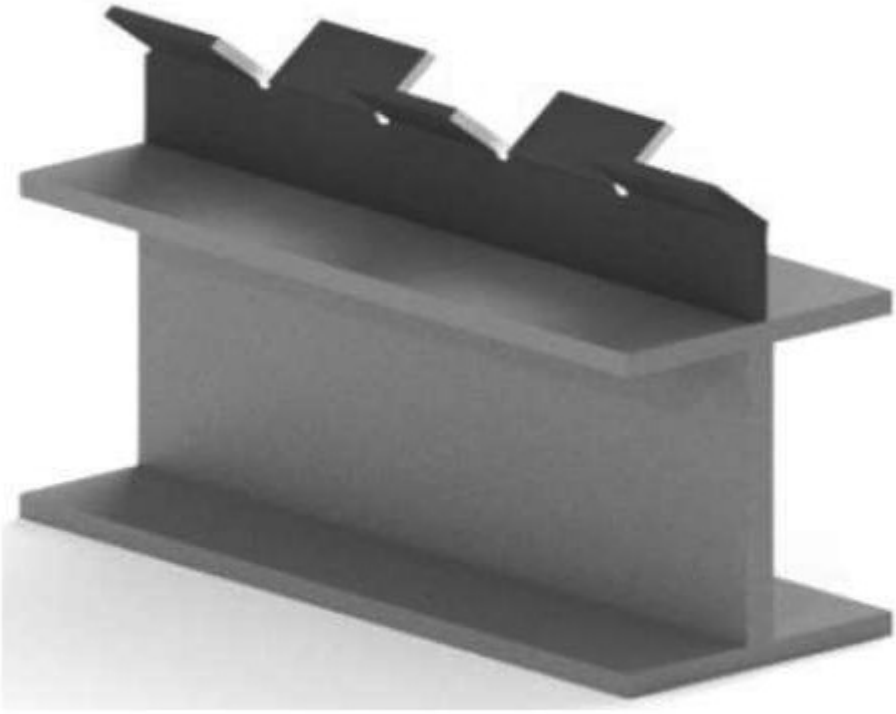

Figure 3.4 Y-shaped perfobond rib shear connectors [15]

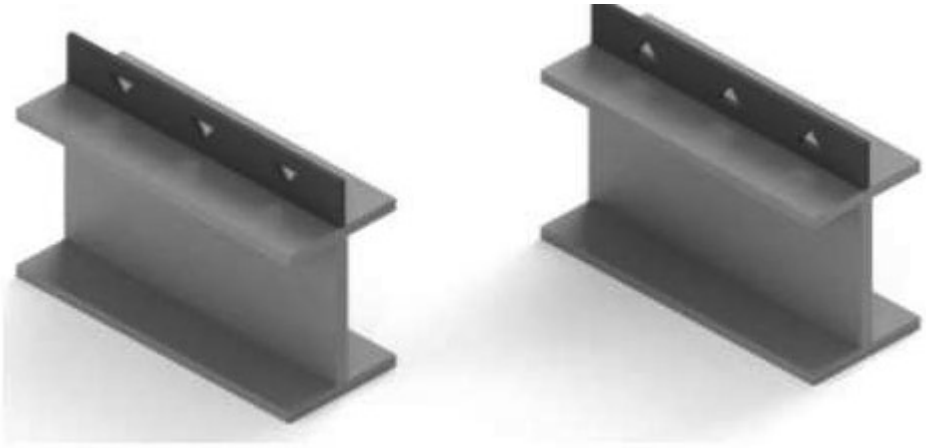

Figure 3.5 (a) triangular-apex in front of the flange; (b) triangular-apex in conflict with the flange[15]

Su et al. used PBL to establish another push-out testing framework while surveying the performance of perfobond rib connectors to separate the influence of contact and example size on main execution. Su et al. investigated the shear obstruction limit of PBL in a composite support span trim with cross

over rebar and cement. Zhan et al. performed detailed push-out experiments (Figure 6) on PBL and headed stud shear connections in composite designs to investigate the effect of increased outer stress on shear connector conductivity. The application of outside pressure when the grinding impact was used considerably improved the strength and solidity of headed studs[19].

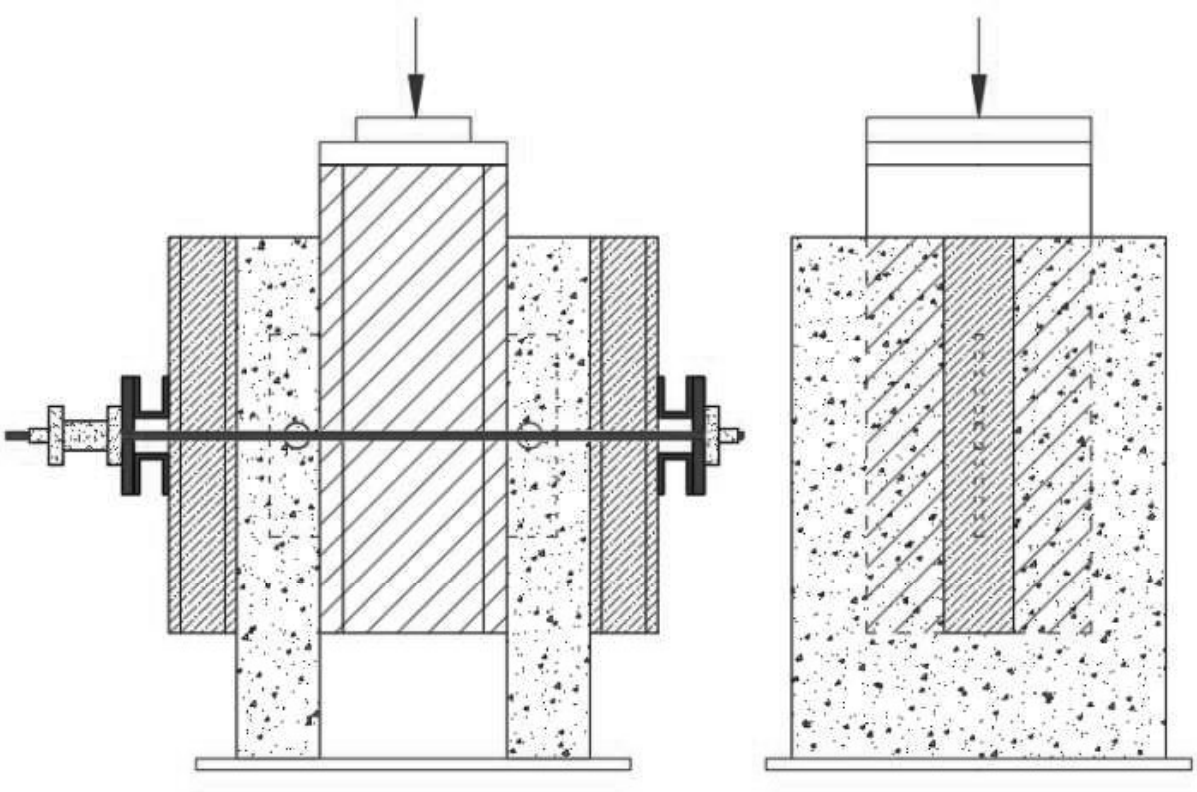

Figure 3.6 External pressure on a test block for the push-out test [19]

3.3.2 FRP PBL shear connectors

FRP accoutrements are employed as shear connection backing to ameliorate flexural firmness, get excellent consumption resistance, and increase the primary strength limit. To advance the participated linking between a pultruded FRP I- brace and significant corridor, Zou etal[21]. used punctured FRP caricatures as shear connectors. Gwon etal[24]. performed a drive- eschewal test on a compound cement FRP module with FRP PBL connections in a one- piece design to determine the shear strength of FRP connectors. Cho etal. demonstrated the significance of the number and size of caricature holes in FRP PBL connector perpetration [37].

Zhang etal. reported contextual data for mystification- shaped (PZ) and clothoidal (CL) compound dowels (Figure3.7) for use as shear connectors in compound shafts [35].

The data has been used to develop specialized rules that will be used to induce instructions for structural design principles, ultimate limit countries, manufacture, and structure. The symmetric shape of CL and PZ compound dowels allows for the bidirectional and invariant distribution of shear force in compound structures. These dowels' compass connectors give good fatigue resistance and suitable strength to fatigue cracks [8].

Heckler etal. presented a fatigue design approach for PZ nonstop shear connections used in prefabricated compound ray assembly. Dudziski etal. delved fatigue cracks and fatigue continuity of compound dowels using a ray test and FE analysis of modified CL- shaped compound dowels. Lorenc etal. delved the cargo- carrying capability of PZ shear connections in full- scale drive-eschewal tests under static ladings using shear resistance. During testing, affecting aspects similar as dowel size, web consistence, and sword quality were delved [13].

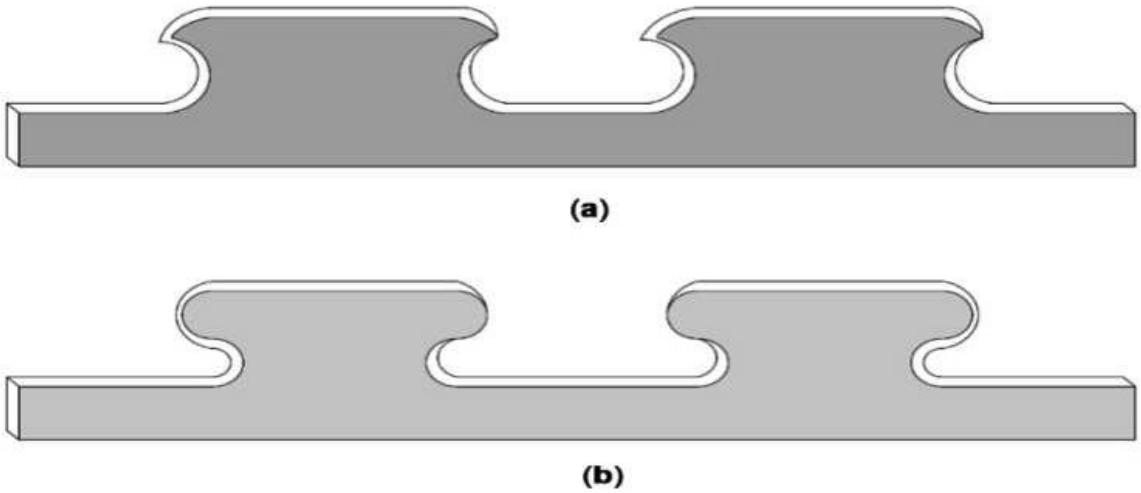

Figure 3.7 (a) Clothoidal and (b) puzzle shape composite dowels used as shear connectors [13]

3.3.4 C-shaped angle and channel shear connectors

By and large, the low strength of headed studs and issues with the stockpile of cross over rebar in PBL openings prompted the possibility of C-type shear associations being created. The laid-out constructability advantages of channel associations were credited to their twice higher shear strength than that of the headed stud and their preferable workplace for building up over that of PBL connectors [22]. C-molded connectors are accessible in two structures: point and channel profile.

Shariati et al. examined channel and point shear (Figure 3.8) associations implanted in high strength concrete (HSC) to assess the exhibition of shear strength and flexibility under static and cyclic push-

out loadings.

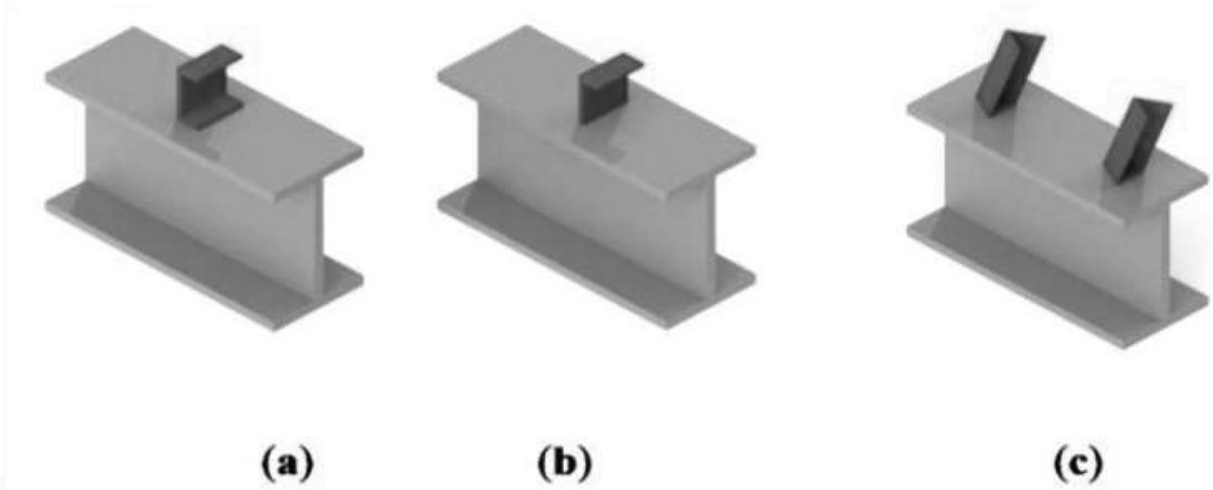

Figure 3.8 Channel shear connector (a), angle shear connector (b), and inclined V-shaped angle shear connector (c) [22]

3.4 Review of Analysis Method

3.4.1 General

The analysis styles are important to prompt the structure model results. The seismic effect of the structures was adding for the formerly time and thus the engineers were dealing to grasp a far better due to help the structures to fail. Nonlinear time history analysis was espoused during this study under two loading conditions. Nonlinear time- history analyses were executed to prompt the seismic parameter results like axial forces, andinter-story drift rates while earthquake side weight was affected to design the structure.

Purpose of Pushover Analysis the end of pushover analysis is to estimate its strength and deformation conditions in seismic structure design using static inelastic analysis and compare these conditions to the available capacity. By doing so, it's to gauge the anticipated performance of the structural system. Power position of interest. The standing relies on the standing

for pivotal performance parameters including global drift, interlayer drift, inelastic element deformation (formalized with connection absolute or yield value), inter-element deformation, and element and connection forces. (For rudiments and connections that cannot absorb inelastic deformation).

Inelastic static pushover analysis is constantly seen as the simplest way of predicting seismic and deformation conditions that compare the division of internal force that happens when a structure is exposed to inertial force. Of weight- bearing behavior. Pushovers are anticipated to produce information about multitudinous responses' characteristics that can't be attained from elastic static or dynamic analysis. the following is an illustration of analogous response characteristics

The realistic force demands on potentially brittle rudiments, like axial force, demands on columns, force demands on brace connections, moment demands on shaft- to- column connections, shear force demands in deep ferroconcrete spandrel shafts, shear force demands in unreinforced masonry wall piers, etc. Estimates of the deformation demands for rudiments that bear to deform in- elastically so on dissipate the energy communicated to the structure by ground movements. Consequences of the strength deterioration of individual rudiments on the

behavior of the structural system.

Identification of the critical regions during which the deformation demands are anticipated to be high came the foremost focus of thorough detailing. Identification of the strength discontinuities in plan or elevation which is suitable to end in changes within the dynamic characteristics within the inelastic range. Estimates of their- story drifts that regard for strength or stiffness discontinuities could indeed be affected to control damage and to gauge P- delta goods.

Verification of the wholeness and adequacy of weight path, considering all the downfall of the structural system, all the connections, the stiff nonstructural rudiments of great strength, and also the minstrel systems.

3.4.2 Background to pushover analysis:

The static pushover analysis has no rigorous theoretical foundation. it's supported the idea that the response of the structure will be associated with the response of a constant single-degree- of- freedom (SDOF) system. this suggests that the response is controlled by one mode and the form of this mode remains constant throughout the time history response.

Easily, both hypotheticals are incorrect, but airman studies conducted by several investigators have indicated that these hypotheticals beget rather good prognostications of the most seismic response of multi-degree-of-freedom (MDOF) structures, handed their response is dominated by a single mode.

The expression of the original SDOF system is not unique, but the abecedarian underpinning supposition common to any or all approaches is that the veered shape of the MDOF system will be represented by a shape vector that continues to be constant throughout the time history, no matter the quantum of distortion. Accepting this supposition and defining the relative relegation vector X of an MDOF system as X ¼ Uxt,(xt = roof relegation), the governing equation of an MDOF system are frequently written as Figure 3.9 Pushover analysis procedures [43].

3.4.3 Time History Analysis

A time history analysis is a step-by-step analysis of the building's dynamic response to identifying the loads that may vary over time. The seismic response of a structure under the dynamic loading of a typical earthquake is determined via time history analysis.

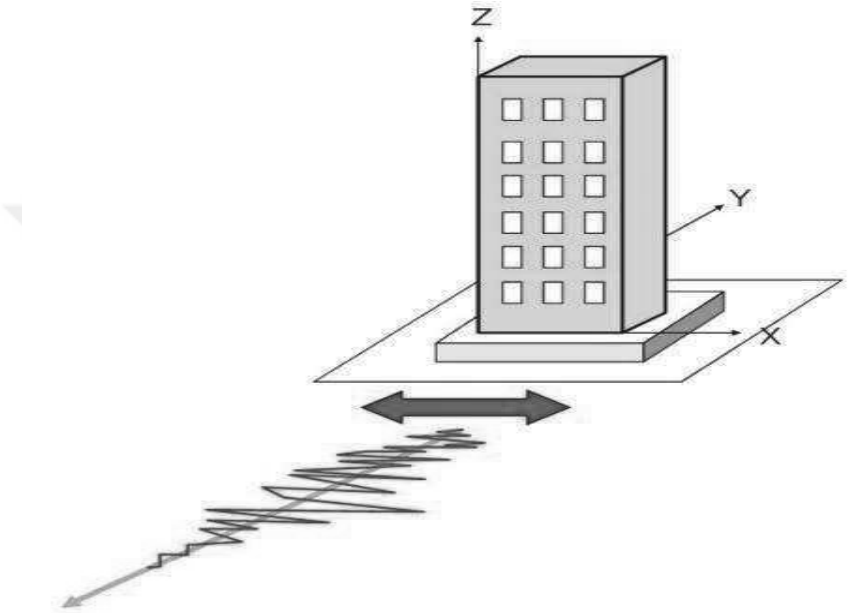

Figure 3.10 Schematic Representation of a Building Model Subjected to Seismic Excitation in the X-Direction [25]

In this method, nonlinear analysis has been considered to determine irregular structure responses when subjected to different earthquake excitation under two loading cases.

Time history is a dynamic analysis method, so the Equation of motion of multi-degree of freedom systems (MDOF) is given in Equation (4.1) and (4.2).

$$M\ddot{u} + C\dot{u} + Ku = -M\ddot{u}_t \qquad (4.1)\ [23]$$

$$\ddot{u}_t = \ddot{u}_r + \ddot{u}_g \qquad (4.2)\ [23]$$

Where,

M = mass of the structure

C = damping coefficient

K = stiffness

$\ddot{u}_t$ = total acceleration

$\ddot{u}_r$ = relative acceleration or structural acceleration

$\ddot{u}_g$ = ground motion acceleration

$\dot{u}$ = relative velocity

u = relative displacement

3.4.4 Nonlinear Time History Analysis

In this study, the response of the structure under seismic excitations has been examined by using the nonlinear step- by- step time history system. This approach allowed us to estimate the structure's response through dynamic analysis by subjugating the structure model to a group of ground movements. The analysis is carried out for further than one ground stir to perform the nonlinear dynamic analysis. Seismic design canons described dynamic analysis for medium and altitudinous structures; thus, the nonlinear dynamic analysis system has been used to determine the irregular structure model's seismic responses.

Seismic analysis is a type of earthquake engineering that's used to snappily understand how structures reply when they're subordinated to earthquake excitations. preliminarily, structures were simply erected to repel gravitational loads. Seismic analysis, on the other hand, has been developed in recent times, which allowed the structure to be anatomized and designed using ground stir data through structural software. In this study, direct integration was used which is more sensitive to time way without affecting the result.

Geometric nonlinearity including the p- delta effect was used during nonlinear direct integration time history analysis. The damping rate is assumed to be 5 while the Newmark system was taken to break nonlinear equations. The gamma and beta values for the Newmark system are taken as and0.25 independently.

3.4.5 P-Delta Effect

The p-Delta effect is also termed geometric nonlinearity, which is related to the equilibrium compatibility relationship of a structural system assigned to its deflected configuration. The p-delta is the application of gravity load on laterally displaced building structures and it increases the story drift and certain parameters while reducing deformation capacity. P-Delta effect tends to include large external forces onto relatively small displacement. However, in general, p-delta can be classified into two types, one is P- Δ (large p-delta or big p-delta) and the other is P- δ (small p-delta) effects. The two sources of the p-Delta effect are shown in Figure 3.11 and described as flows:

a) P- δ (small p-delta) effect: P- δ effect related to local deformation relative to the element chord between end nodes. The small p-delta effect is very important for local buckling load and the moment which may affect the structural behavior of the building.

b) P- Δ (large p-delta) effect: The p -Δ an effect related to the displacement of the member at the

ends. The large p-delta effect is very essential for structural behavior under axial loading. For implementing the large p-delta effect in nonlinear analysis gravity load should be presented. As shown in Figure 3.4, gravity loading influences the response of the structure under lateral loading.

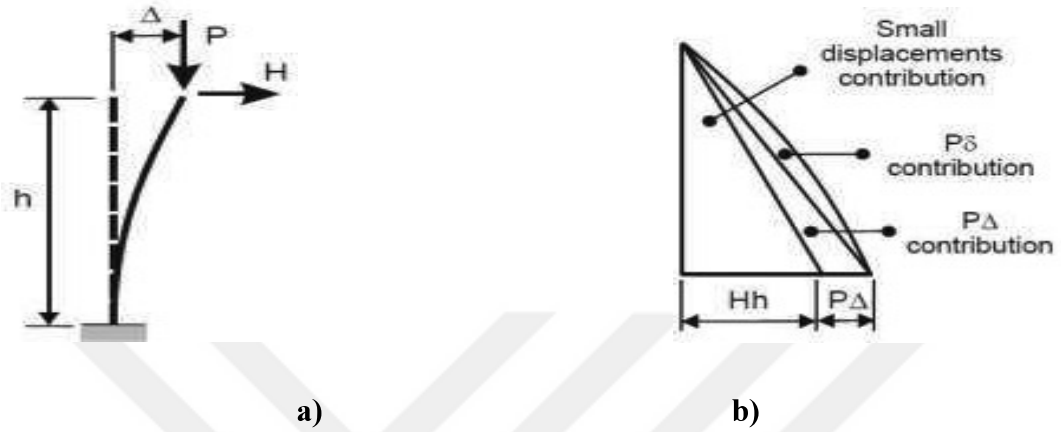

Figure 3.11: P-Delta effect [32]

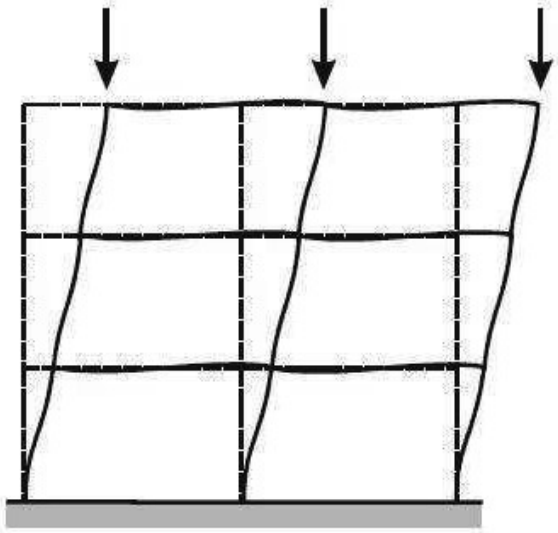

Figure 3.12: P-Delta effect about structure [32]

3.7 Properties of Plastic Hinges and Their Definition

Plastic hinges are defined the deformation that happen at the beam or column section where plastic bending take place. In nonlinear time history analysis, users may imitate post-yield behavior by inserting concentrating plastic hinges to the frames. Elastic behavior happens on

top of member length, while deformation after elastic limit happens in the hinges. Plasticity is related with the force displacement behavior (axial and shear) or moment rotation (torsion or bending). However, the hinges can be assigned to any of the six degrees of freedom.

The plastic hinges are very important for checking the building performance under seismic excitations. For plastic hinge formation the behavior of stress strain ductile material like steel, they end elastic limit of the body by starting from plastic behavior. Then the strain and stress will be altered at different rate as shown in Figure 3.13.

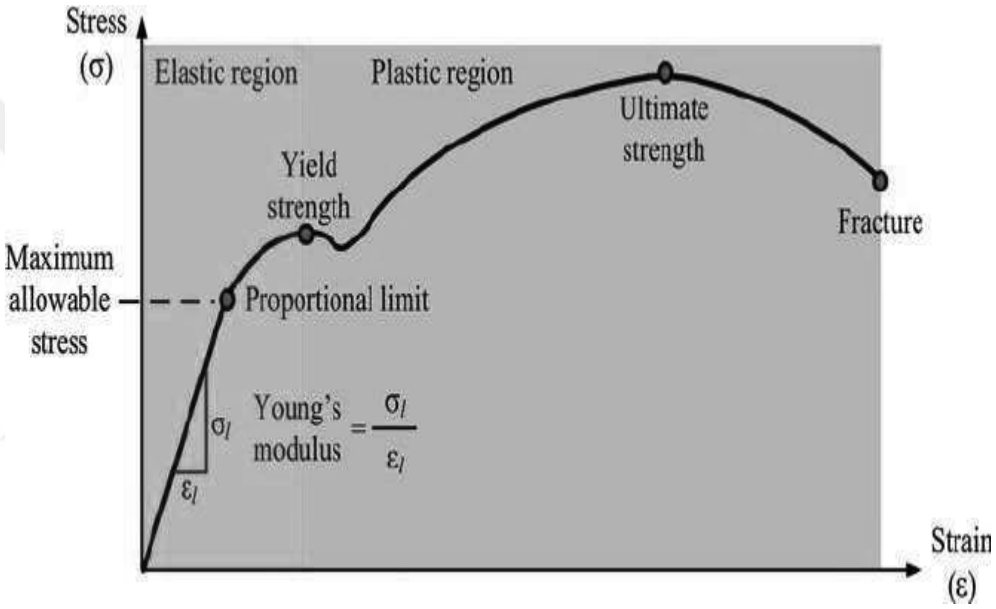

Figure 3.13: Stress-Strain Relationship [38]

In this study plastic hinges were assigned at the end of beams and columns in all models. moreover, the plastic hinges in beams are assigned M3 degree of freedom while column are assigned at the P-M2-M3 degree of freedom inside SAP2000 software.

CHAPTER 4

NUMERICAL MODELING

4.1 Introduction

This chapter presents the modeling of one story-one bay reinforced concrete frame and steel inner frames with or without vertical or vertical and horizontal connectors. Twelve different 2D models have been used for this study. The models have been analyzed by using sap2000 v23.1.0. Nonlinear Pushover Analysis has been conducted to study the nonlinear behavior of individual frames and their combinations with different configurations. Nonlinear time history analysis has been used to study the energy consumption of different elements of the models. Four Input ground motions have been taken in both components and scaled to ASCE 7-22 target spectrum by using the Seismomatch software.

4.2 Material Definitions

Materials' specifications in this study are based on SI units (N, mm, C) and for the Concrete and structural steel and rebars and connectors are as shown in the below:

4.2.1 Concrete

In this study C25 concrete is used for modeling RC columns and RC beams with a material property which are shown in the table 4.1.

Name	C25
Weight per unit Volume	2.500E-06
Modulus of Elasticity, E	26875
Poisson, U	0.15
Specified concrete compression strength, F'c	25 N/mm2

Table 4.1 Concrete Material Properties

4.2.2 Structural Steel

In this study ST37 Structural Steel is used for modeling inner steel frames with a material property which are shown in the table 4.2 .

Name	ST37
Weight per unit Volume	7.850E-05
Modulus of Elasticity, E	200000
Poisson, U	0.3

Minimum yield stress, F_y	240
Minimum tensile stress, F_u	370

Table 4.2 Structural Steel Material Properties

4.2.3 Rebars' Steel

Name	AIII
Weight per unit Volume	7.697E-05
Modulus of Elasticity, E	200000
Poisson, U	0.3
Minimum yield stress, F_y	400
Minimum tensile stress, F_u	600

Table 4.3 AII Rebar Steel Material Properties

Name	AII
Weight per unit Volume	7.850E-05
Modulus of Elasticity, E	200000
Poisson, U	0.3
Minimum yield stress, F_y	340
Minimum tensile stress, F_u	500

Table 4.4 AII Rebar Steel Material Properties

4.3 Sections Definitions

4.3.1 RC Frame Sections

4.3.1.1 RC Column's Section

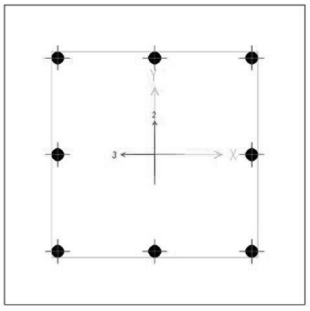

Dimensions (height * withs)	350 mm * 350 mm
Concrete Material	C25

Main Rebars	AIII – 8 * 14mm d
Confinement rebars	AII – 10 mm d @ 150 mm
Clear cover	45 mm

Table 4.5 RC Columns Section Details

4.3.1.2 RC Beam's Section

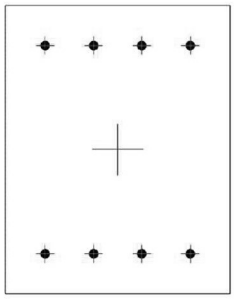

Dimensions (height * withs)	450 mm * 350 mm
Concrete Material	C25
Main Rebars	AIII – 8 * 14mm d
Confinement rebars	AII – 10 mm d @ 150 mm
Clear cover	45 mm

Table 4.6 RC Beams Section Details

4.3.2 Steel Frame Sections

Three different standard steel box sections are defined and their details are as shown below:

4.3.2.1 TUBO260X130X10

Material	ST 37
Outside depth (t3)	260 mm
Outside width (t2)	130 mm
Flange thickness (tf)	10 mm
Web thickness (tw)	10 mm
Corner radius	0 mm

Table 4.7 TUB 260 Steel Section Details

4.3.2.2 TUBO300X150X12.5

Material	ST 37
Outside depth (t3)	300 mm
Outside width (t2)	150 mm
Flange thickness (tf)	12.5 mm

Web thickness (tw)	12.5 mm
Corner radius	0 mm

Table 4.8 TUB 300 Steel Section Details

4.3.2.3 TUBO380X190X12.5

Material	ST 37
Outside depth (t3)	380 mm
Outside width (t2)	190 mm
Flange thickness (tf)	12.5 mm
Web thickness (tw)	12.5 mm
Corner radius	0 mm

Table 4.9 TUB 380 Steel Section Details

4.3.3 Connectors

Three different sections are defined to be used as shear connectors which are 10mm d rebar, 30mm d rebar and 60mm d rebar. Used material in all three is AIII rebar material.

4.4 Model's Definitions

4.4.1 Models' General Parameters

In this study we have four primary models and twelve combined models in which the outer RC frame is same in all but the differences are in the sections of inner steel frame and diameter of shear connectors. All models are defined in four major groups; first group namely OM group, consists of the models which all have 30mm d rebars as vertical connectors and in the second group namely HM models there is only horizontal connectors and in the third group we have two special combination of vertical and horizontal connectors and the fourth group is SM models which have vertical and horizontal connectors with different steel frame sections and connectors.

Name	Height	Width	Length (Axis to Axis)
RC Outer Frame	3.00 m	5.20 m	-
ST Inner Frame	2.40 m	4.00 m	-
Vertical Connector	-	-	0.60 m
Horizontal Connector	-	-	0.60 m

Table 4.10 Models' General Parameters

4.4.2 General Concepts

In the defining the characteristics of the inner and outer frames in order to have general concept and broad results, we defined individual frame characteristics as are shown below:

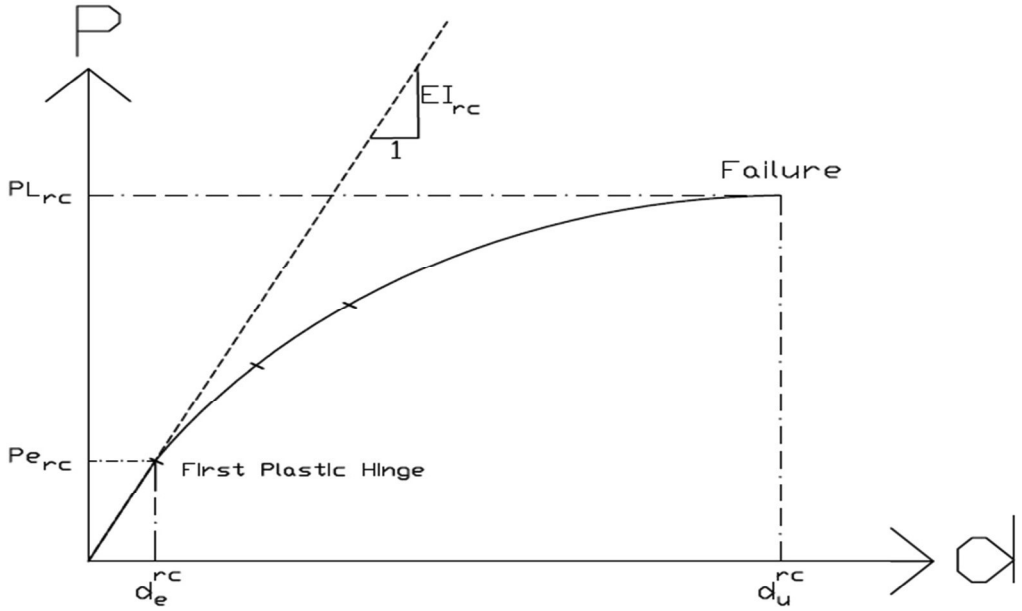

$$\eta^{rc}{}_{s} = d^{rc}u/d^{rc}e$$

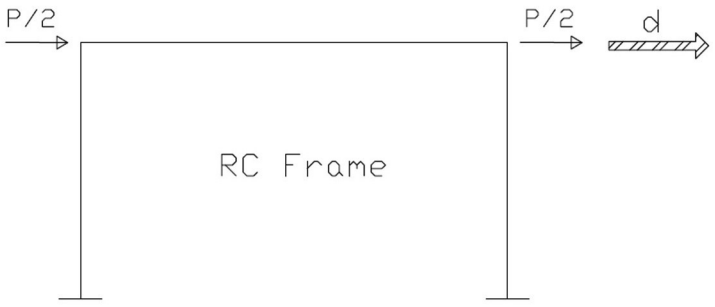

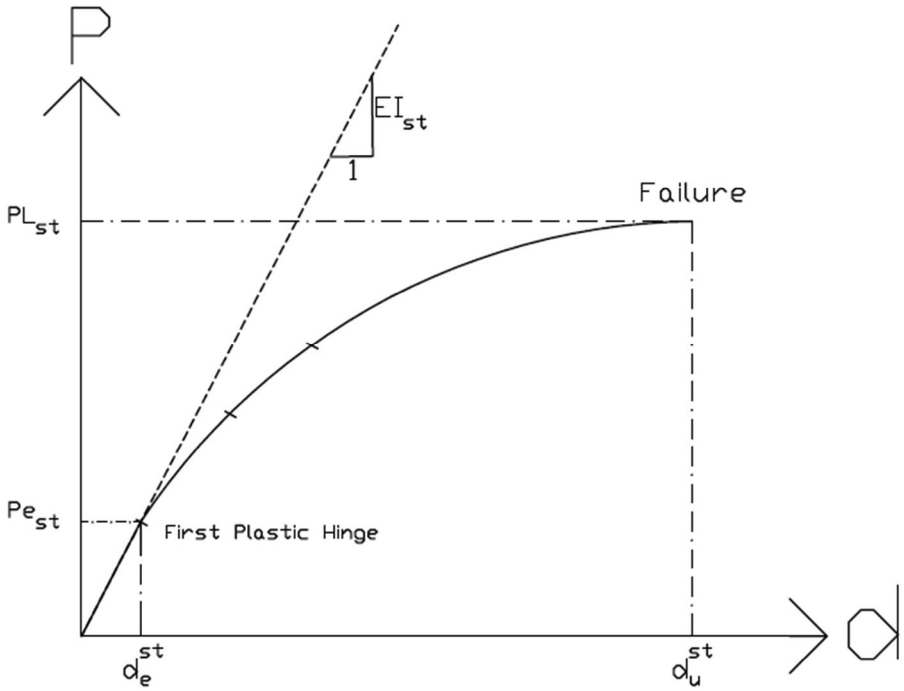

$\eta^{st}{}_s = d^{st}u/d^{st}e$

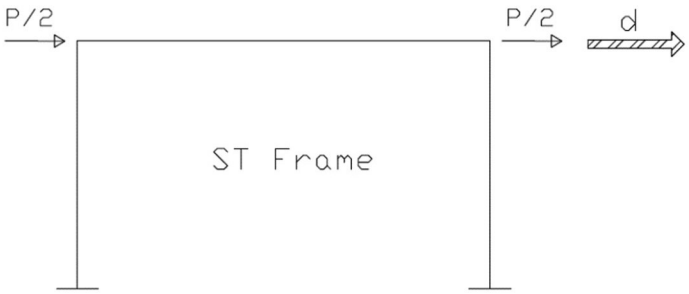

Then we defined three parameters in order to generalize selecting the inner frame with respect to outer frame:

$RR = EI_{st} / EI_{rc}$ Ratio of initial rigidities of frames

$RD = \eta^{st}{}_s / \eta^{rc}{}_s$ Ratio of displacement ductilities

$RL = PL_{st} / PL_{rc}$ Ratio of limit loads

4.4.3 Models Specifications and Parameters

The elements and parameters of each defined model are summarized in the tables below:

Model	RC beam	RC Column	ST Frame	Vertical Sh.C	Horizontal Sh.C	RR	RD	RL
OM1	B1	C1	TUBO260X130X10	10 * 30mm d	-	0.62	0.42	2.82
OM2	B1	C1	TUBO300X150X12.5	10 * 30mm d	-	1.17	0.41	4.66
OM3	B1	C1	TUBO380X190X12.5	10 * 30mm d	-	2.37	0.41	7.64

Table 4.1 OM models Specifications

Model	RC beam	RC Column	ST Frame	Vertical Sh.C	Horizontal Sh.C	RR	RD	RL
HM1	B1	C1	TUBO260X130X10	-	12 * 30mm d	0.62	0.42	2.82
HM2	B1	C1	TUBO300X150X12.5	-	12 * 30mm d	1.17	0.41	4.66
HM3	B1	C1	TUBO380X190X12.5	-	12 * 30mm d	2.37	0.41	7.64

Table 4.2 HM models Specifications

Model	RC beam	RC Column	ST Frame	Vertical Sh.C	Horizontal Sh.C	RR	RD	RL
SM1	B1	C1	TUBO260X130X10.0	10 * 10mm d	12 * 10mm d	0.62	0.42	2.82
SM2	B1	C1	TUBO260X130X10.0	10 * 30mm d	12 * 30mm d	0.62	0.42	2.82
SM3	B1	C1	TUBO260X130X10.0	10 * 60mm d	12 * 60mm d	0.62	0.42	2.82
SM4	B1	C1	TUBO300X150X12.5	10 * 10mm d	12 * 10mm d	1.17	0.41	4.66
SM5	B1	C1	TUBO300X150X12.5	10 * 30mm d	12 * 30mm d	1.17	0.41	4.66
SM6	B1	C1	TUBO300X150X12.5	10 * 60mm d	12 * 60mm d	1.17	0.41	4.66
SM7	B1	C1	TUBO380X190X12.5	10 * 10mm d	12 * 10mm d	2.37	0.41	7.64
SM8	B1	C1	TUBO380X190X12.5	10 * 30mm d	12 * 30mm d	2.37	0.41	7.64
SM9	B1	C1	TUBO380X190X12.5	10 * 60mm d	12 * 60mm d	2.37	0.41	7.64

Table 4.3 SM models Specifications

4.4.4 General Models

As mentioned above, we have one RC frame and three different steel frames which other models are generated by different combinations of these four basic models. These models' details are shown in the table below:

Model	RC beam	RC Column	ST Frame	Vertical Connectors	Horizontal Connectors
M1(RC Frame)	B1	C1	-	-	-
M2	-	-	TUBO260X130X10.0	-	-
M3	-	-	TUBO300X150X12.5	-	-
M4	-	-	TUBO380X190X12.5	-	-

Table 4.11 M Models' General Parameters

4.4.5 OM Models

The models in this group consist of an outer RC frame with a steel inner frame which are connected by only vertical connectors. In the all models, RC frame sections and connectors' diameters are kept constant. In the all models, 30mm d rebars are used as vertical connectors.
The specifications of all models in this group are as shown in the table below:

Model	RC beam	RC Column	ST Frame	Vertical Connectors	Horizontal Connectors
OM1	B1	C1	TUBO260X130X10.0	10 * 30mm d	-
OM2	B1	C1	TUBO300X150X12.5	10 * 30mm d	-
OM3	B1	C1	TUBO380X190X12.5	10 * 30mm d	-

Table 4.12 OM Models' General Parameters

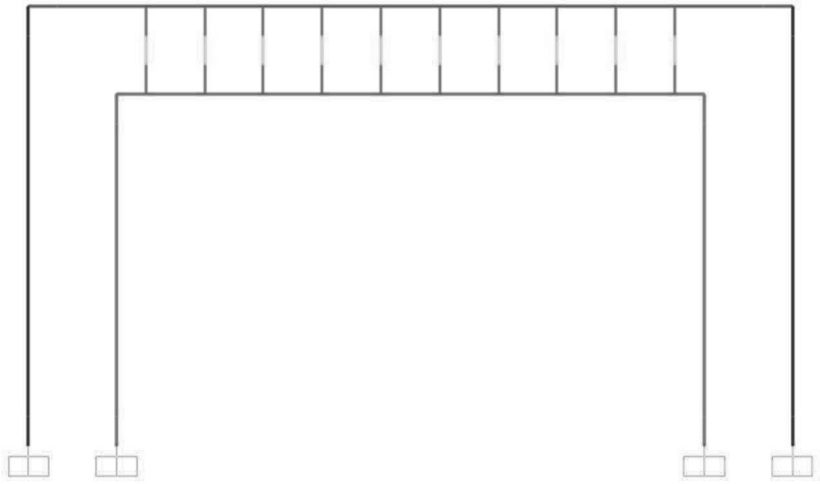

Figure 4.1 OM Models General Configuration

4.4.6 HM Models

The models in this group consist of an outer RC frame with a steel inner frame which are connected by only horizontal connectors. In the all models, RC frame sections and connectors' diameters are kept constant. In the all models, 30mm d rebars are used as horizontal connectors.

The specifications of all models in this group are as shown in the table below:

Model	RC beam	RC Column	ST Frame	Vertical Connectors	Horizontal Connectors
HM1	B1	C1	TUBO260X130X10.0	-	12 * 30mm d
HM2	B1	C1	TUBO300X150X12.5	-	12 * 30mm d
HM3	B1	C1	TUBO380X190X12.5	-	12 * 30mm d

Table 4.12 HM Models' General Parameters

Figure 4.2 HM Models General Configuration

4.4.7 SM Models

The models in this group consist of an outer RC frame with a steel inner frame which are connected by vertical and horizontal connectors. In the all models, RC frame sections are kept constant while the sections of steel inner frame and sections of the vertical and horizontal connectors are differing in each model.

The specifications of all models in this group are as shown in the table below:

Model	RC beam	RC Column	ST Frame	Vertical Connectors	Horizontal Connectors
SM1	B1	C1	TUBO260X130X10.0	10 * 10mm d	12 * 10mm d
SM2	B1	C1	TUBO260X130X10.0	10 * 30mm d	12 * 30mm d
SM3	B1	C1	TUBO260X130X10.0	10 * 60mm d	12 * 60mm d
SM4	B1	C1	TUBO300X150X12.5	10 * 10mm d	12 * 10mm d
SM5	B1	C1	TUBO300X150X12.5	10 * 30mm d	12 * 30mm d
SM6	B1	C1	TUBO300X150X12.5	10 * 60mm d	12 * 60mm d
SM7	B1	C1	TUBO380X190X12.5	10 * 10mm d	12 * 10mm d
SM8	B1	C1	TUBO380X190X12.5	10 * 30mm d	12 * 30mm d
SM9	B1	C1	TUBO380X190X12.5	10 * 60mm d	12 * 60mm d

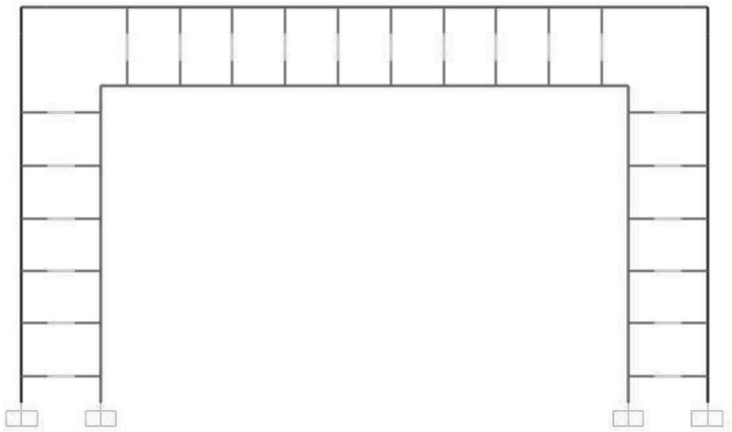

Figure 4.3 SM Models General Configuration

4.4.8 NM Models

The NM models are some specific combination of connectors which are proposed to be studied after getting results from SM models and two models are defined in this group which are shown in bellow:

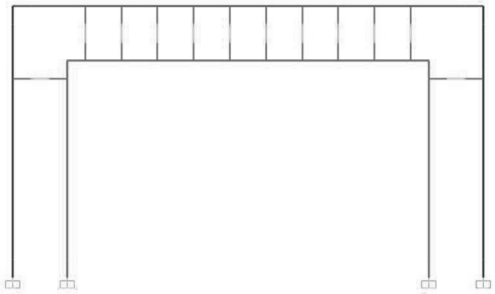

Figure 4.4 NM1 Model

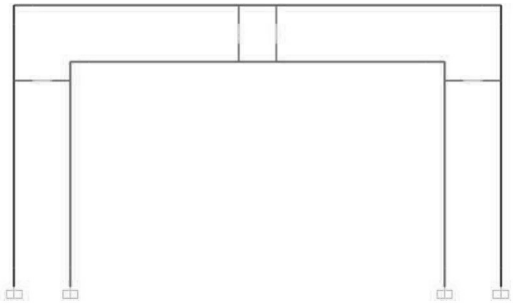

Figure 4.5 NM2 Model

4.5 Plastic hinges

In order to consider material wise nonlinear behavior of models, different concentrated plasticities or plastic hinges are defined and assigned to the elements. The definitions and details of the plastic hinges are provided so they can model the hole plastic behavior of each section and element.
The details of all defined and assigned plastic hinges are provided in the table below:

Hinge Name	Assigned Element	Hinge Type	Plastic behavior	Hysteresis Type	Symmetry Condition	Load Capacity After Point E
RC Column P.H	RC Columns	Deformation Controlled	P-M3	Takeda Model	Symmetric	Drops to Zero
RC Beam P.H	RC Beams	Deformation Controlled	M3	Takeda Model	Symmetric	Drops to Zero
ST Column P.H	ST Columns	Deformation Controlled	P-M3	Takeda Model	Symmetric	Drops to Zero
ST Beam P.H	ST Beams	Deformation Controlled	M3	Takeda Model	Symmetric	Drops to Zero
ST Connector P.H1	ST Connectors	Deformation Controlled	P-M3	Takeda Model	Symmetric	Drops to Zero
ST Connector P.H2	ST Connectors	Deformation Controlled	V	Takeda Model	Symmetric	Drops to Zero

Table -

4.6 Nonlinear Load Cases

In this study we defined two nonlinear load cases, first one is the Nonlinear Pushover and the second one is the Nonlinear Time History. Nonlinear pushover load case is used to study retrofitting results in general and the effects of orientation and distribution of the connectors and nonlinear time history load case is used to study the energy consumption of different elements of the models in the real earthquake records.

4.6.1 Nonlinear Pushover Load Case

The Nonlinear Pushover load case is defined as a nonlinear static load case with load pattern according to assigned lateral loads to the top of the RC columns. It starts from zero initial conditions and increases the lateral load by 1kN increment in each step. Load application control is full load and the joint no 14(top point of the left RC column) is the point that displacements are monitored.

4.6.2 Nonlinear Time History Load Case

The Nonlinear Time History load case is defined as a nonlinear dynamic load case and we selected four ground motion records to define four different load cases. It starts from zero initial conditions and then assigns accelerations to the model in the X direction. Mass source1 is used as mass source.

4.7 Ground Motion Data

4.7.1 Selection of Ground Motions

The earthquake records used for this study have been obtained from the PEER database. The Peak ground acceleration (PGA) ranges from 0.5 to 0.8g, and the magnitude of the ground motions ranges from 5.5 to 7.5

Table 4.6: Selected Ground Motion Records

Earthquake Name	Year	Station Name	Magnitude	Mechanism	Rjb (km)	Rrup (km)	Vs30 (m/sec)
"Morgan Hill"	1984	"Gilroy Array #6"	6.19	strike slip	9.85	9.87	663.31
"Loma Prieta"	1989	"Hayward City Hall - North"	6.93	Reverse Oblique	54.97	55.11	735.44
"Northridge-01"	1994	"Mt Wilson - CIT Seis Sta"	6.69	Reverse	35.53	35.88	680.37
"Kobe_ Japan"	1995	"MZH"	6.9	strike slip	69.04	70.26	609

4.7.2 Scaling of Ground Motion Records

Seismo match software was used to scale earthquake records and bring them to a consistent intensity level. Scaling allows multiple ground motion recordings and the structure's seismic reaction to being combined. Target response spectra is selected from ASCE 7-22 and for the stiff soil. The target spectrum is shown as bellow:

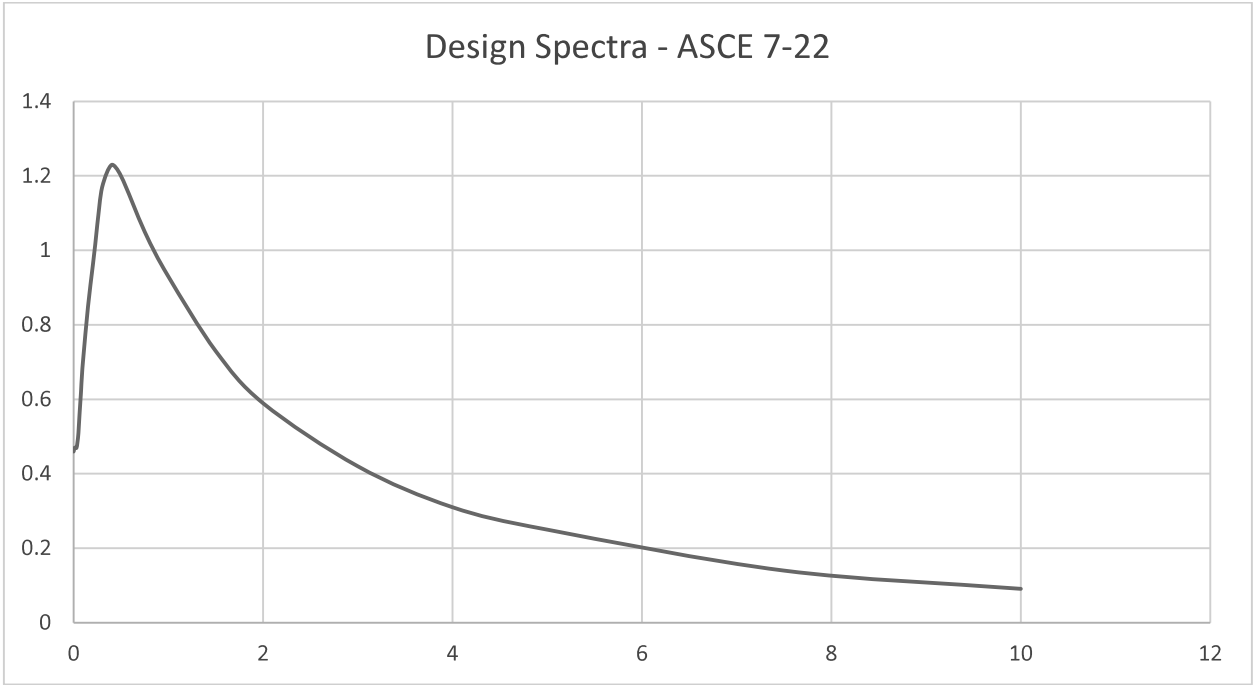

Time history records of selected earthquakes are plotted bellow in unscaled version and scaled version:

- Morgan Hill Earthquake:

Unscaled:

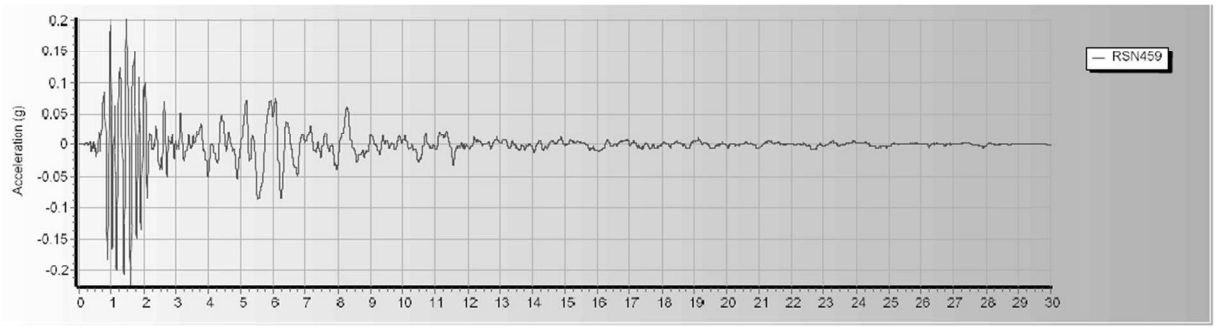

Scaled:

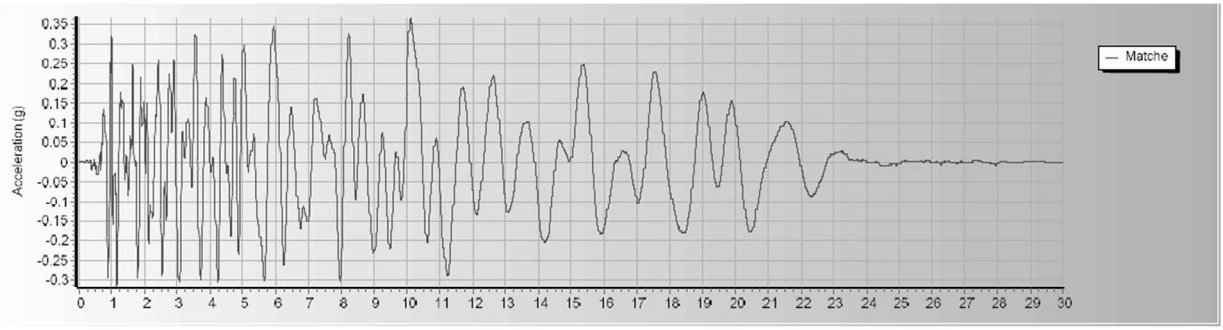

- Loma Prieta Earthquake :

Unscaled :

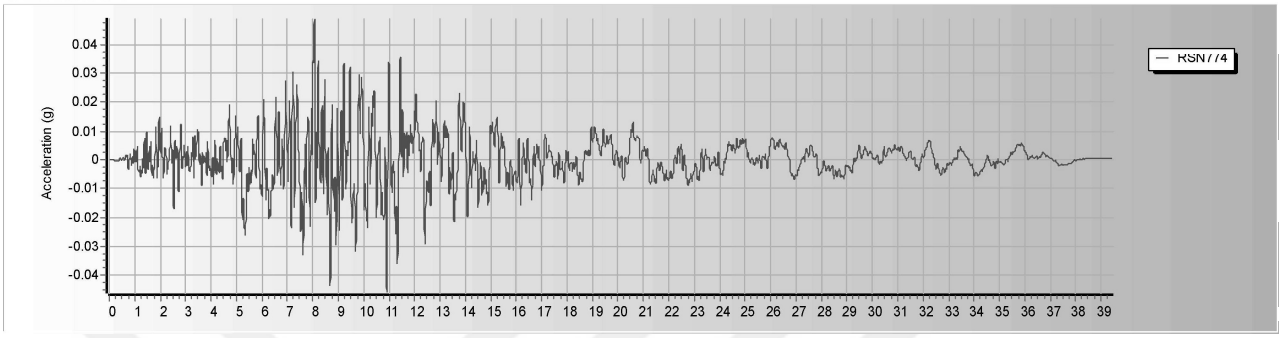

Scaled:

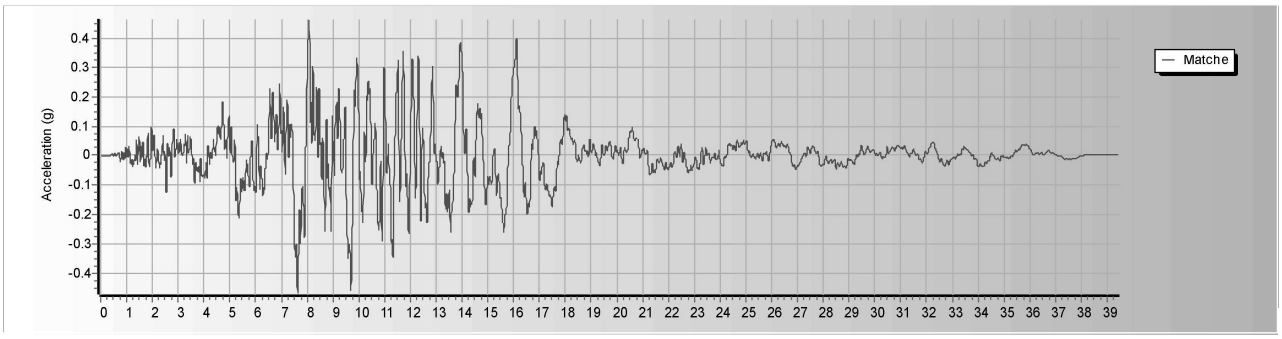

- Northridge Earthquake:

Unscaled :

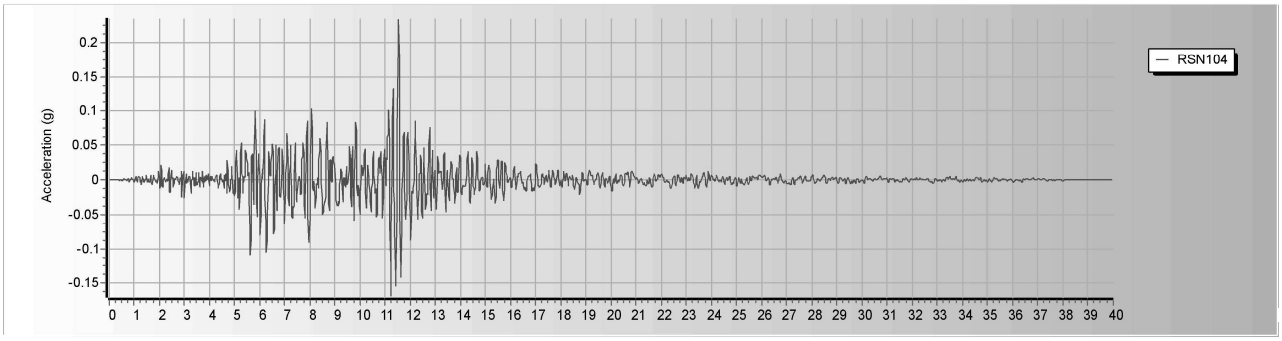

Scaled :

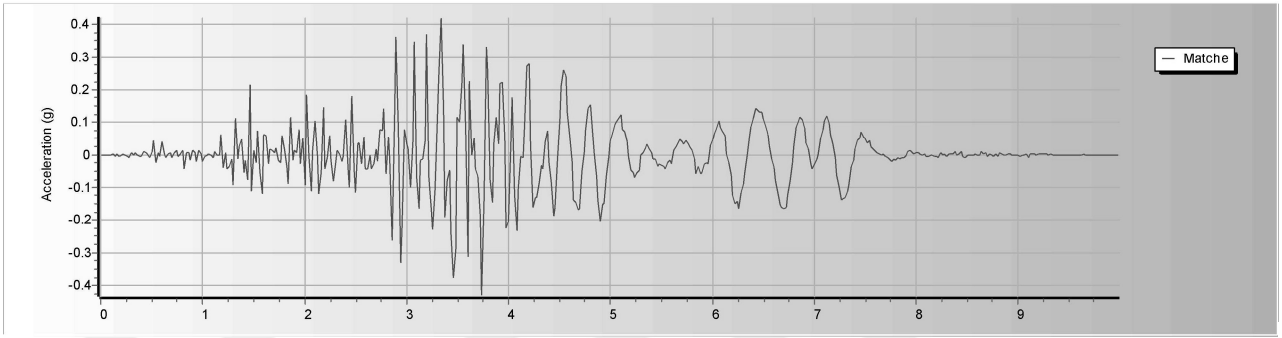

- Kobe Earthquake :

Unscaled :

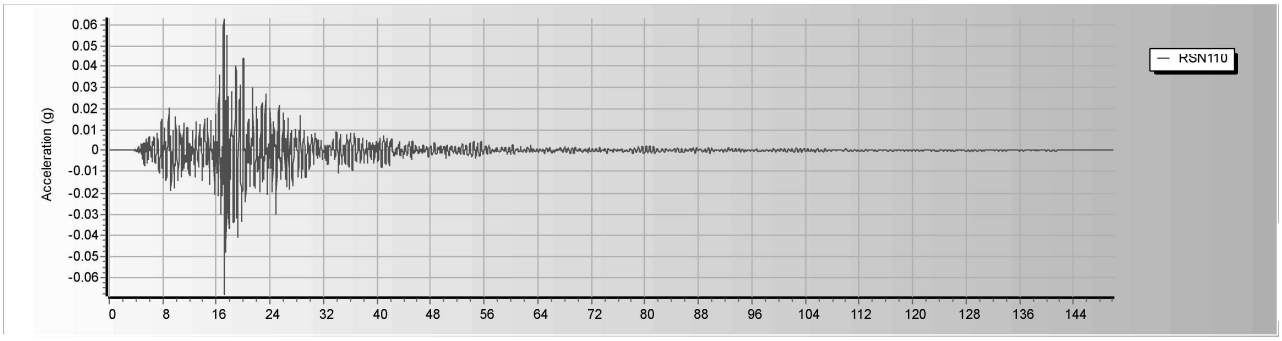

Scaled :

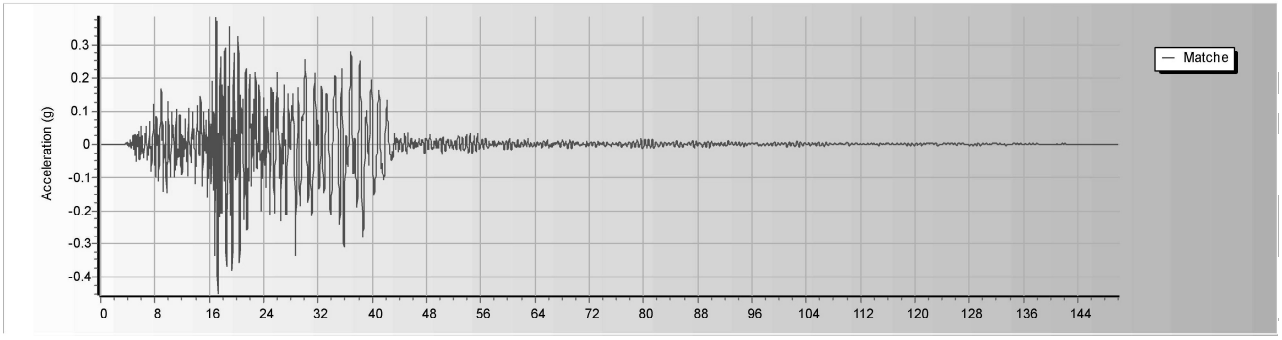

CHAPTER 5

ANALYSIS RESULT AND DISCUSSION

5.1 General

In this study seventheen models are defined to study the indvidual rehebilitation results of each combination of the outer RC frame and Steel inner frame and horizontal and vertical connections and to be able to compare models to study and compare the efficency of ecah model and select and propose the most effective case.

The results are presented in two gropus:

a) Nonlinear Pushover Analyisis Results. b) Nonlinear Tome History Analysis Result .

The first group result are used to stusy the efficency of vertical and horizontal connectors and the effects of the distribution of connectors and the effects of axial and shear rigidities of connectors to the general bavior of the models as well.

The second group results are used to study the energy consumption of elements in each differernt cobinations and will show how the connectors are disipiating earthquake energy in each model.

5.2 Analysis Results

5.2.1 Nonlinear Pushover Analysis Results

In this part the results are presented in two parts, the results of general behavior of models and the results of connectors' internal forces in each of the models. The pushover curve and the lateral load carrying capacity of the models at elastic point and maximum load point are presented for each defined model and then the internal forces of connectors which have contribution in conveying lateral loads from outer frame to inner frame are presented.

5.2.1.1 M Models' Pushover Curves

In this part pushover curves of the M Models are presented.

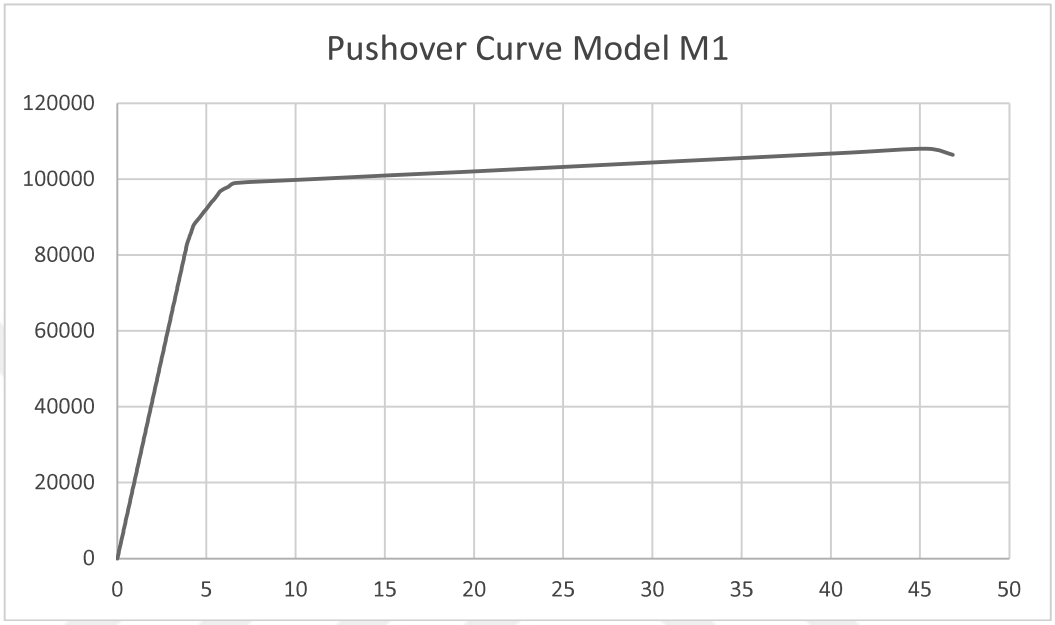

M1 Model P.O Curve

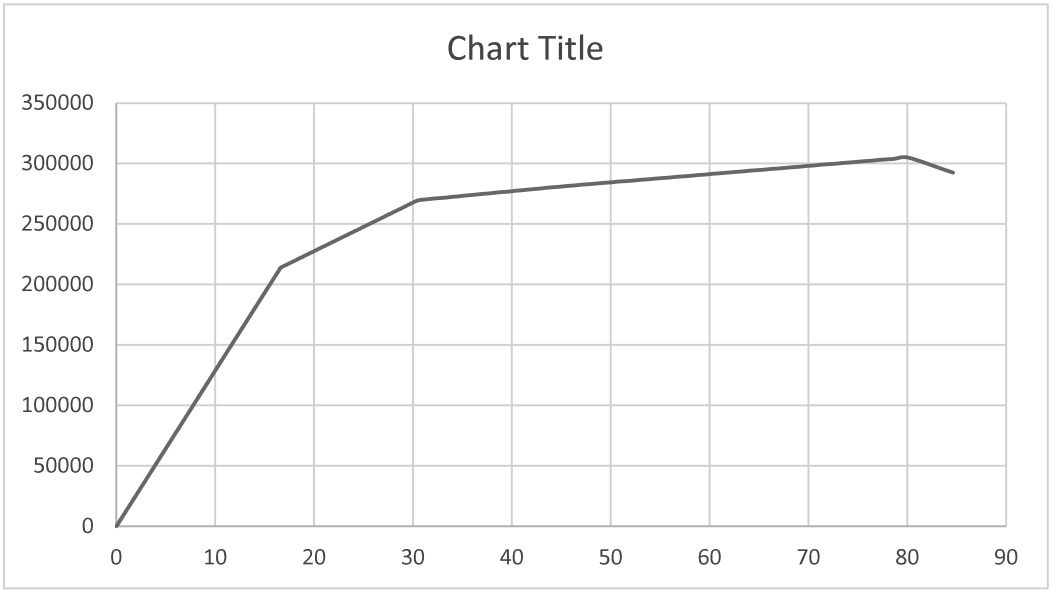

M2 Model P.O Curve

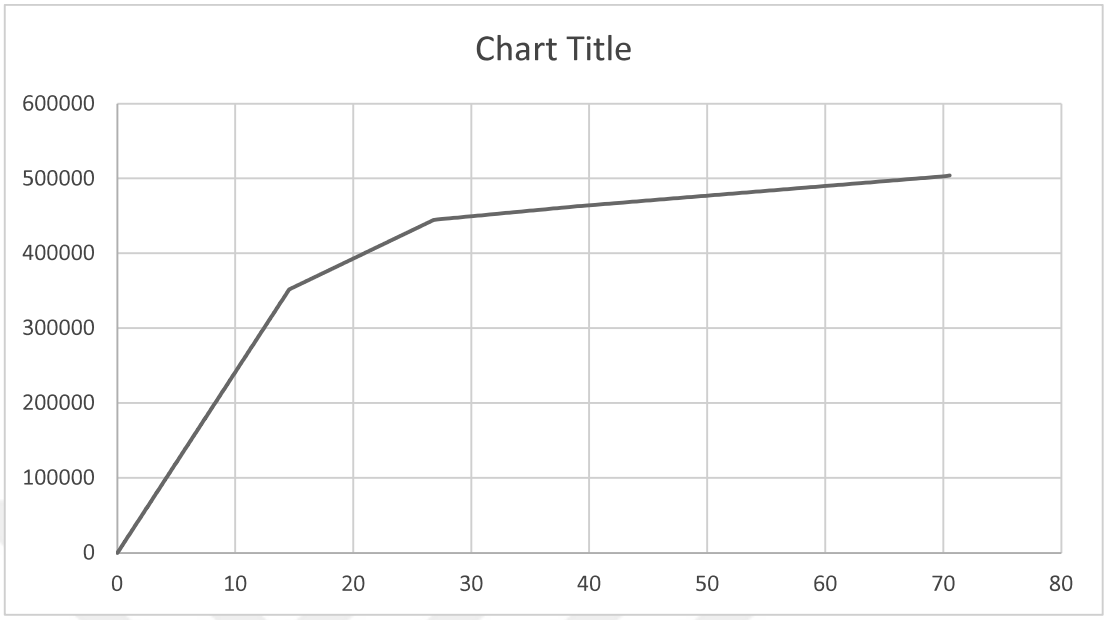

M3 Model P.O Curve

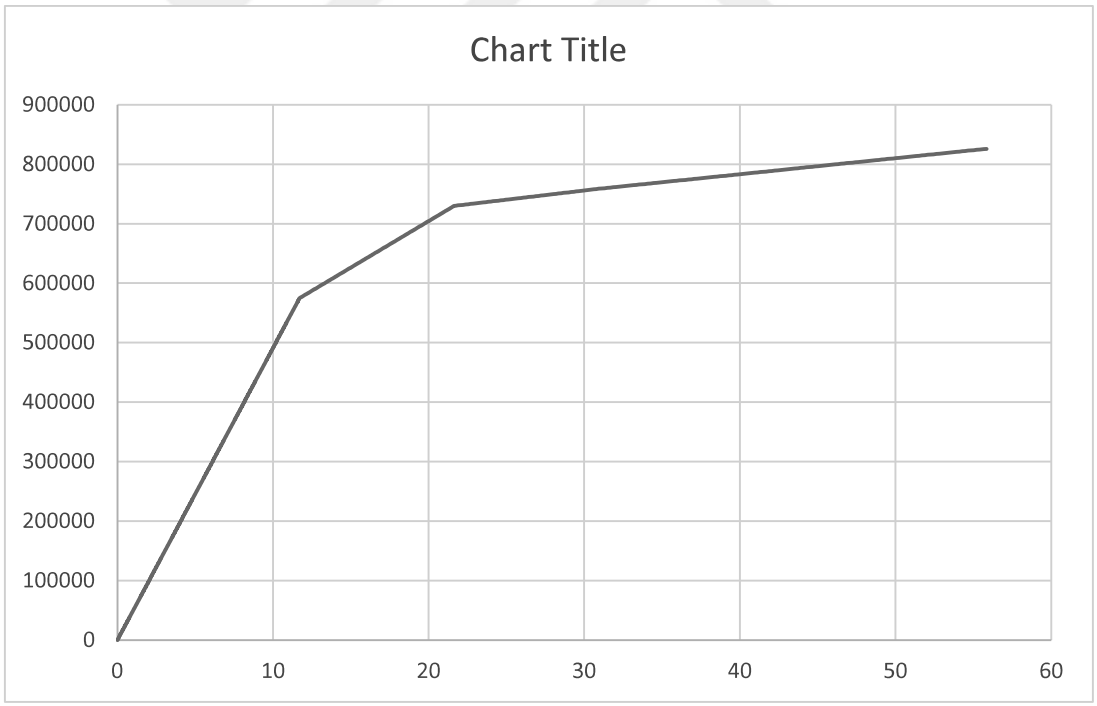

M4 Model P.O Curve

5.2.1.2 OM Models' Pushover Curves

In This Part pushover curves of the OM models are presented. Pushover curves of the general models are plotted and simultaneously the pushover curves of the outer RC frame and inner steel frame are plotted as well. The black line is the pushover curve of the structure and blue line and red line are pushover curves of RC frame and steel frame respectively.

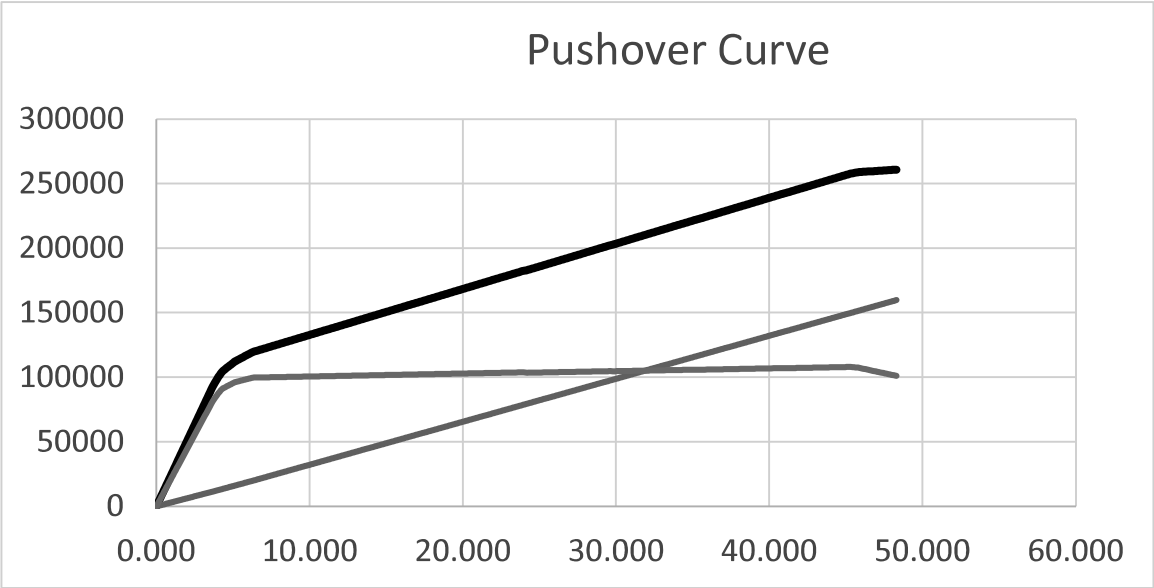

OM1 Model P.O Curve

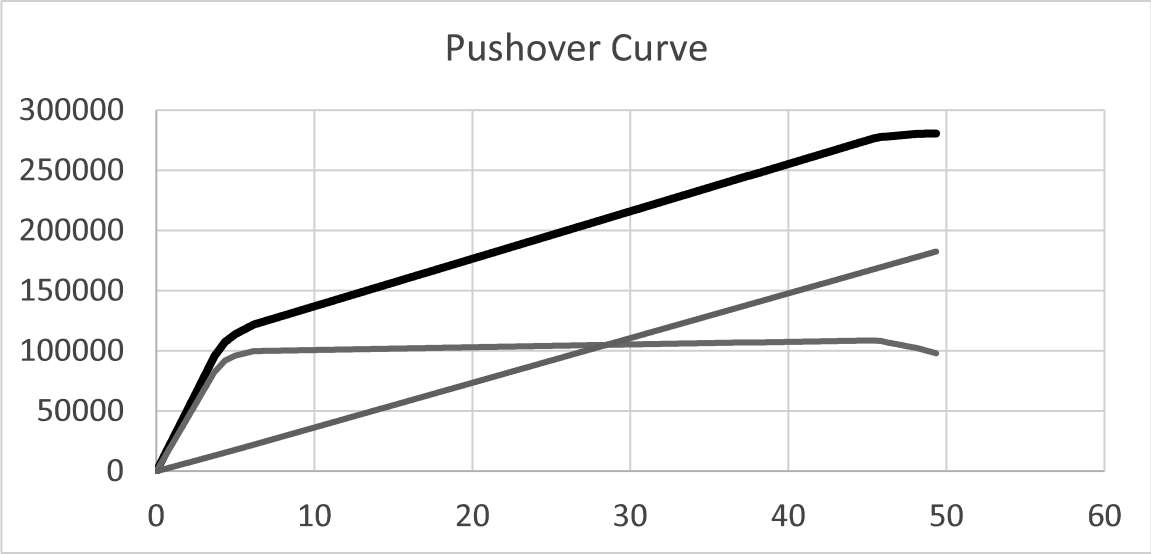

OM2 Model P.O Curve

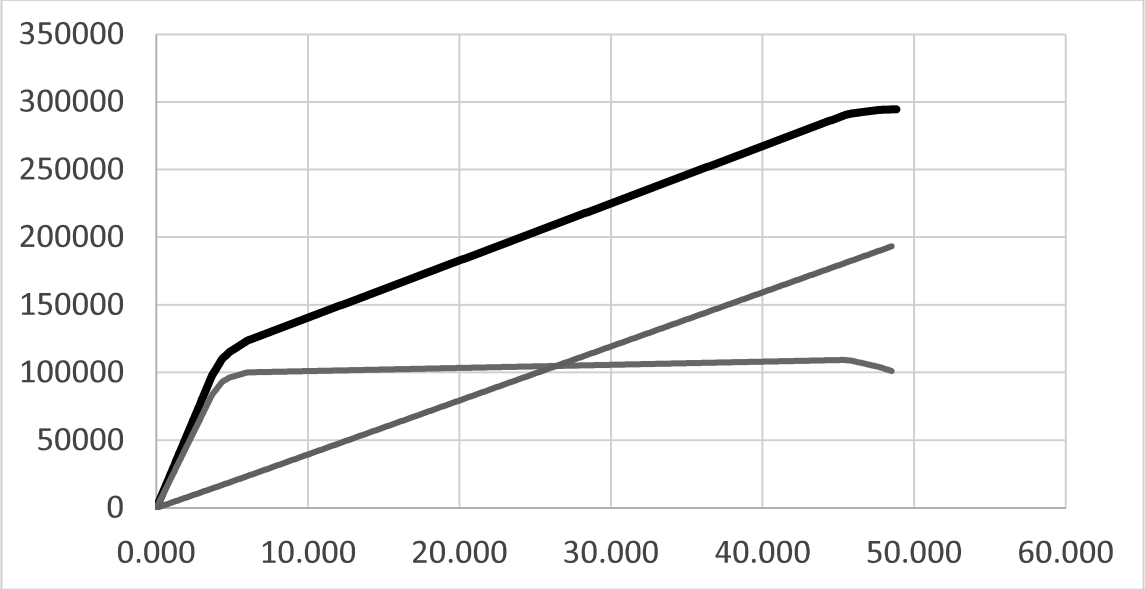

OM3 Model P.O Curve

5.2.1.3 HM Models' Pushover Curves

In This Part pushover curves of the HM models are presented. Pushover curves of the general models are plotted and simultaneously the pushover curves of the outer RC frame and inner steel frame are plotted as well. The black line is the pushover curve of the structure and blue line and red line are pushover curves of RC frame and steel frame respectively.

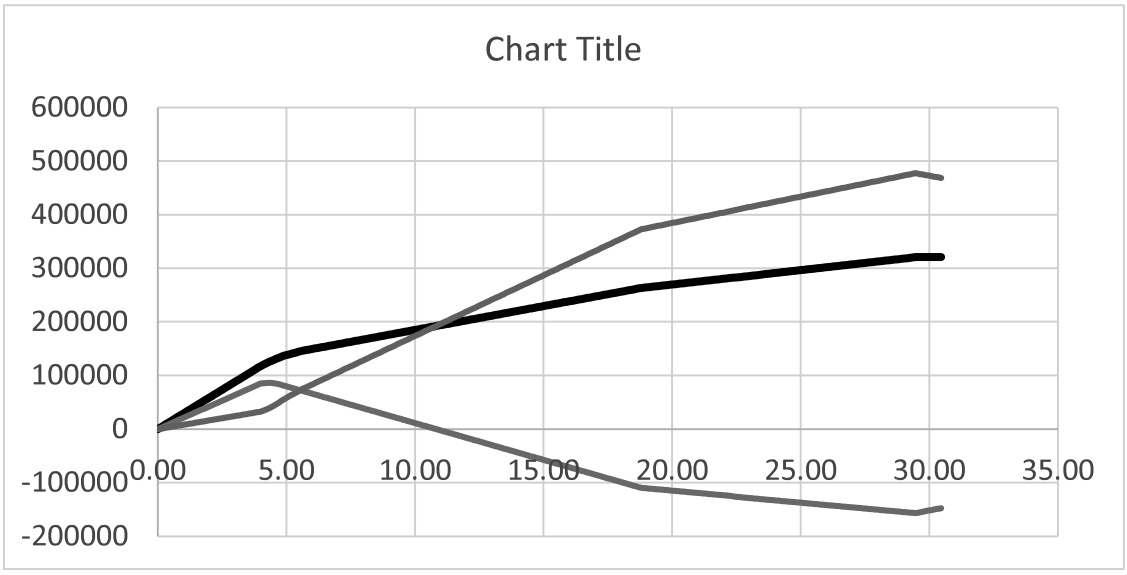

HM1 Model P.O Curve

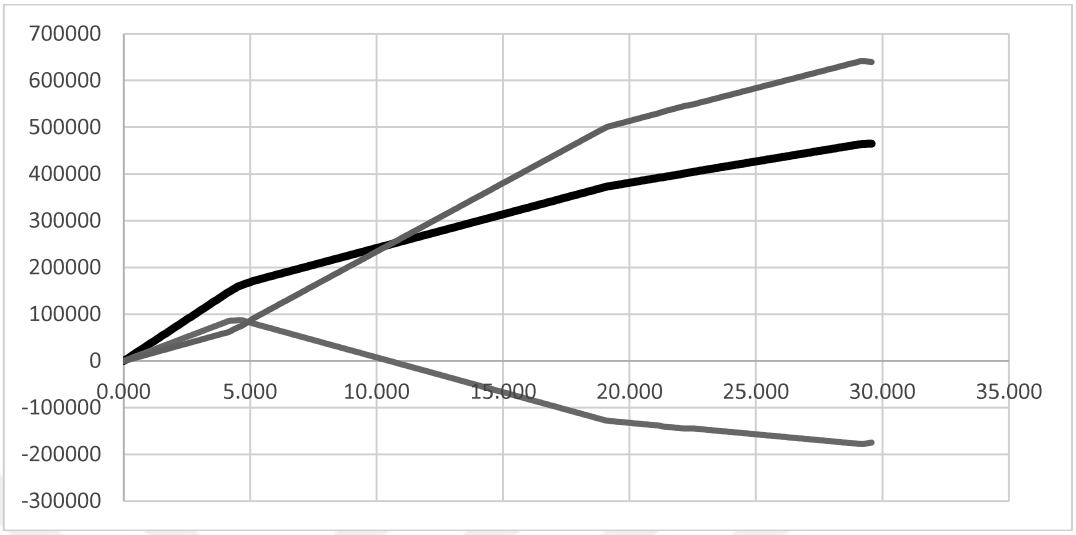

HM2 Model P.O Curve

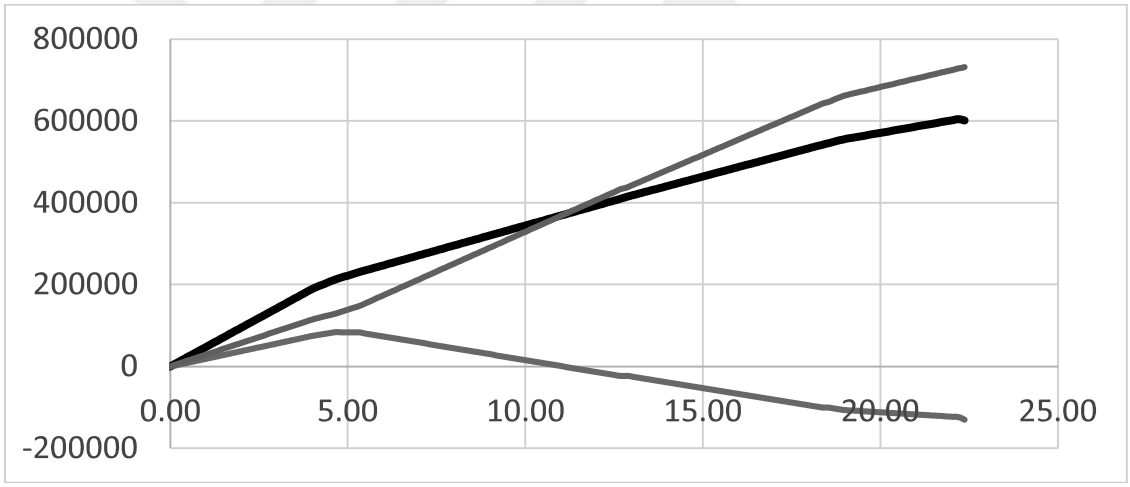

HM3 Model P.O Curve

5.2.1.4 SM Models' Pushover Curves

In This Part pushover curves of the SM models are presented. Pushover curves of the general models are plotted and simultaneously the pushover curves of the outer RC frame and inner steel frame are plotted as well. The black line is the pushover curve of the structure and blue line and red line are pushover curves of RC frame and steel frame respectively.

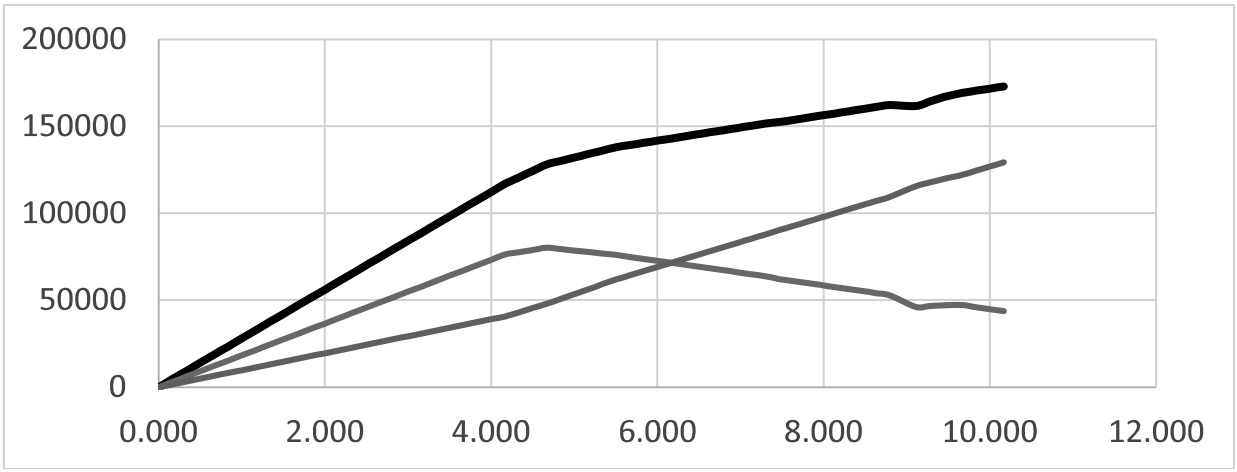
200000
150000
100000
50000
0
0.000
2.000
4.000
6.000
8.000
10.000
12.000

SM1

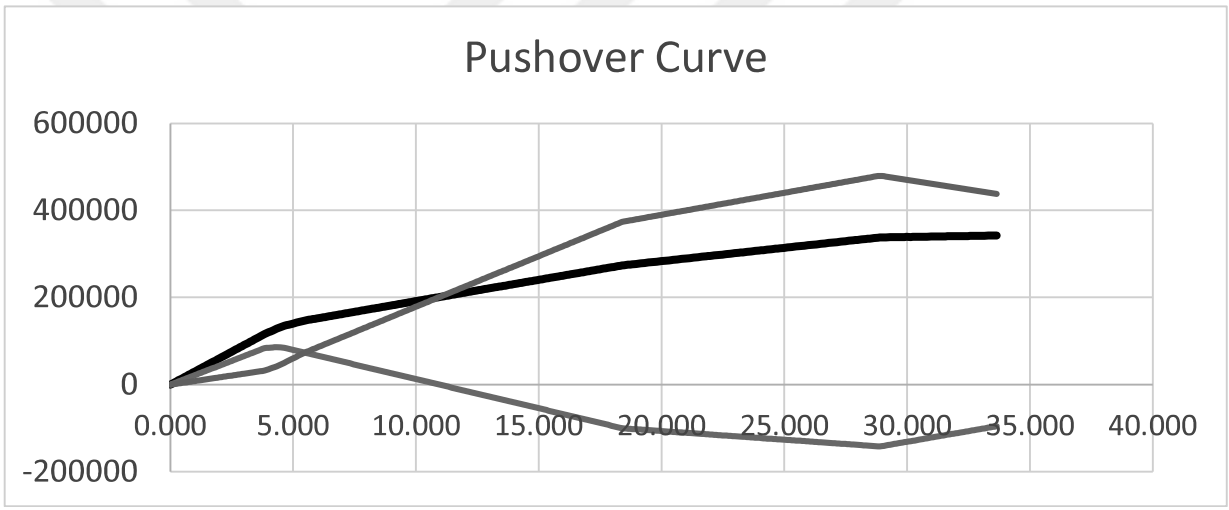
Pushover Curve
600000
400000
200000
0
-200000
0.000
5.000
10.000
15.000
20.000
25.000
30.000
35.000
40.000

SM2

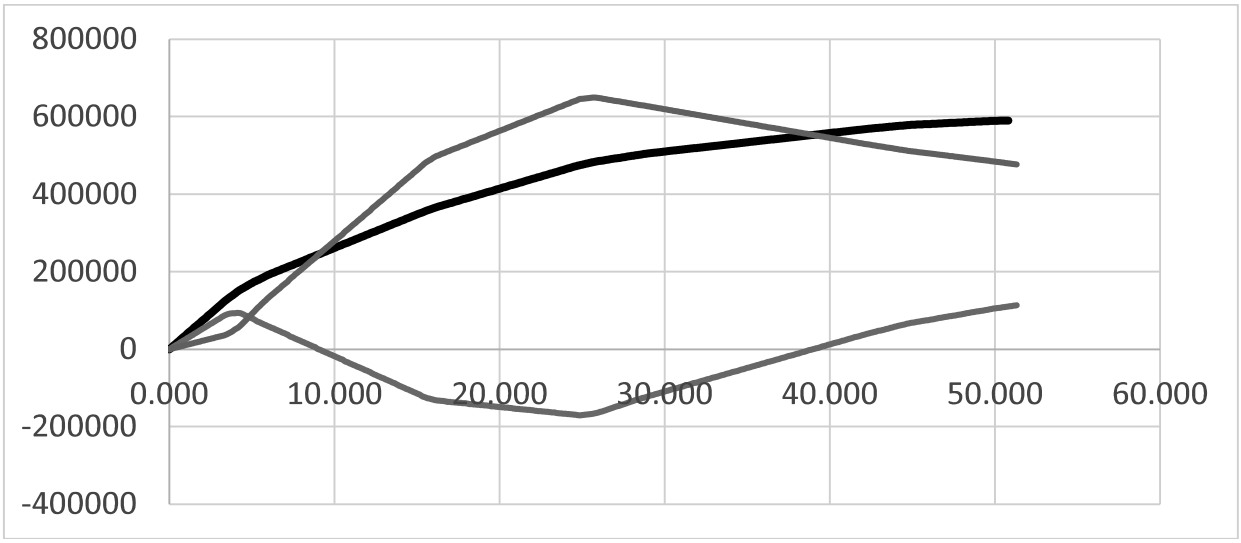
800000
600000
400000
200000
0
-200000
-400000
0.000
10.000
20.000
30.000
40.000
50.000
60.000

SM3

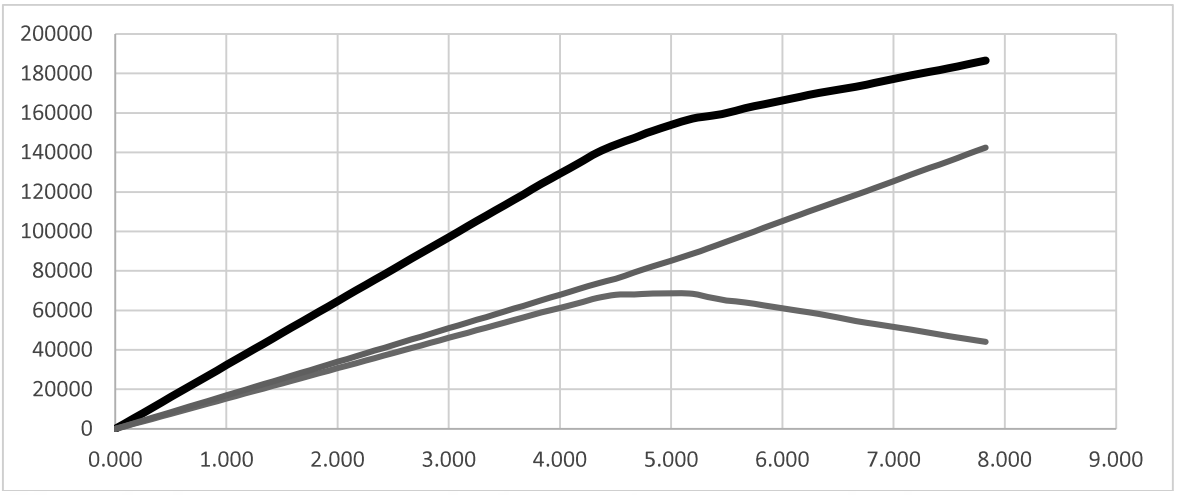
200000
180000
160000
140000
120000
100000
80000
60000
40000
20000
0
0.000
1.000
2.000
3.000
4.000
5.000
6.000
7.000
8.000
9.000

SM4

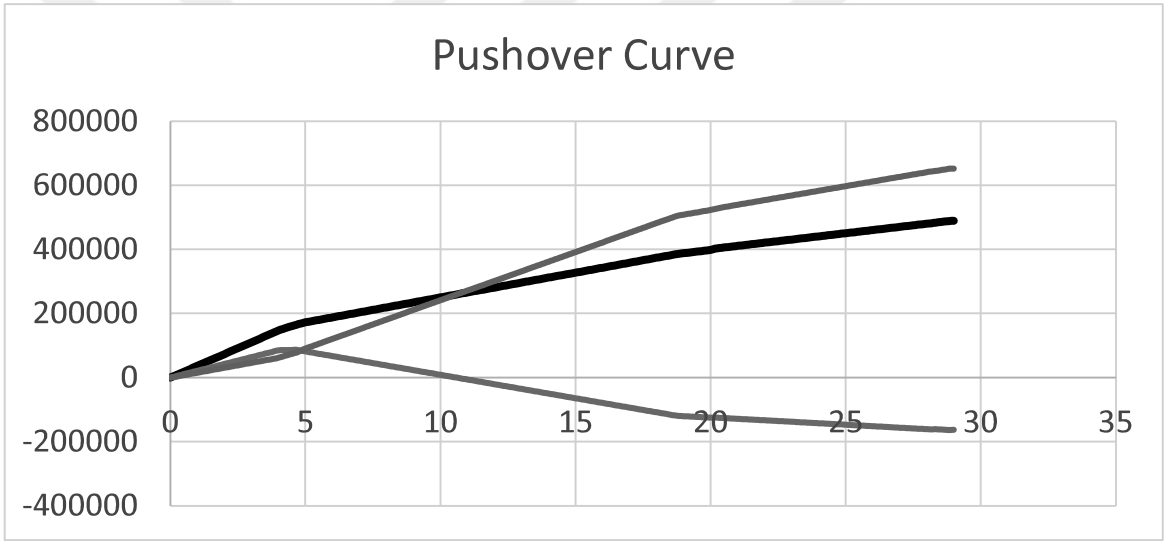
Pushover Curve
800000
600000
400000
200000
0
-200000
-400000
0
5
10
15
20
25
30
35

SM5

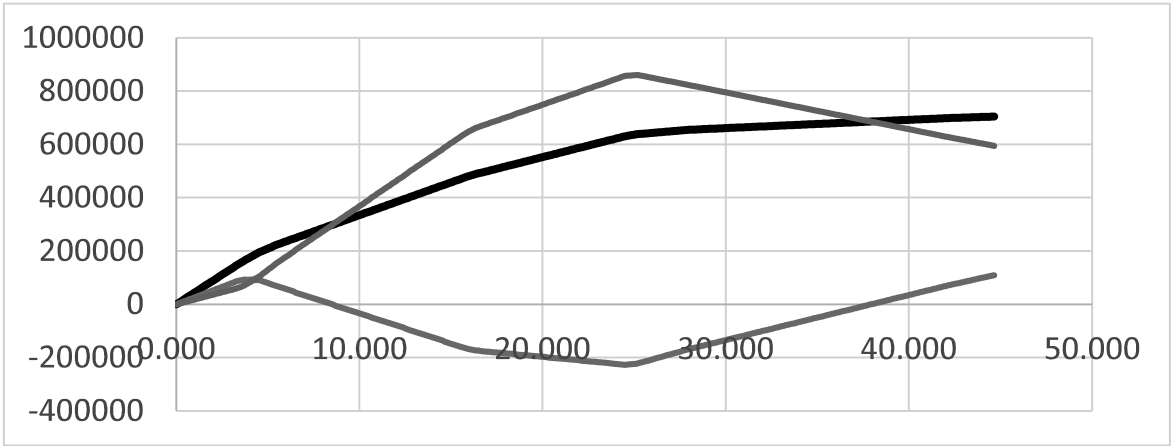
1000000
800000
600000
400000
200000
0
-200000
-400000
0.000
10.000
20.000
30.000
40.000
50.000

SM6

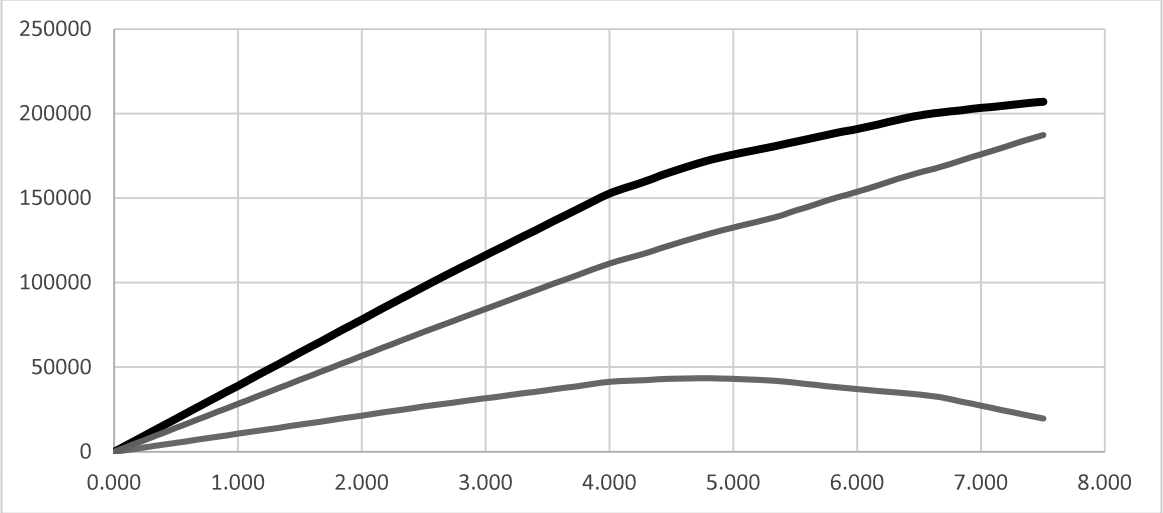
250000
200000
150000
100000
50000
0
0.000
1.000
2.000
3.000
4.000
5.000
6.000
7.000
8.000

SM7

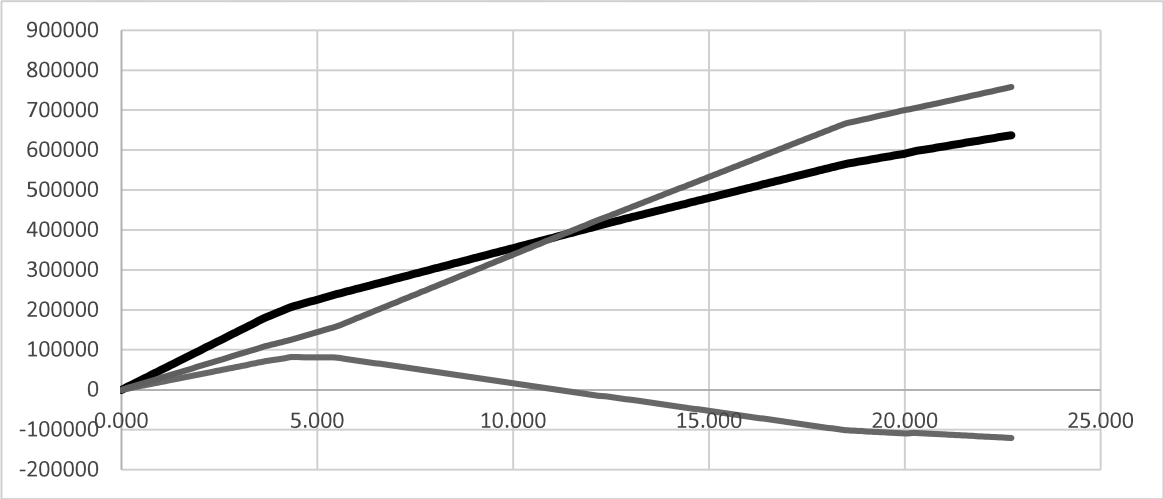
900000
800000
700000
600000
500000
400000
300000
200000
100000
0
-100000
-200000
0.000
5.000
10.000
15.000
20.000
25.000

SM8

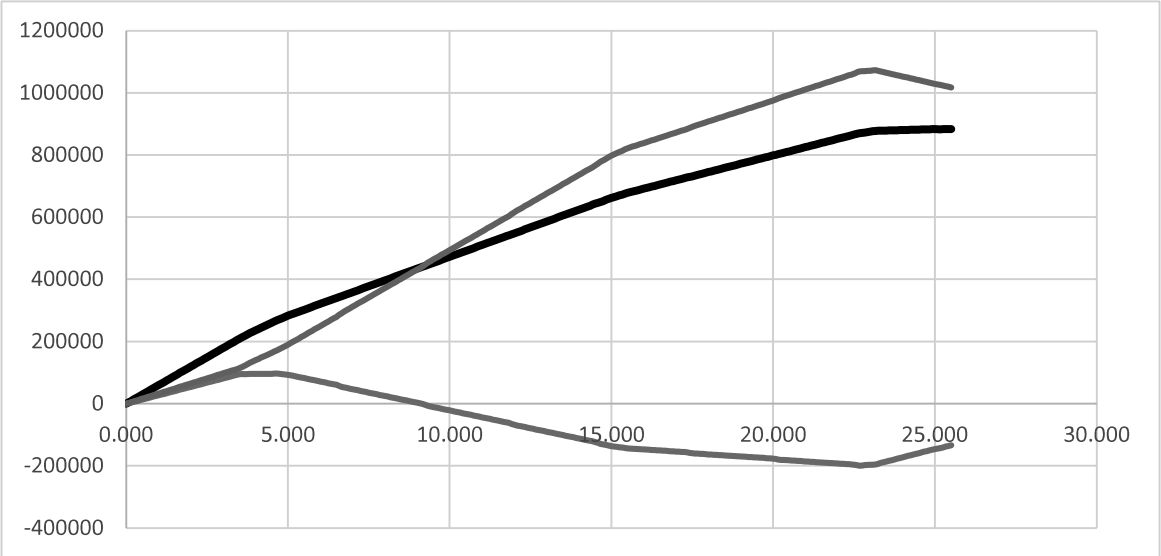
1200000
1000000
800000
600000
400000
200000
0
-200000
-400000
0.000
5.000
10.000
15.000
20.000
25.000
30.000

SM9

5.2.1.5 NM Models' Pushover Curves

In This Part pushover curves of the NM models are presented. Pushover curves of the general models are plotted and simultaneously the pushover curves of the outer RC frame and inner steel frame are plotted as well. The black line is the pushover curve of the structure and blue line and red line are pushover curves of RC frame and steel frame respectively.

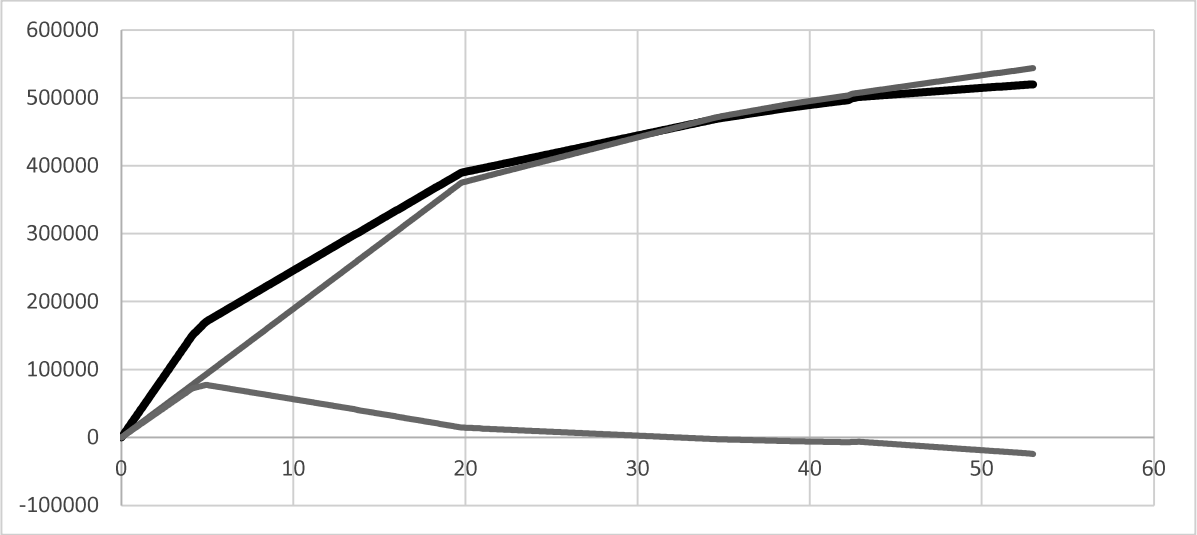

NM1

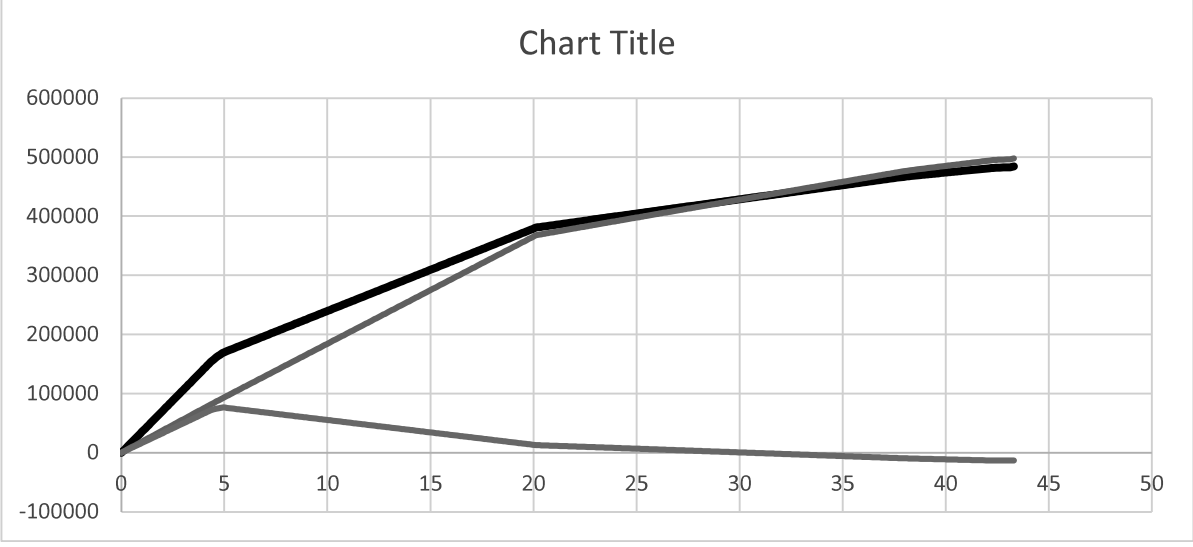

NM2

5.2.1.6 Models' Numerical results

In this part numerical result of the nonlinear pushover analysis are presented, results contain general behavior results of the models and the internal forces of the connectors as well. In order to compare the results, at the first step the results of the general behavior of the models are presented and the results of the internal forces of the connectors are presented at the second step.

5.2.1.6.1 Models' General Behavior Numerical results

The results of the General behavior of the models are presented here in order to compare the efficiency of vertical and horizontal connectors and the effect of the ratio of the rigidity of inner steel frame to outer RC frame.

Model	Pe (N)	de (mm)	Pu (N)	du (mm)	EI (n/mm)	ζ (mm/mm)
M1(RC Frame)	81000.0	3.91	108000.0	45.40	20726.7	11.62
M2	214000.0	16.61	305000.0	80.10	12883.8	4.82
M3	352000.0	14.56	503000.0	70.01	24175.8	4.81
M4	575000.0	11.70	825000.0	55.39	49145.3	4.73

Table Group M Models Results

Model	Pe (N)	de (mm)	Pu (N)	du (mm)	EI (n/mm)	ζ (mm/mm)
OM1	92719.0	3.66	261135.0	48.16	25333.1	13.16
OM2	95368.0	3.66	280668.0	49.67	26056.8	13.57
OM3	97716.0	3.66	294785.0	49.17	26698.4	13.43

Table Group OM Models Results

Model	Pe (N)	de (mm)	Pu (N)	du (mm)	EI (n/mm)	ζ (mm/mm)
HM1	117675.0	4.00	321186.0	30.29	29418.8	7.57
HM2	148328.0	4.17	465100.0	29.57	35595.9	7.10
HM3	189683	4.00	604727	22.21	47420.8	5.55

Table Group HM Models Results

Model	Pe (N)	de (mm)	Pu (N)	du (mm)	EI (n/mm)	ζ (mm/mm)
NM1	150446.0	4.13	519905.0	52.98	36471.8	12.84
NM2	153391.0	4.33	484612	43.31	35425.2	10.00

Table Group NM Models Results

Model	Pe (N)	de (mm)	Pu (N)	du (mm)	EI (n/mm)	ζ (mm/mm)
SM1	116920.0	4.17	172941	17.84	28058.6	4.28
SM2	116119.0	3.83	342369	33.64	30294.5	8.78
SM3	123110.0	3.33	589582	51.32	36936.7	15.40
SM4	124176.0	3.83	186542	7.82	32396.6	2.04
SM5	146983.0	4.00	489650	29.00	36745.8	7.25
SM6	148491.0	3.33	704969	44.66	44591.9	13.41
SM7	97743.0	2.50	207017	7.50	39097.2	3.00
SM8	180549.0	3.67	637742	22.71	49236.2	6.19
SM9	209363.0	3.50	884139	25.50	59818.0	7.28

Table Group SM Models Results

5.2.1.7 Internal Forces of the Connectors

In this section the internal axial forces of the lateral connectors and internal shear forces of vertical connectors at the stages of first plastic hinge and the final stage are presented and compared in order to get a general conclusion.

5.2.1.7.1 OM Models' Results

5.2.1.7.1.1 OM1 Model

Internal shear forces of the vertical connectors of the OM1 model are presented below:

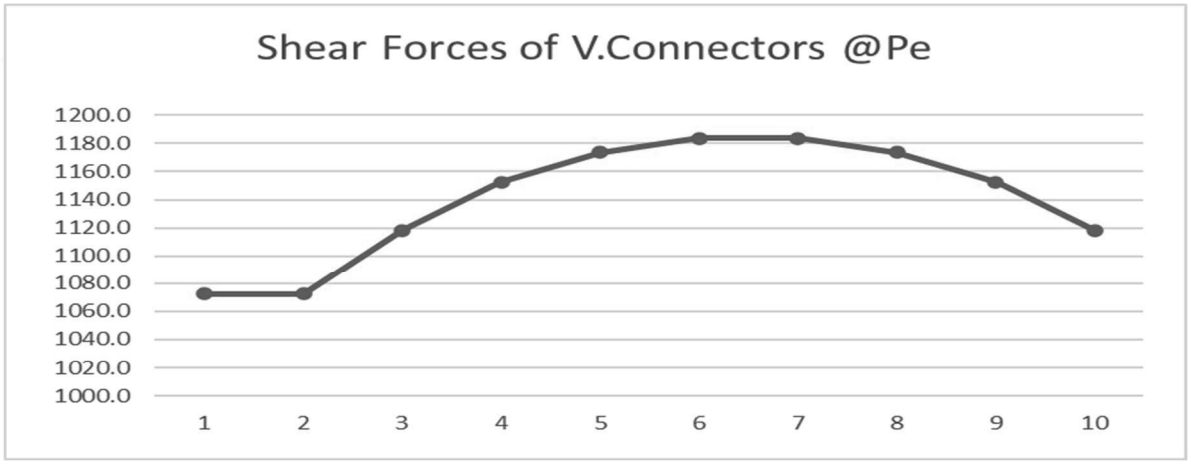

Figure 5.1 Shear Forces of Connectors @ Pe

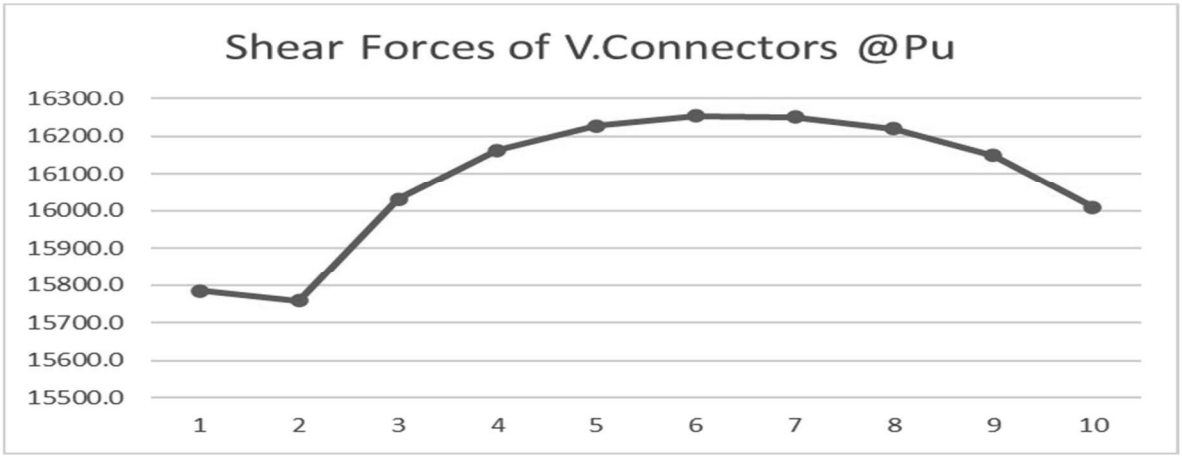

Figure 5.2 Shear Forces of Connectors @ Pu

5.2.1.7.1.2 OM2 Model

Internal shear forces of the vertical connectors of the OM2 model are presented below:

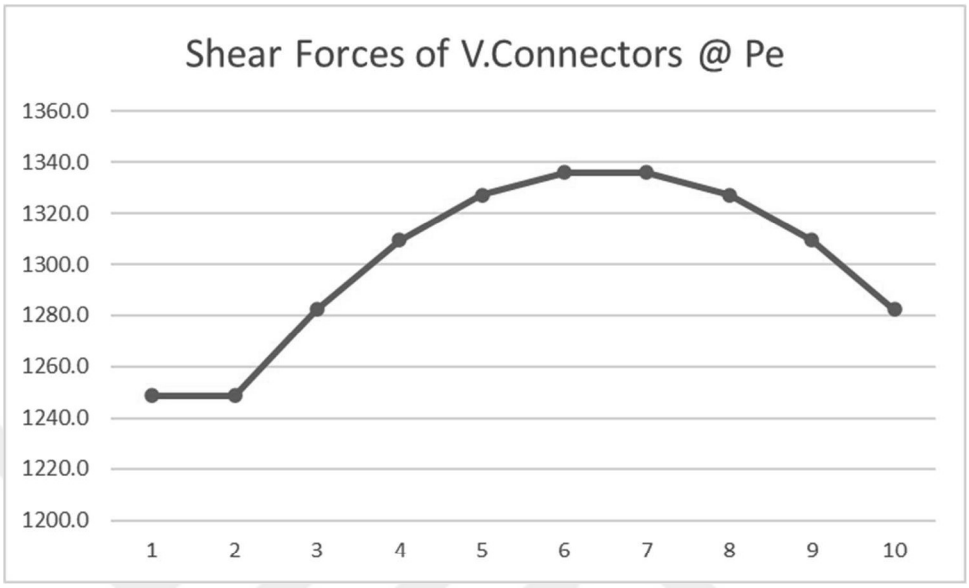

Figure 5.3 Shear Forces of Connectors @ Pe

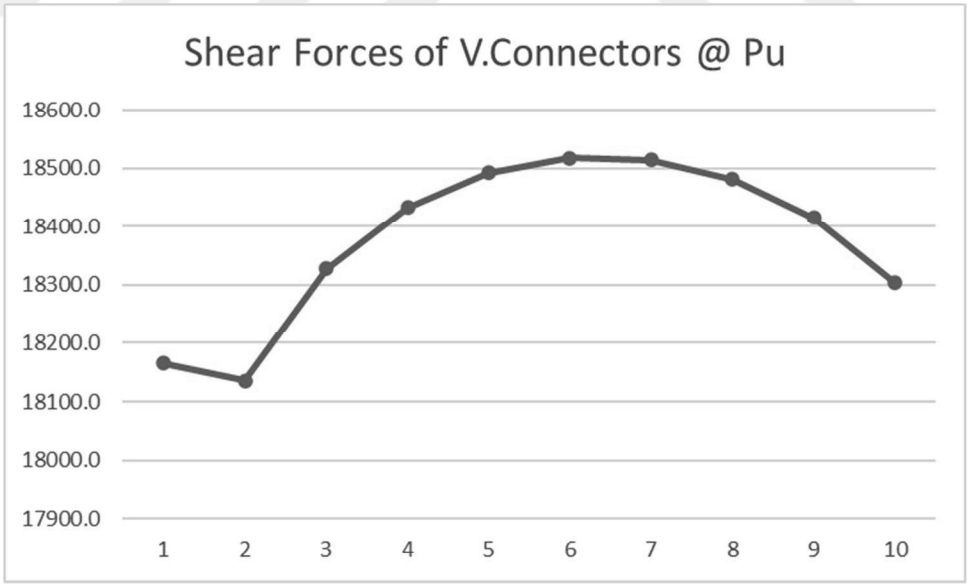

Figure 5.4 Shear Forces of Connectors @ Pu

5.2.1.7.1.3 OM3 Model

Internal shear forces of the vertical connectors of the OM3 model are presented below:

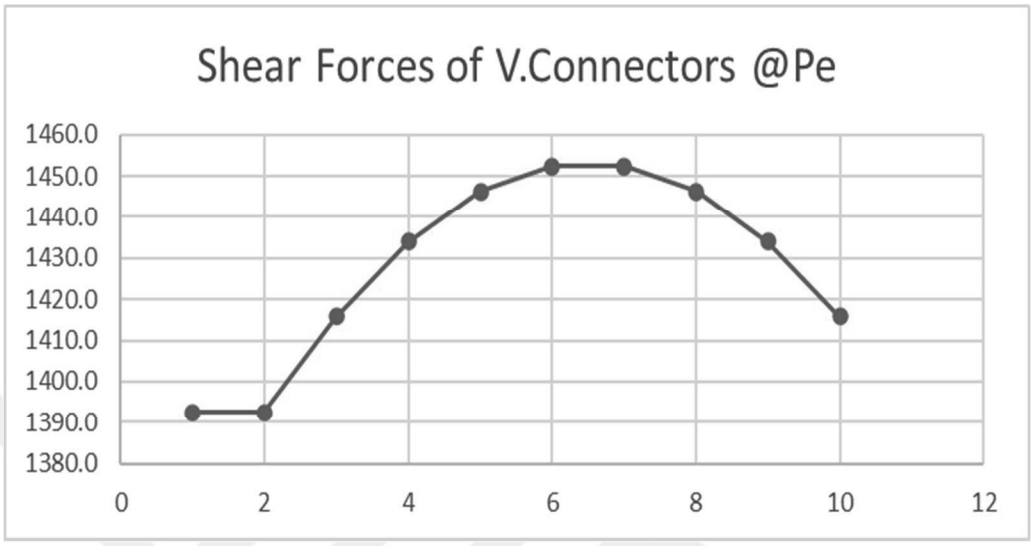

Figure 5.5 Shear Forces of Connectors @ Pe

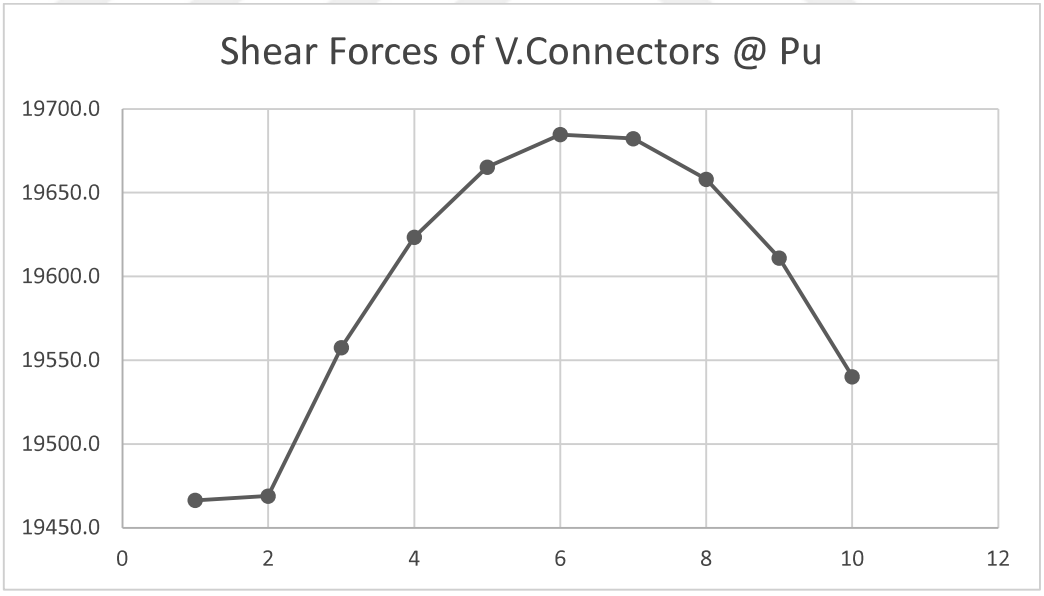

Figure 5.6 Shear Forces of Connectors @ Pu

5.2.1.7.2 HM Models' Results

5.2.1.7.2.1 HM2 Model

Internal Axial forces of the horizontal connectors of the HM2 model are presented below:

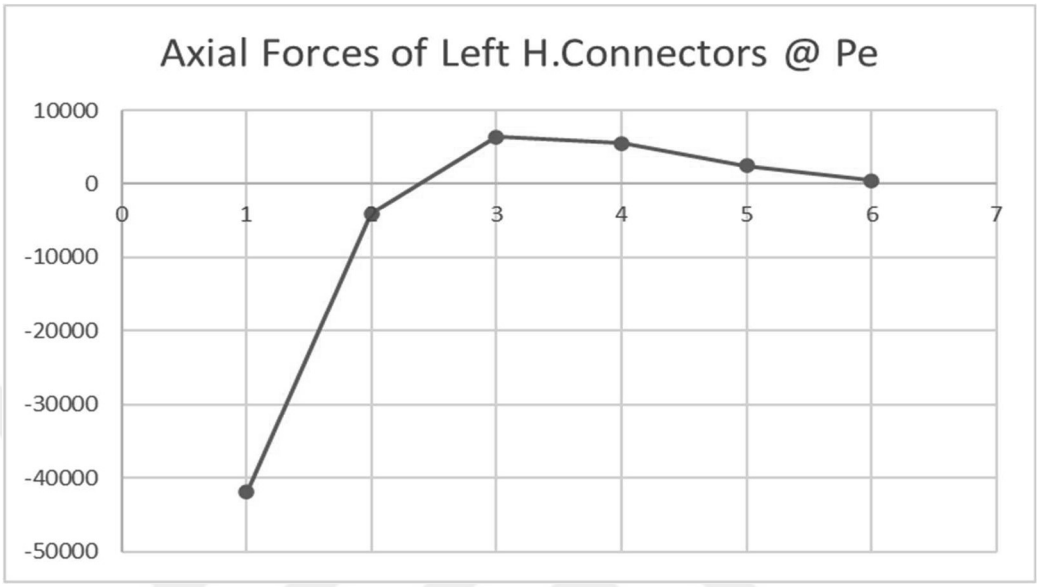

Figure 5.7 Axial Forces of Connectors at right side @ Pe

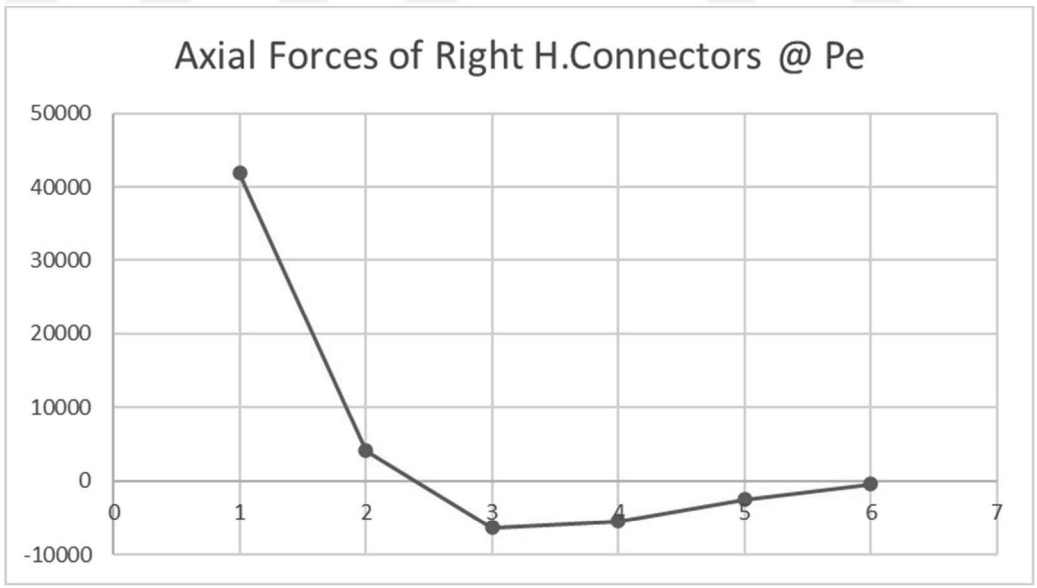

Figure 5.8 Axial Forces of Connectors at left side @ Pe

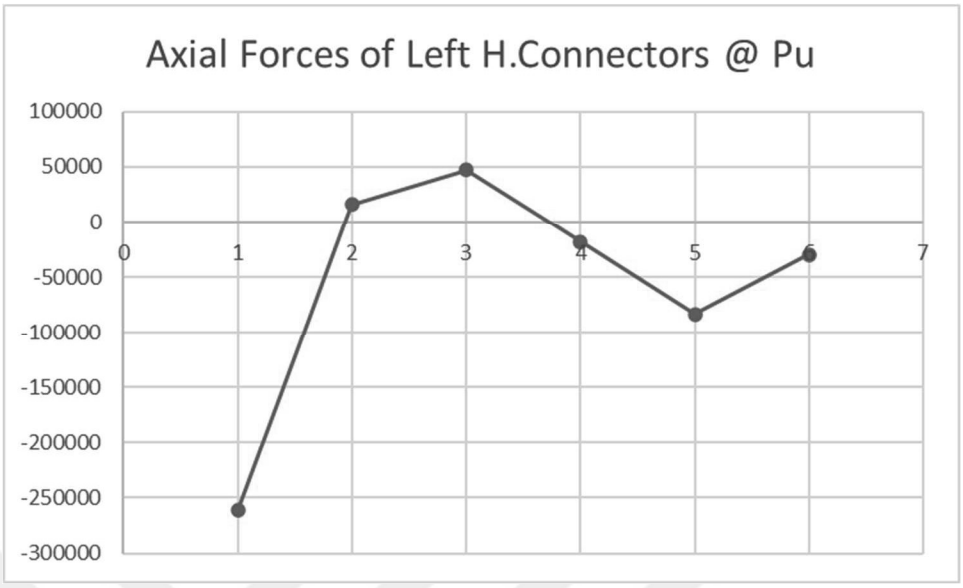

Figure 5.9 Axial Forces of Connectors at right side @ Pu

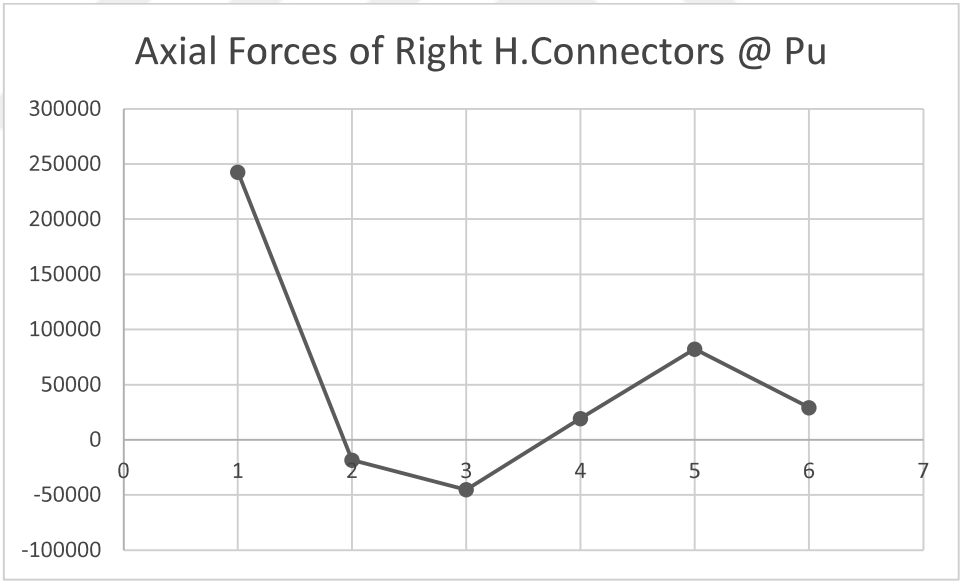

Figure 5.10 Axial Forces of Connectors at left side @ Pu

5.2.1.7.3 SM Models' Results

5.2.1.7.3.1 SM1 Model

Internal Axial forces of the horizontal connectors and the shear forces of the horizontal connectors of the SM1 model are presented below:

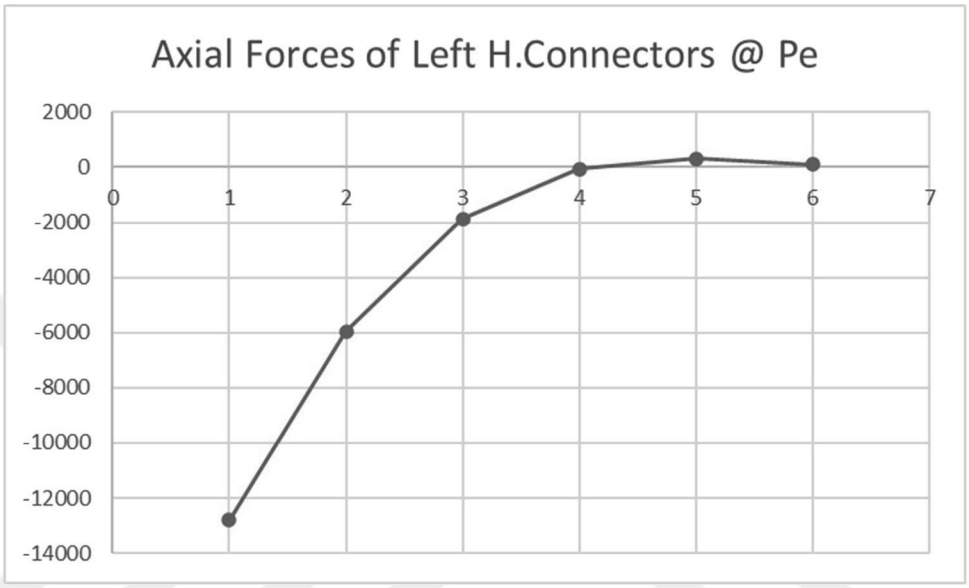

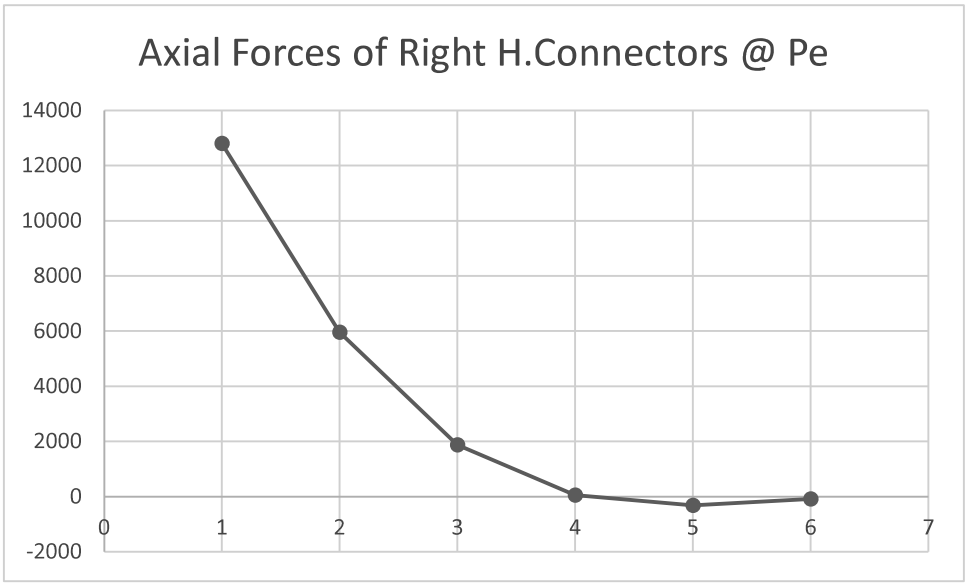

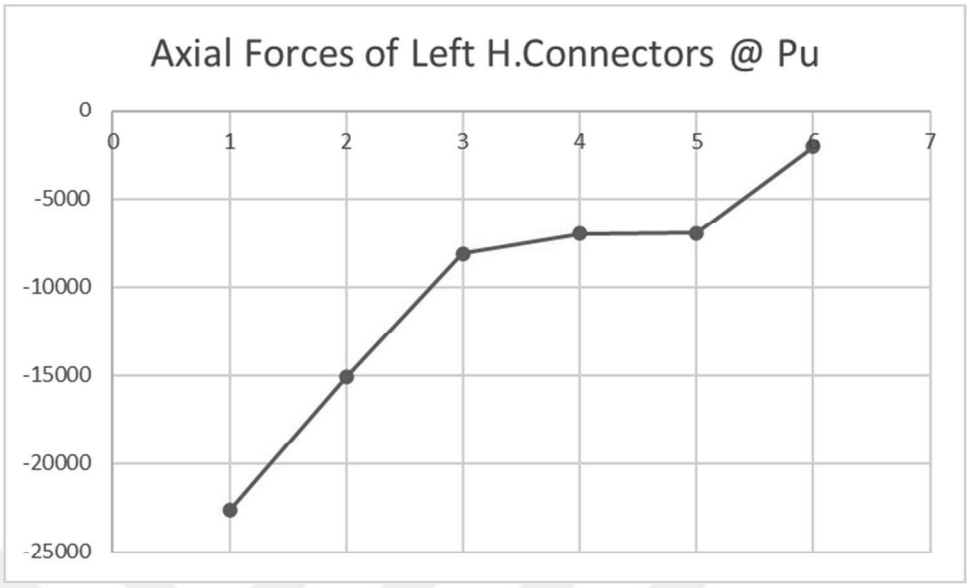
Axial Forces of Left H.Connectors @ Pu
0
-5000
-10000
-15000
-20000
-25000
0
1
2
3
4
5
6
7

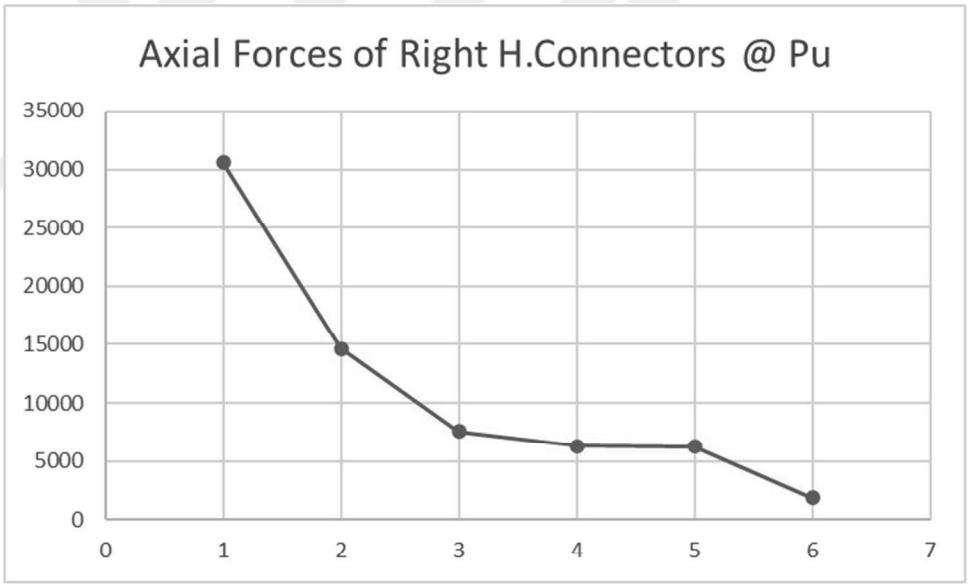
Axial Forces of Right H.Connectors @ Pu
35000
30000
25000
20000
15000
10000
5000
0
0
1
2
3
4
5
6
7

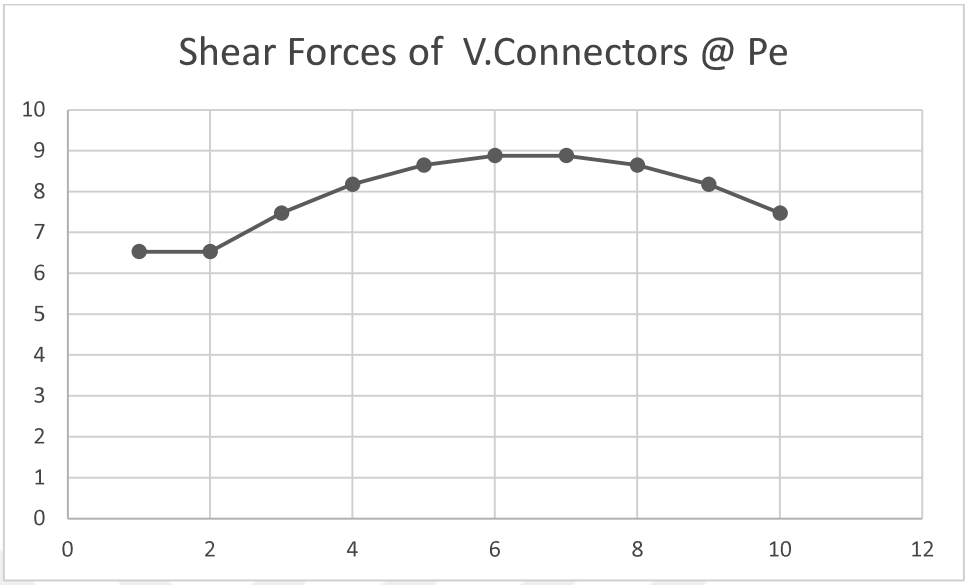

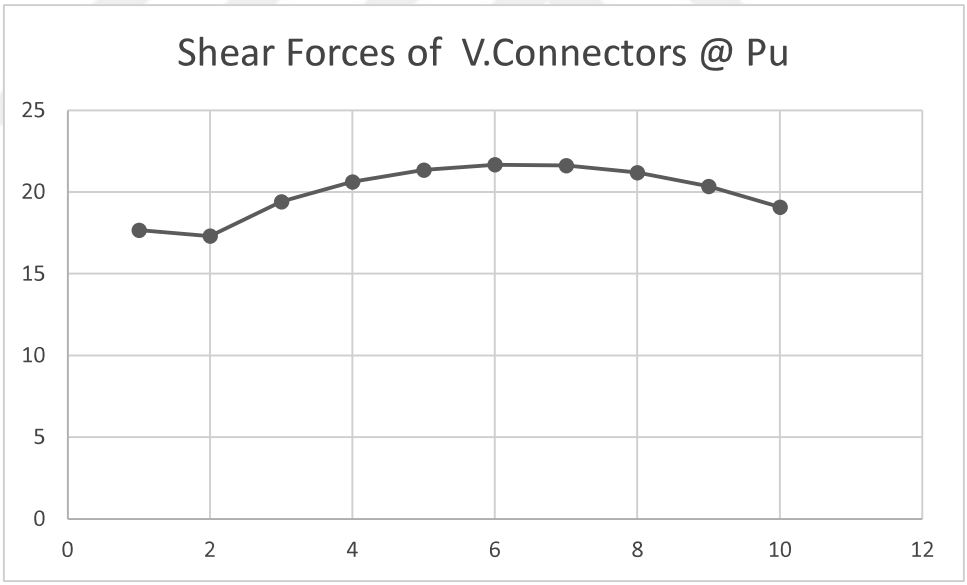

5.2.1.7.3.2 SM2 Model

Internal Axial forces of the horizontal connectors and the shear forces of the horizontal connectors of the SM2 model are presented below:

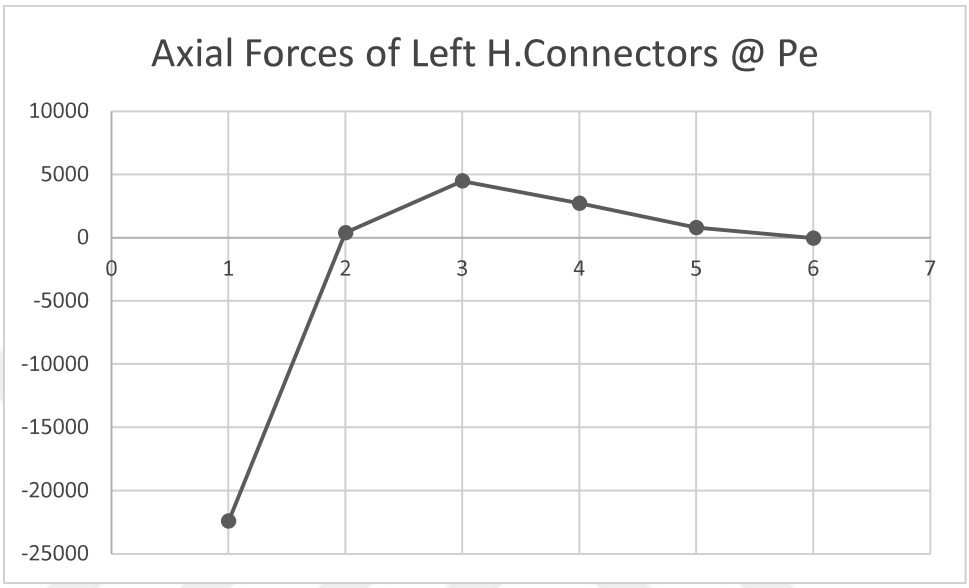

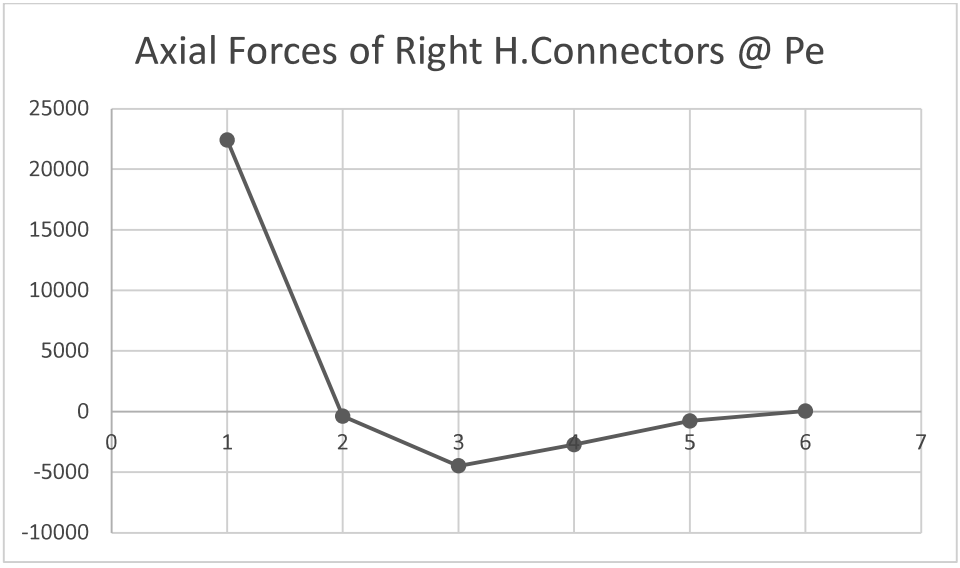

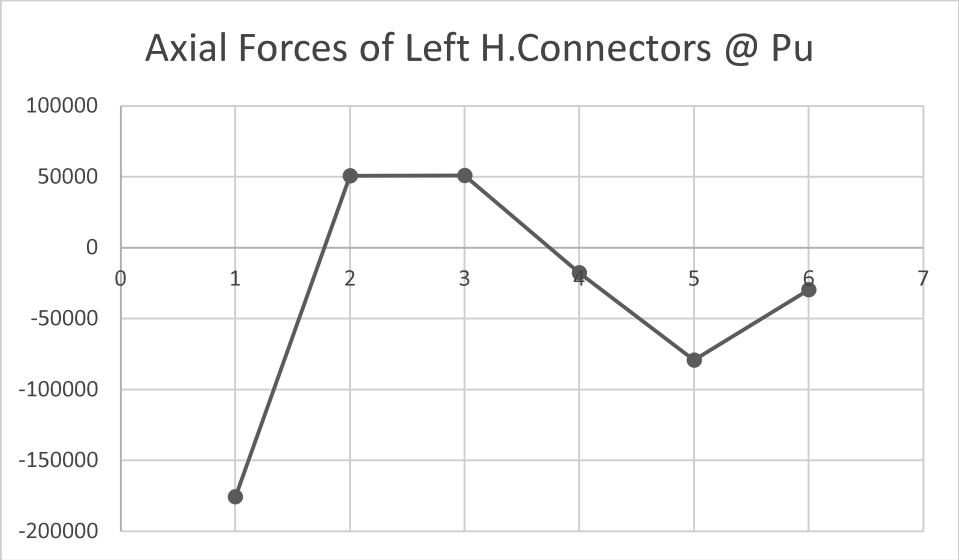
Axial Forces of Left H.Connectors @ Pu
100000
50000
0
-50000
-100000
-150000
-200000
0
1
2
3
4
5
6
7

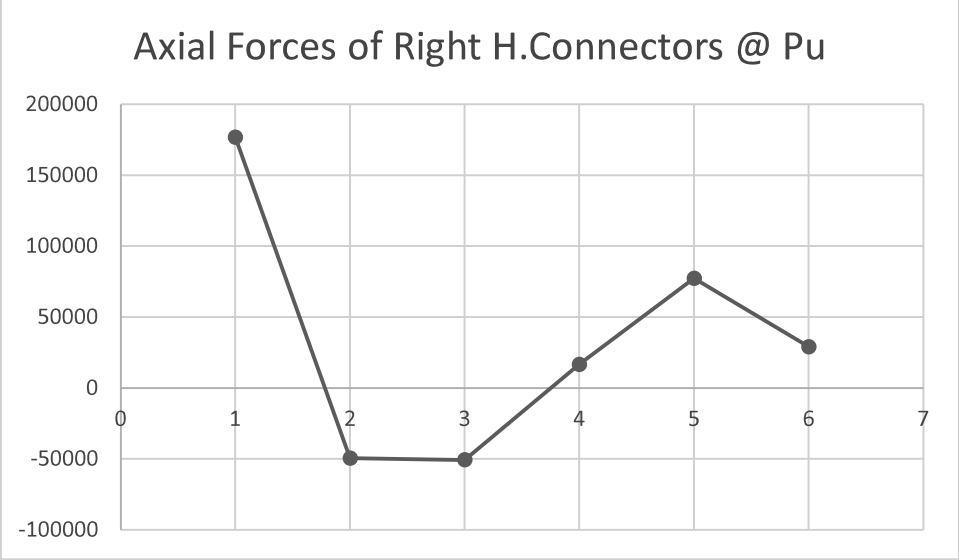
Axial Forces of Right H.Connectors @ Pu
200000
150000
100000
50000
0
-50000
-100000
0
1
2
3
4
5
6
7

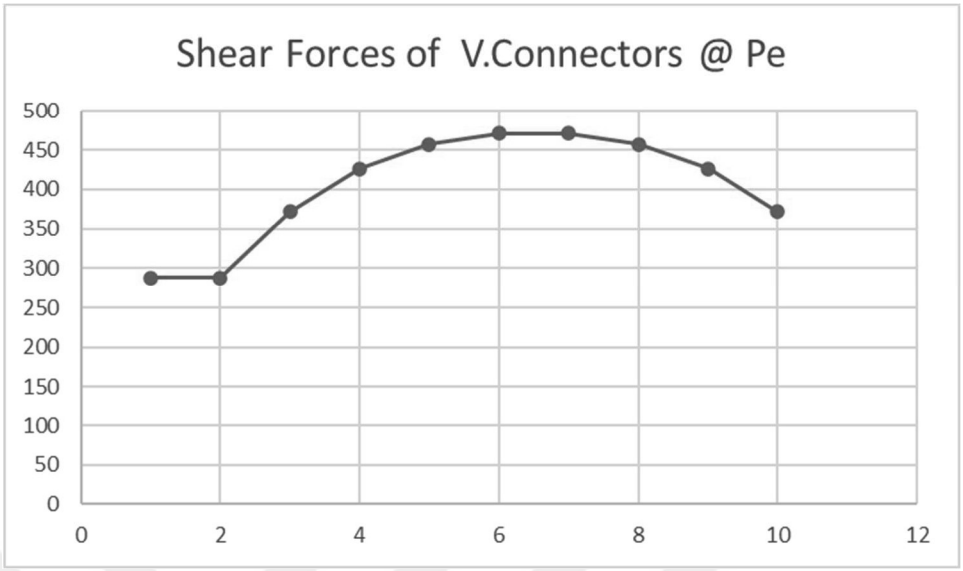
Shear Forces of V.Connectors @ Pe
500
450
400
350
300
250
200
150
100
50
0
0
2
4
6
8
10
12

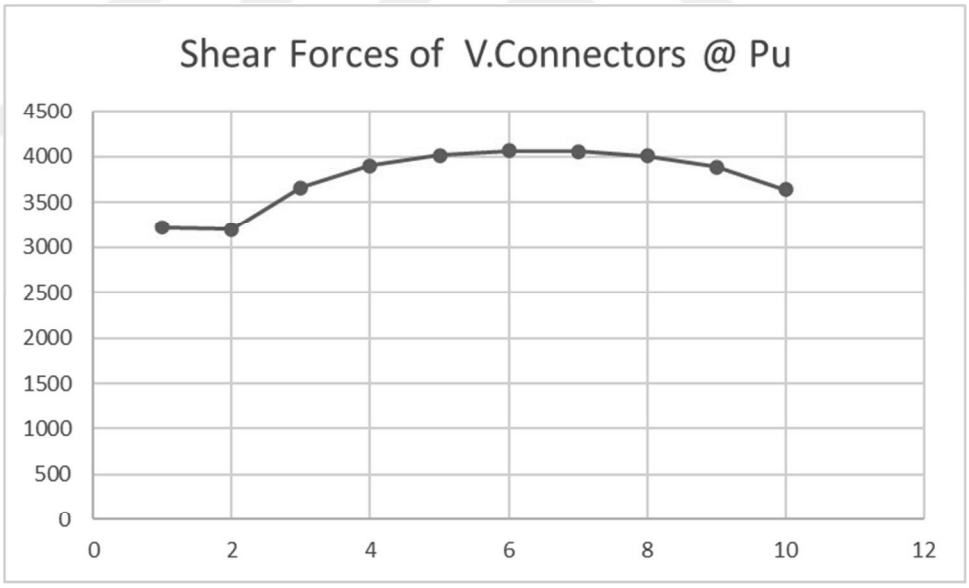
Shear Forces of V.Connectors @ Pu
4500
4000
3500
3000
2500
2000
1500
1000
500
0
0
2
4
6
8
10
12

5.2.1.7.3.3 SM3 Model

Internal Axial forces of the horizontal connectors and the shear forces of the horizontal connectors of the SM3 model are presented below:

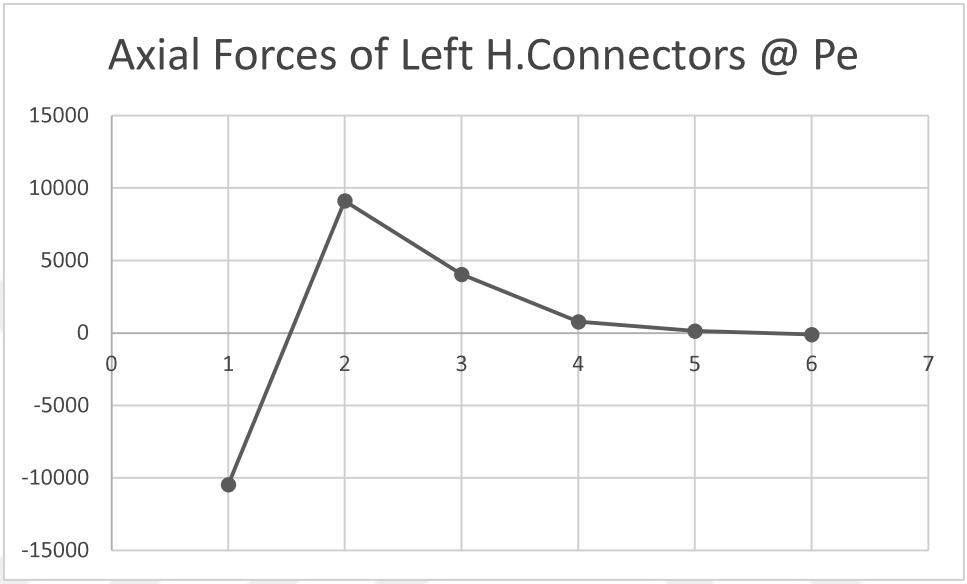

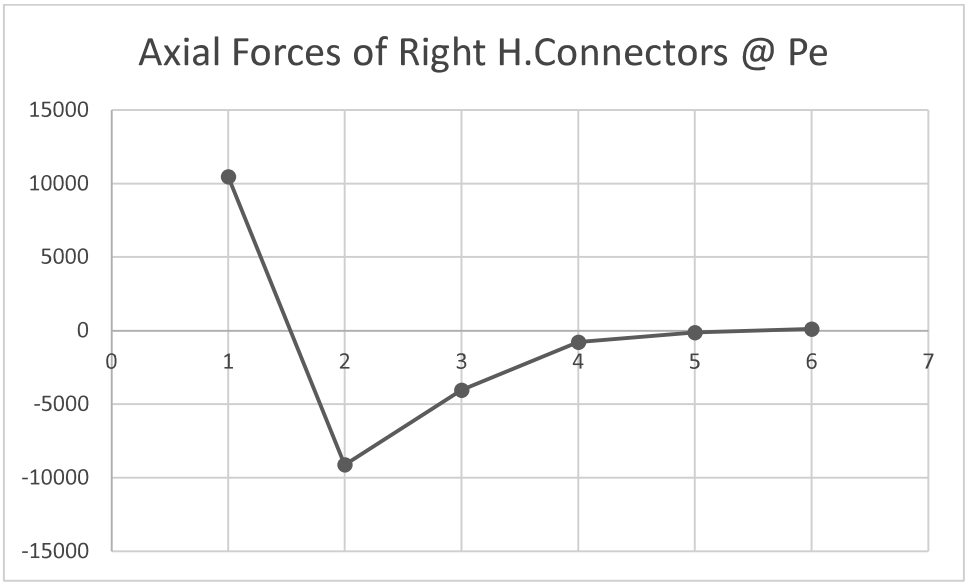

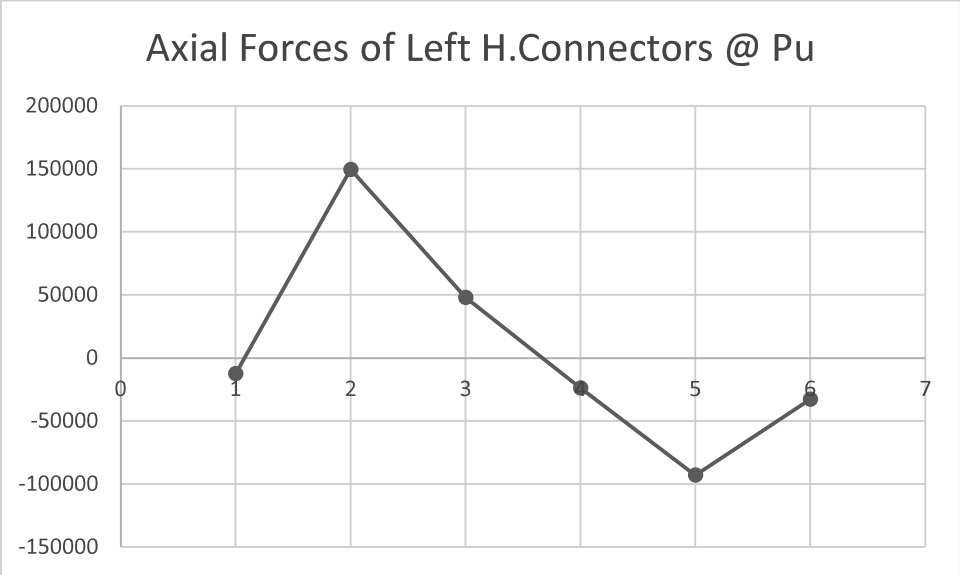
Axial Forces of Left H.Connectors @ Pu
200000
150000
100000
50000
0
-50000
-100000
-150000
0
1
2
3
5
6
7

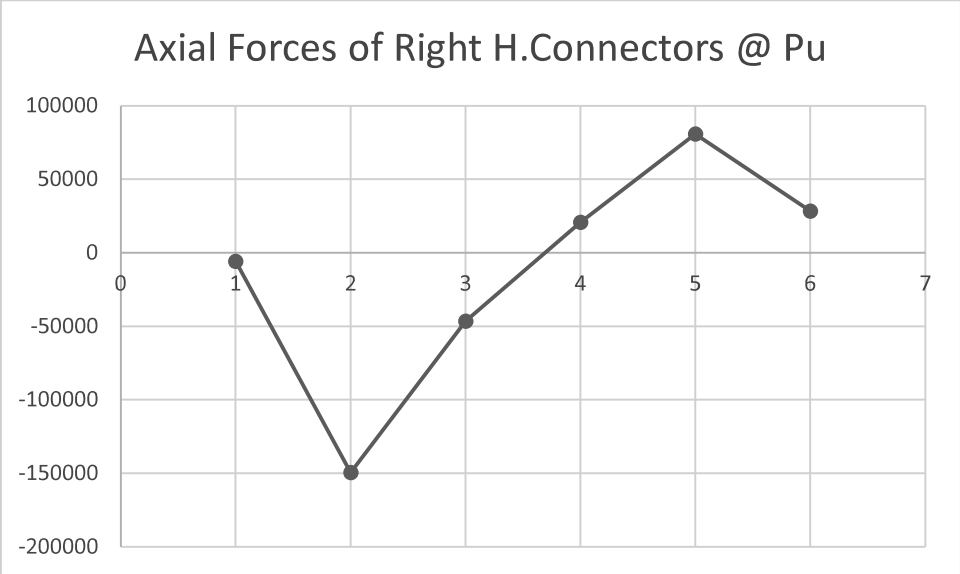
Axial Forces of Right H.Connectors @ Pu
100000
50000
0
-50000
-100000
-150000
-200000
0
1
2
3
4
5
6
7

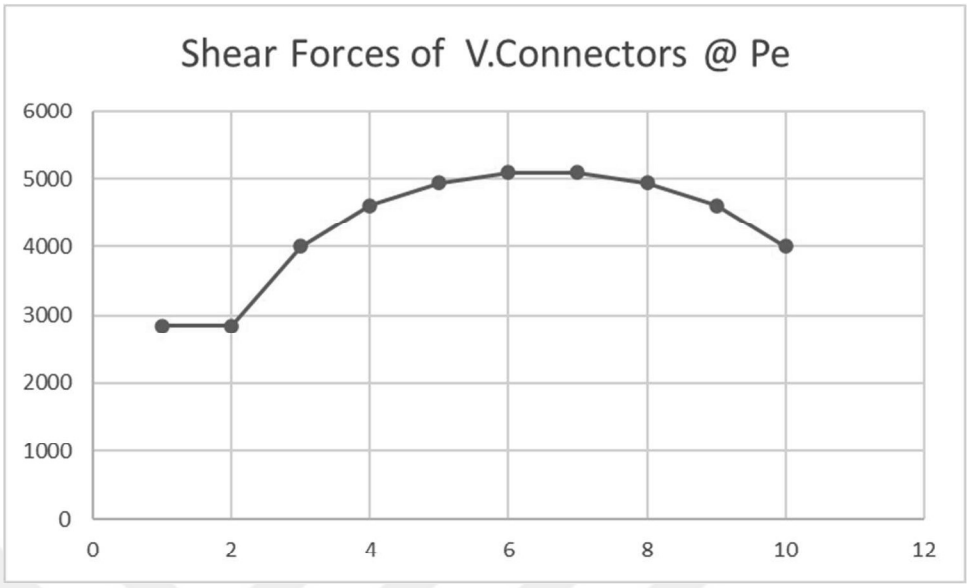
Shear Forces of V.Connectors @ Pe
6000
5000
4000
3000
2000
1000
0
0
2
4
6
8
10
12

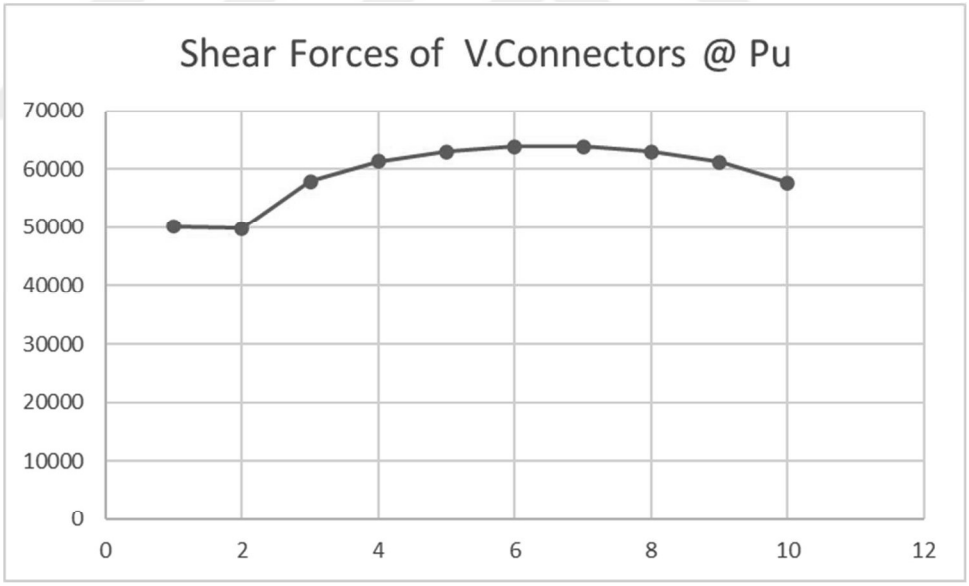
Shear Forces of V.Connectors @ Pu
70000
60000
50000
40000
30000
20000
10000
0
0
2
4
6
8
10
12

5.2.1.7.3.4 SM4 Model

Internal Axial forces of the horizontal connectors and the shear forces of the horizontal connectors of the SM4 model are presented below:

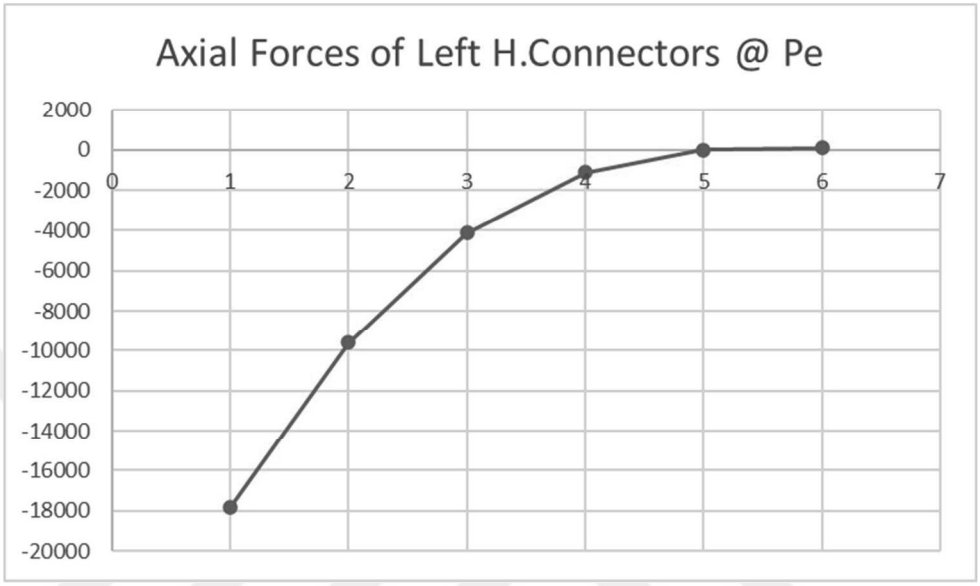

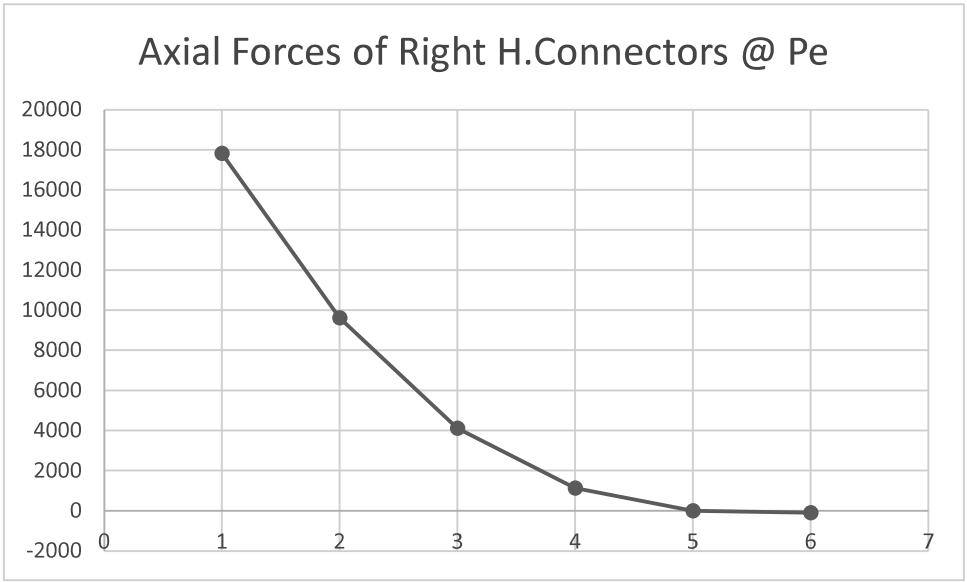

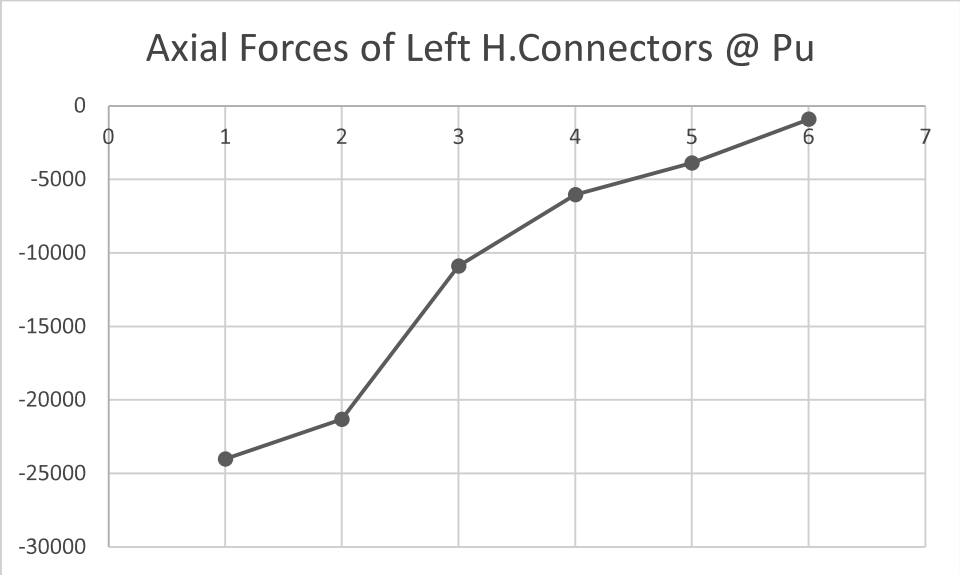
Axial Forces of Left H.Connectors @ Pu
0
-5000
-10000
-15000
-20000
-25000
-30000
0
1
2
3
4
5
6
7

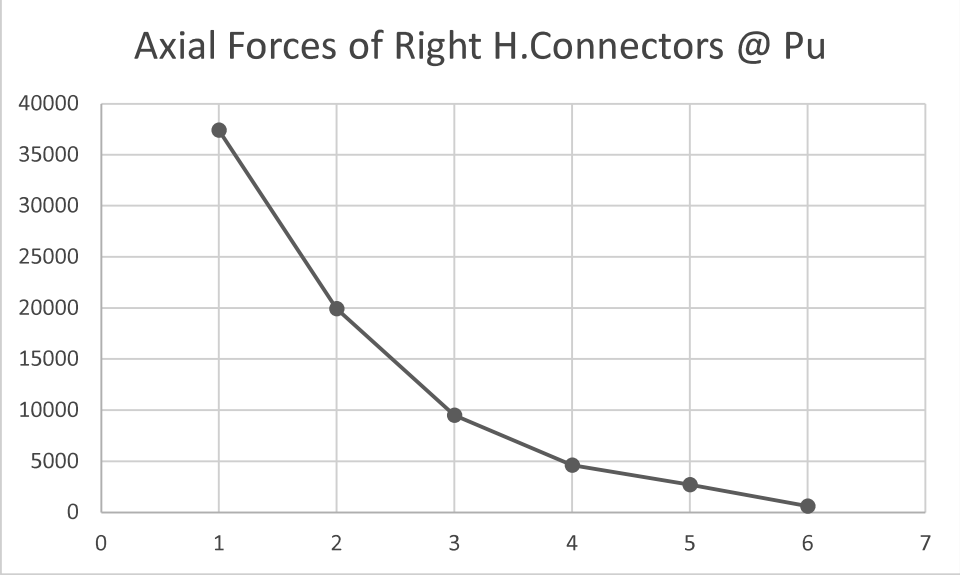
Axial Forces of Right H.Connectors @ Pu
40000
35000
30000
25000
20000
15000
10000
5000
0
0
1
2
3
4
5
6
7

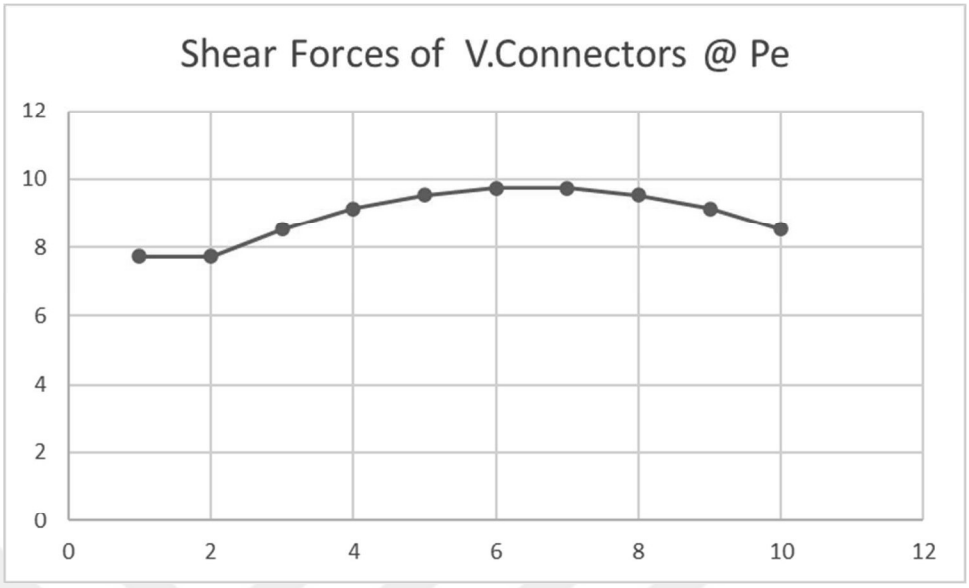
Shear Forces of V.Connectors @ Pe
12
10
8
6
4
2
0
0
2
4
6
8
10
12

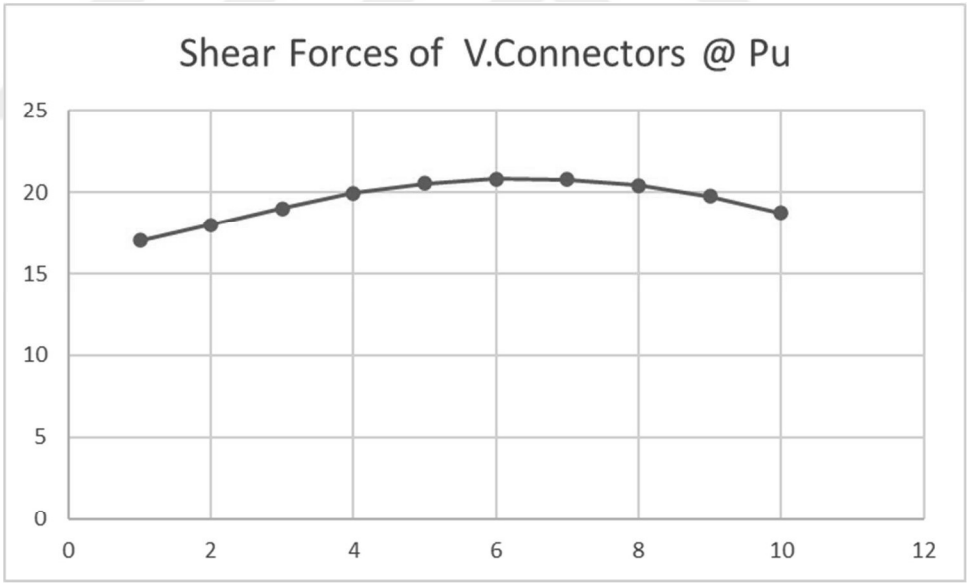
Shear Forces of V.Connectors @ Pu
25
20
15
10
5
0
0
2
4
6
8
10
12

5.2.1.7.3.5 SM5 Model

Internal Axial forces of the horizontal connectors and the shear forces of the horizontal connectors of the SM5 model are presented below:

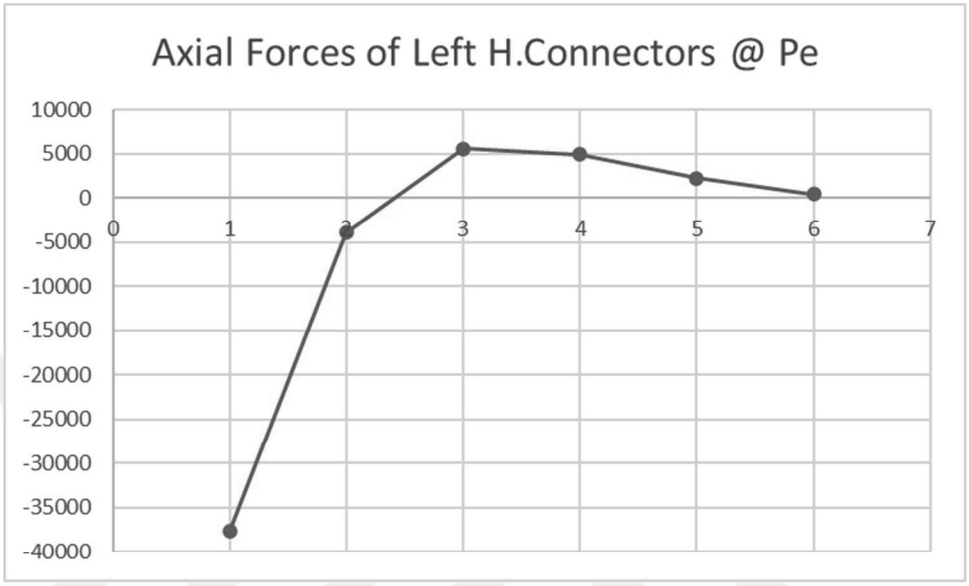

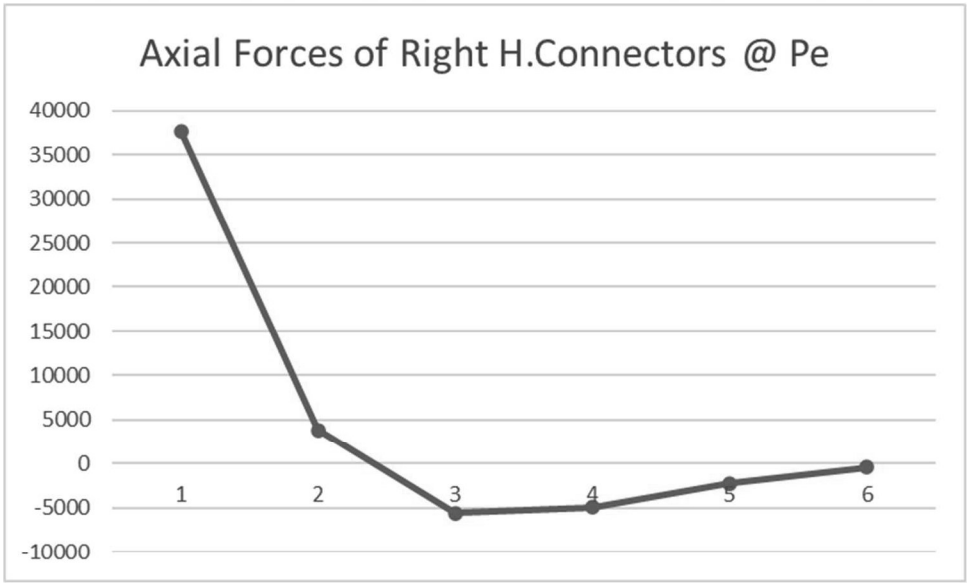

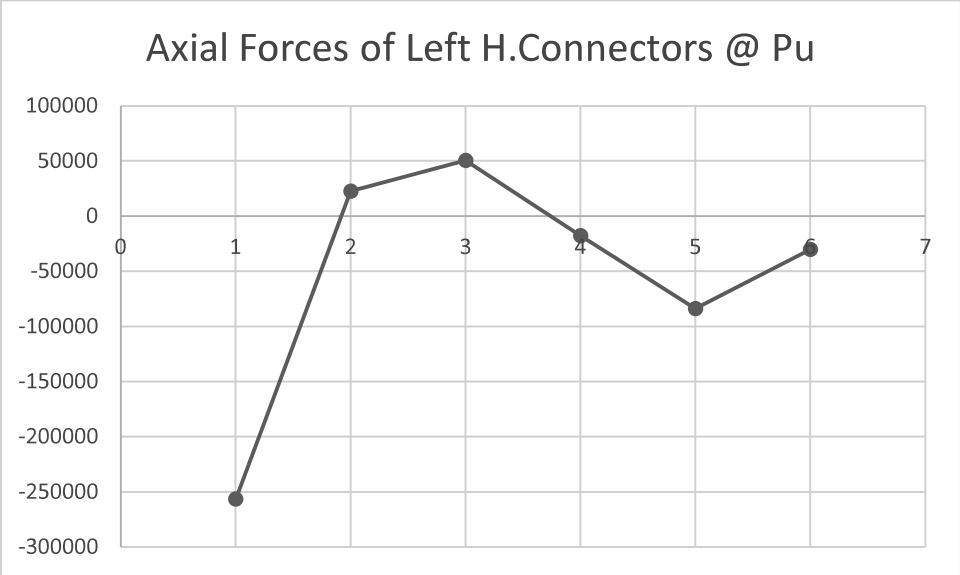
Axial Forces of Left H.Connectors @ Pu
100000
50000
0
-50000
-100000
-150000
-200000
-250000
-300000
0
1
2
3
4
5
6
7

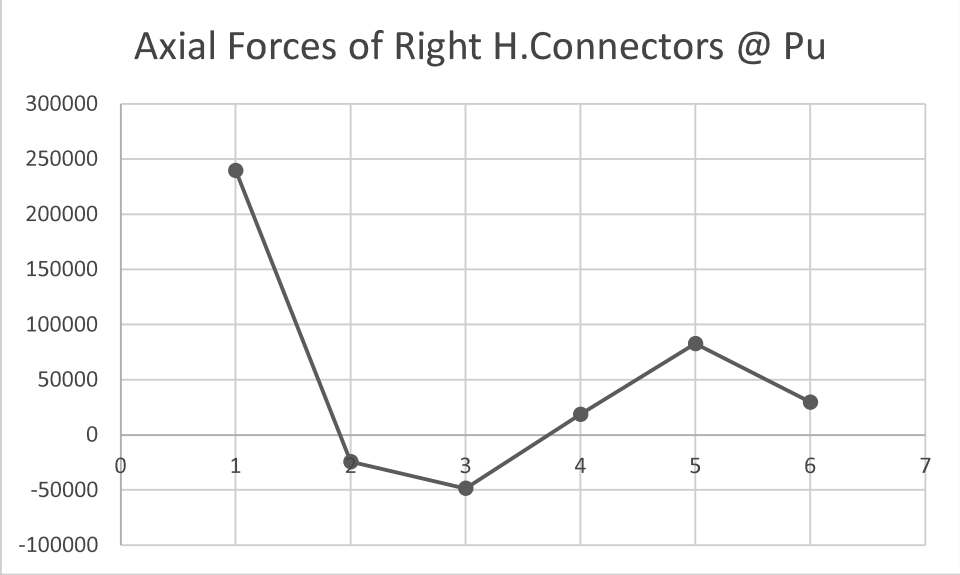
Axial Forces of Right H.Connectors @ Pu
300000
250000
200000
150000
100000
50000
0
-50000
-100000
0
1
2
3
4
5
6
7

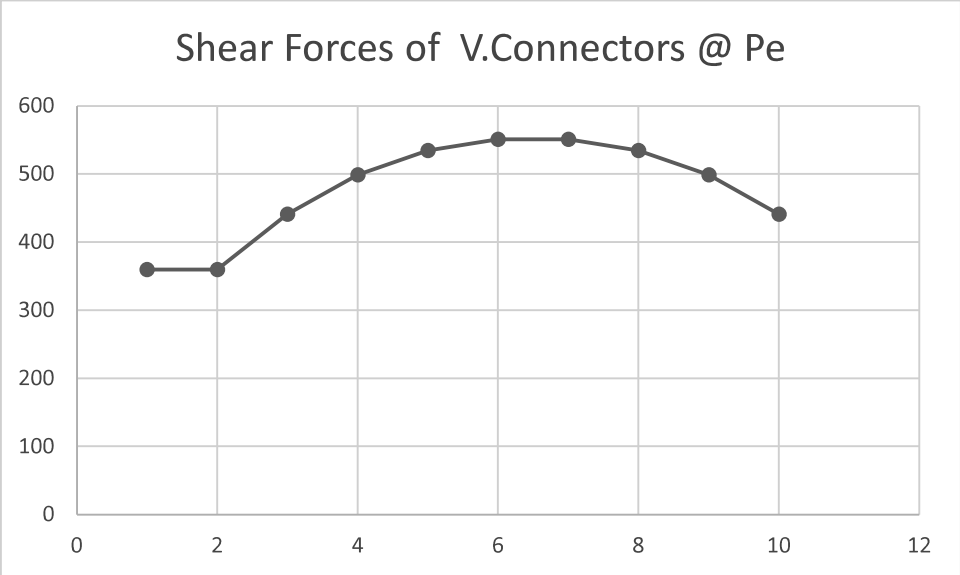

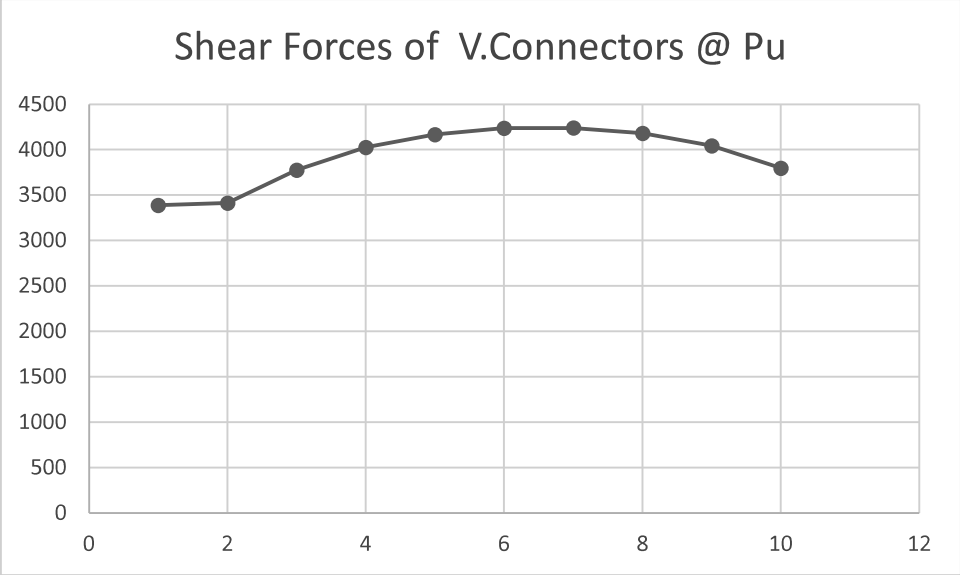

5.2.1.7.3.6 SM6 Model

Internal Axial forces of the horizontal connectors and the shear forces of the horizontal connectors of the SM6 model are presented below:

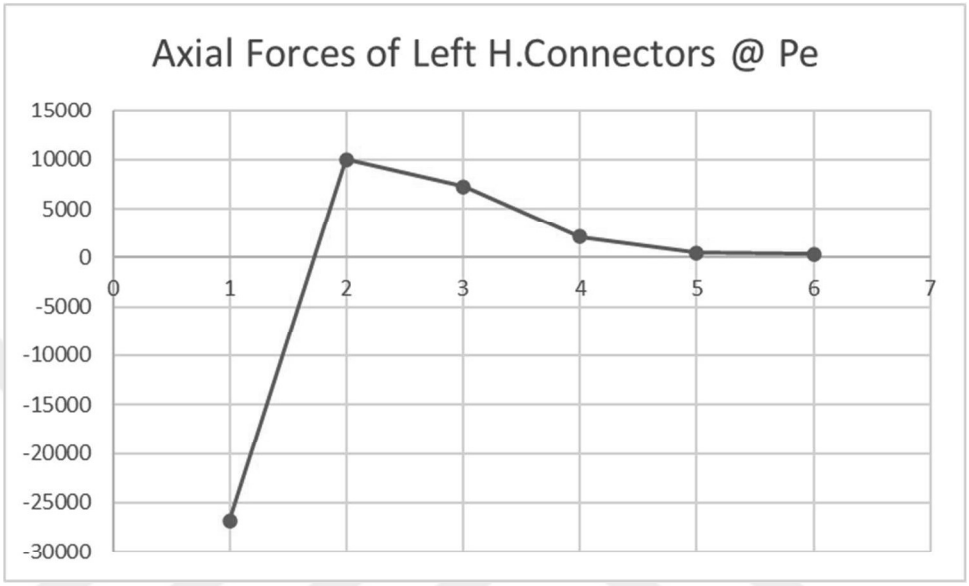

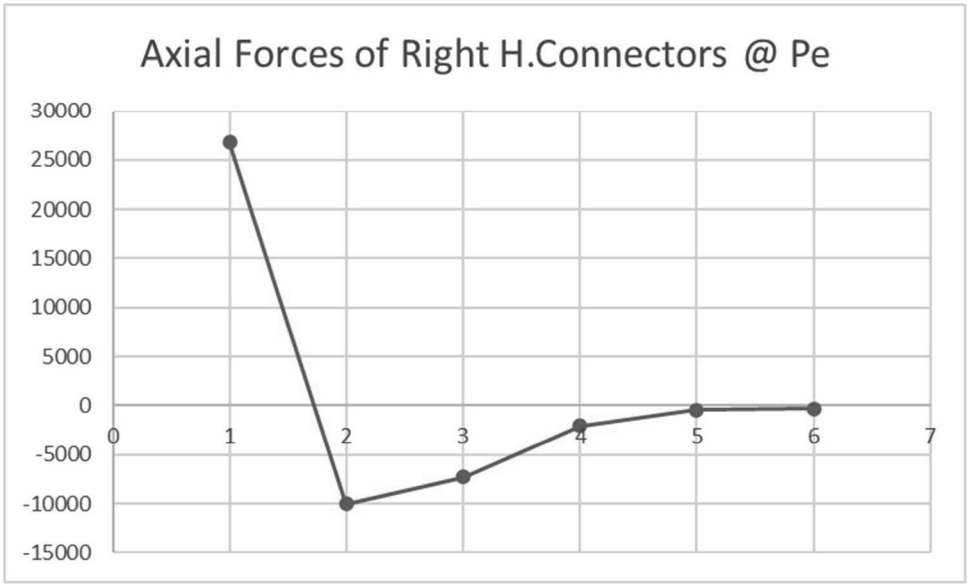

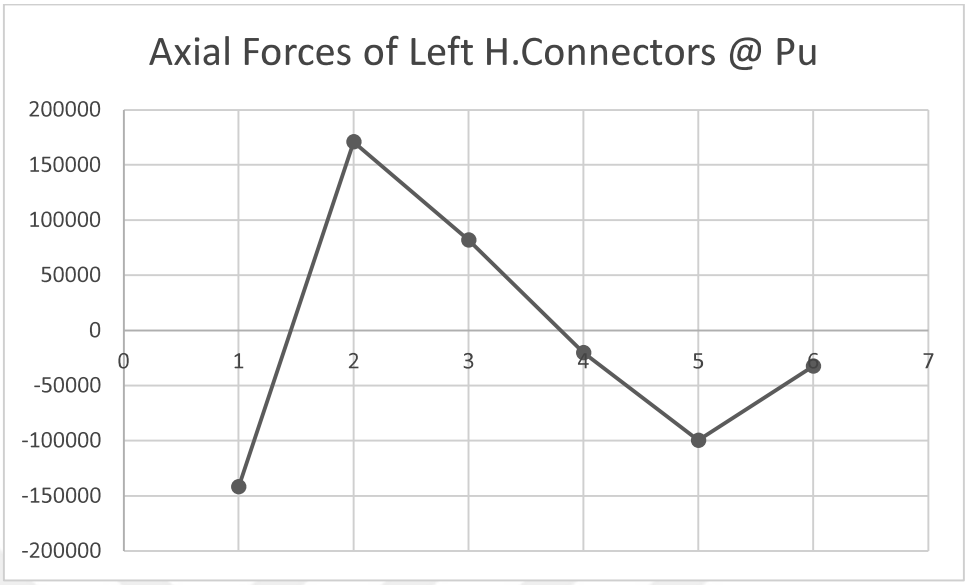
Axial Forces of Left H.Connectors @ Pu
200000
150000
100000
50000
0
-50000
-100000
-150000
-200000
0
1
2
3
4
5
6
7

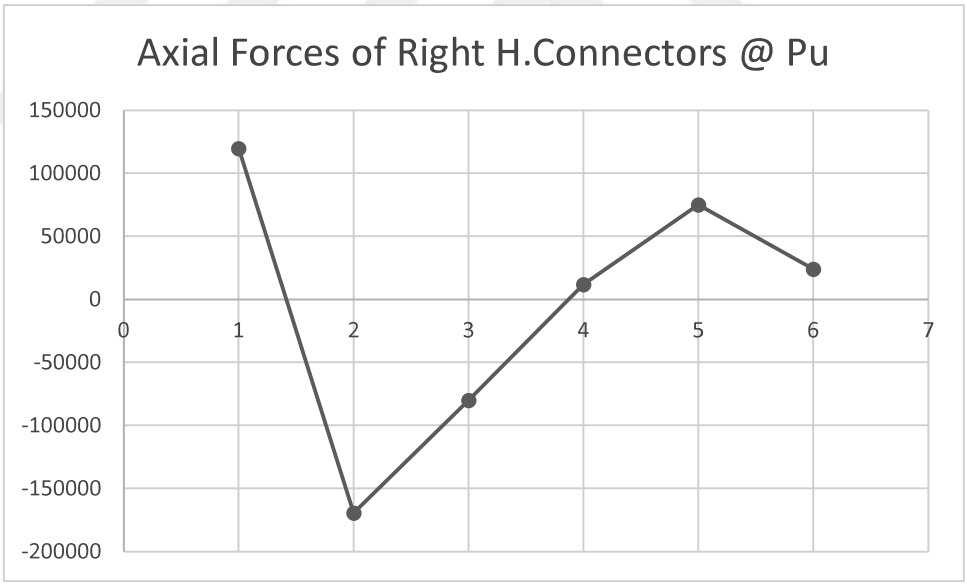
Axial Forces of Right H.Connectors @ Pu
150000
100000
50000
0
-50000
-100000
-150000
-200000
0
1
2
3
4
5
6
7

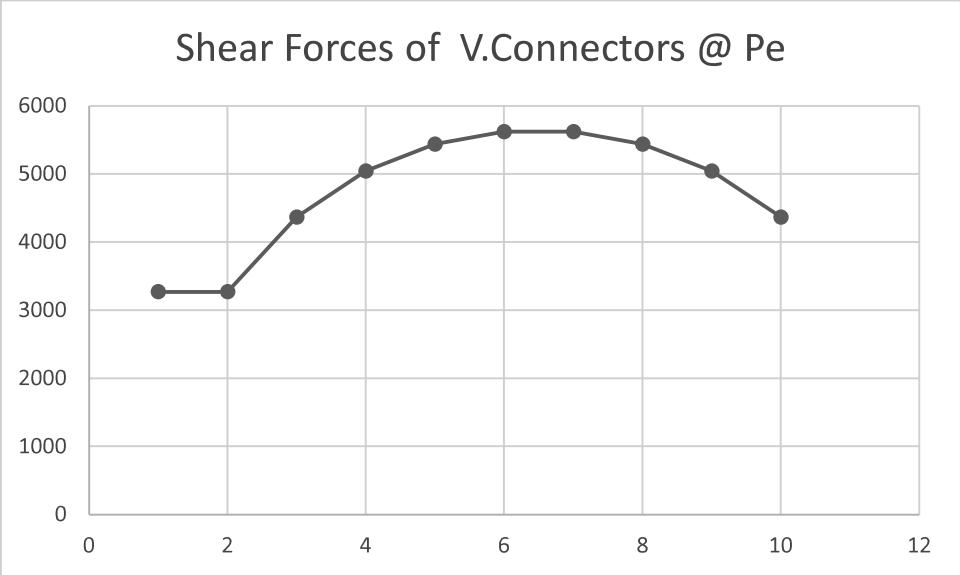

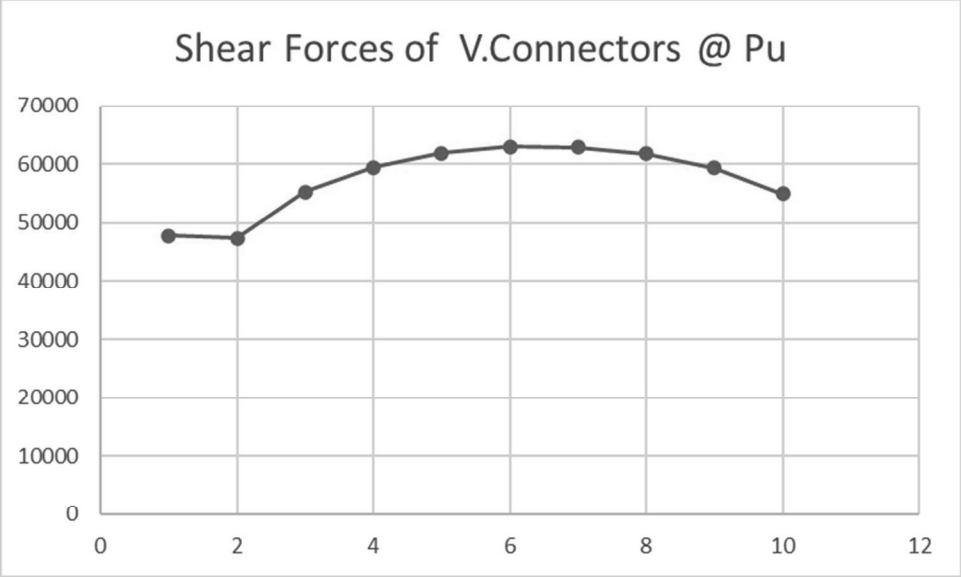

5.2.1.7.3.7 SM7 Model

Internal Axial forces of the horizontal connectors and the shear forces of the horizontal connectors of the SM7 model are presented below:

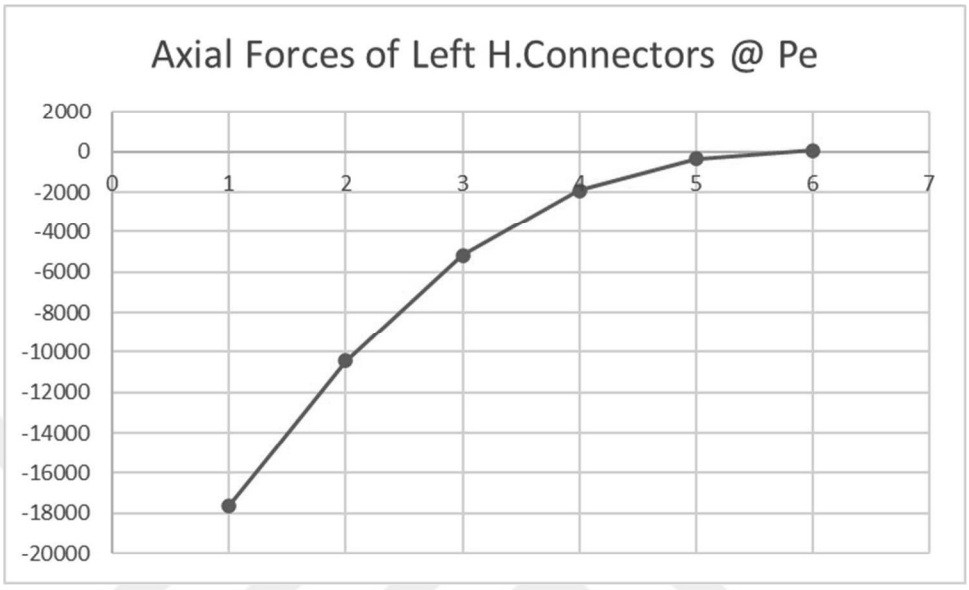

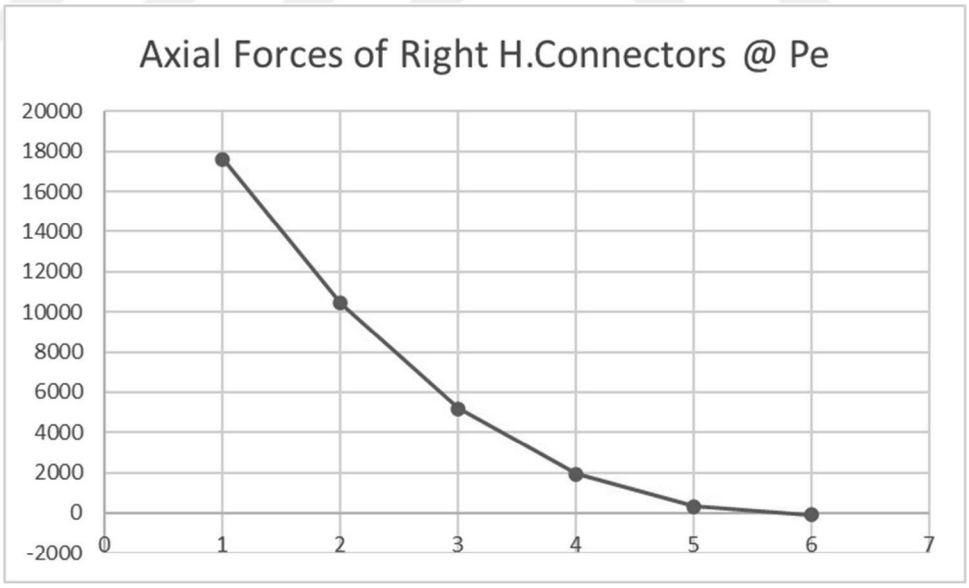

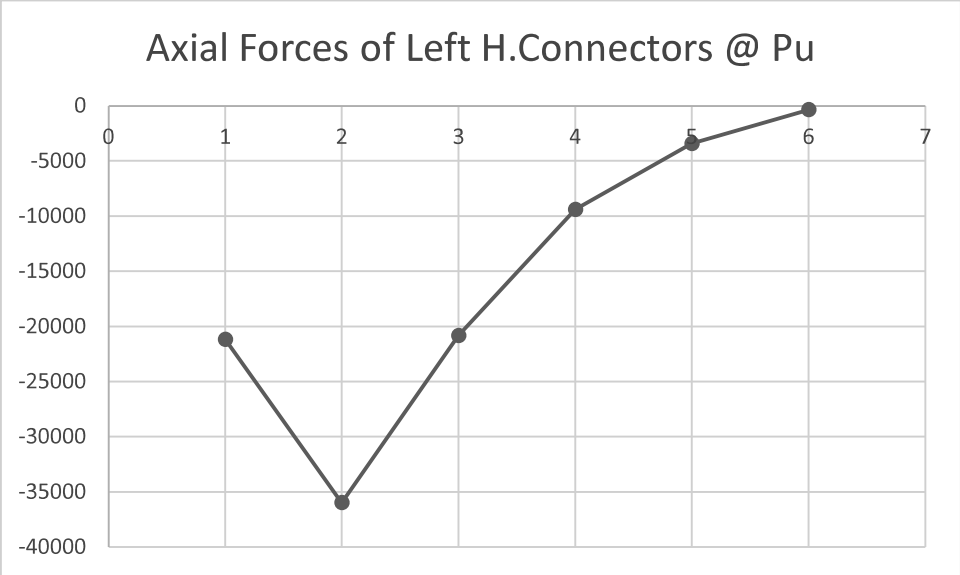
Axial Forces of Left H.Connectors @ Pu
0
-5000
-10000
-15000
-20000
-25000
-30000
-35000
-40000
0
1
2
3
4
5
6
7

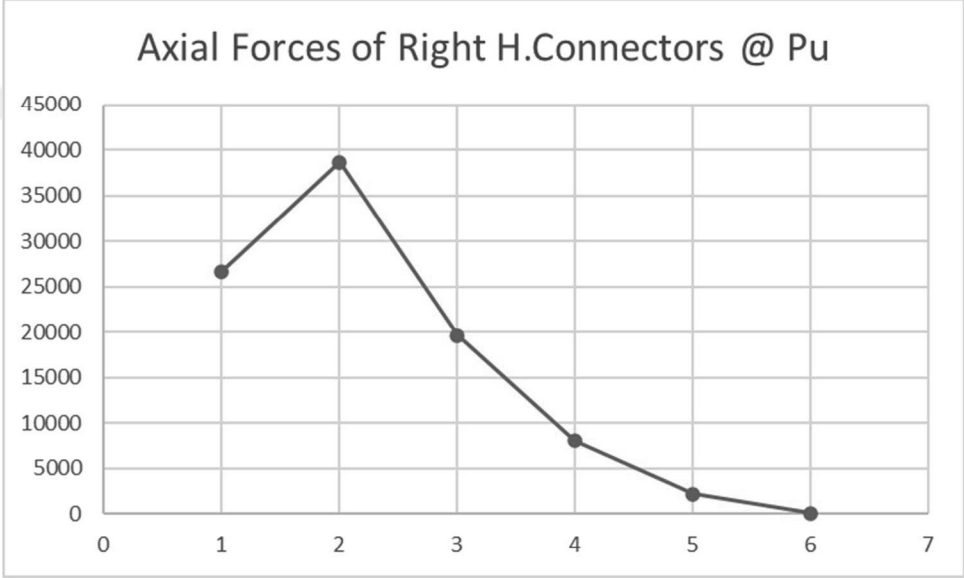
Axial Forces of Right H.Connectors @ Pu
45000
40000
35000
30000
25000
20000
15000
10000
5000
0
0
1
2
3
4
5
6
7

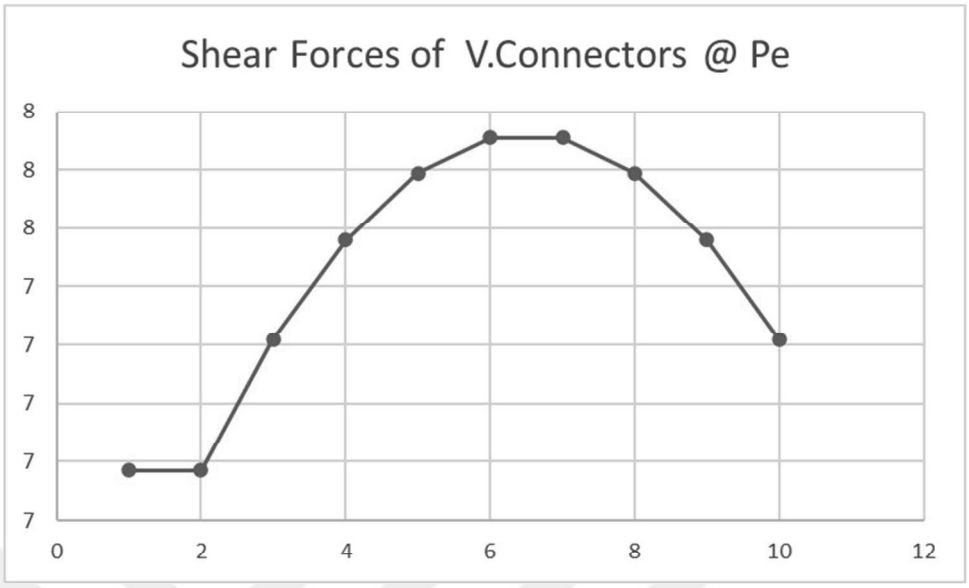
Shear Forces of V.Connectors @ Pe
8
8
8
7
7
7
7
0
2
4
6
8
10
12

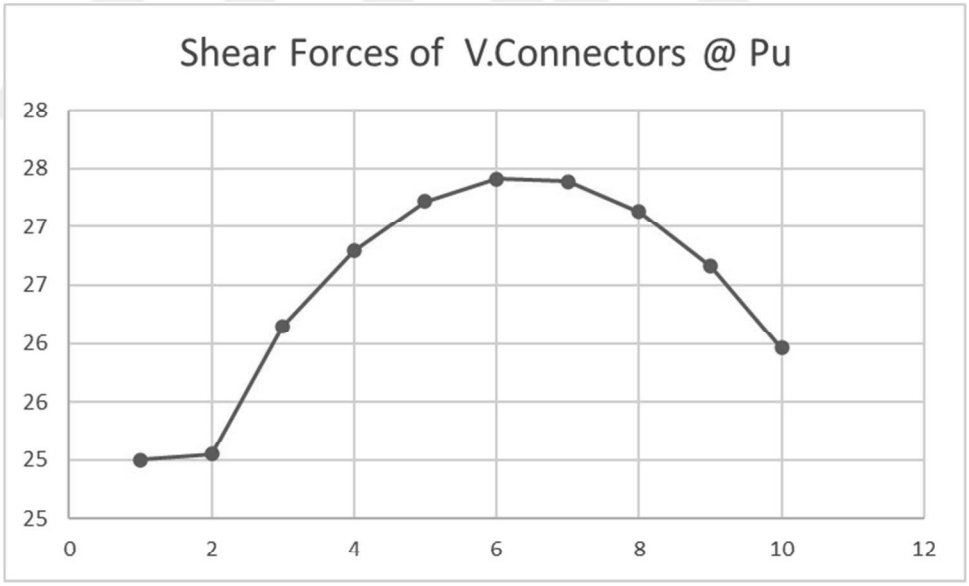
Shear Forces of V.Connectors @ Pu
28
28
27
27
26
26
25
25
0
2
4
6
8
10
12

5.2.1.7.3.8 SM8 Model

Internal Axial forces of the horizontal connectors and the shear forces of the horizontal connectors of the SM8 model are presented below:

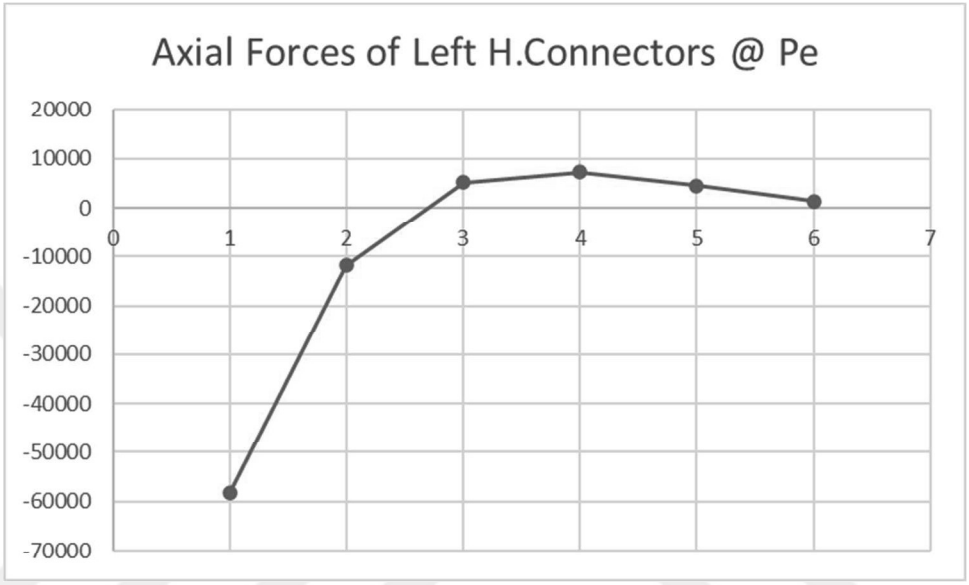

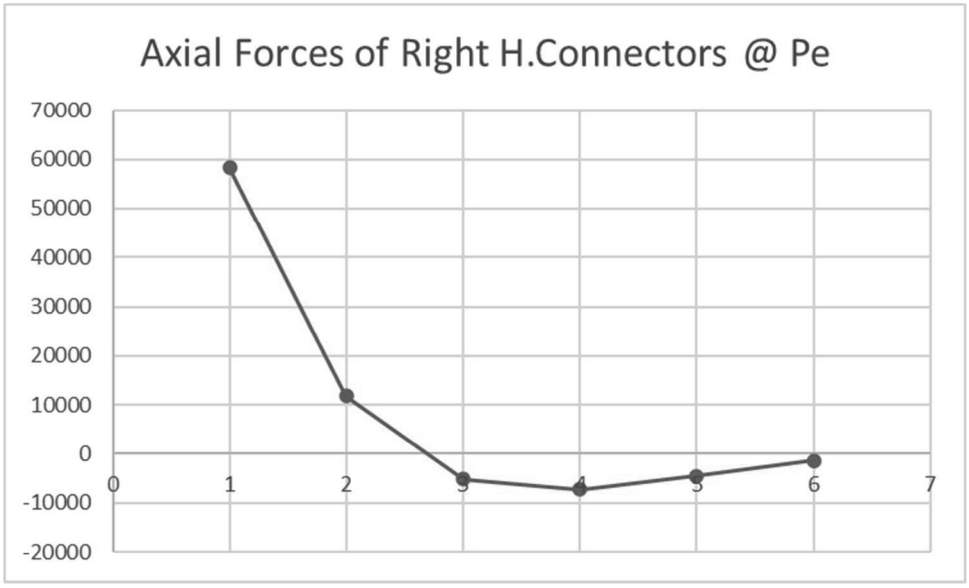

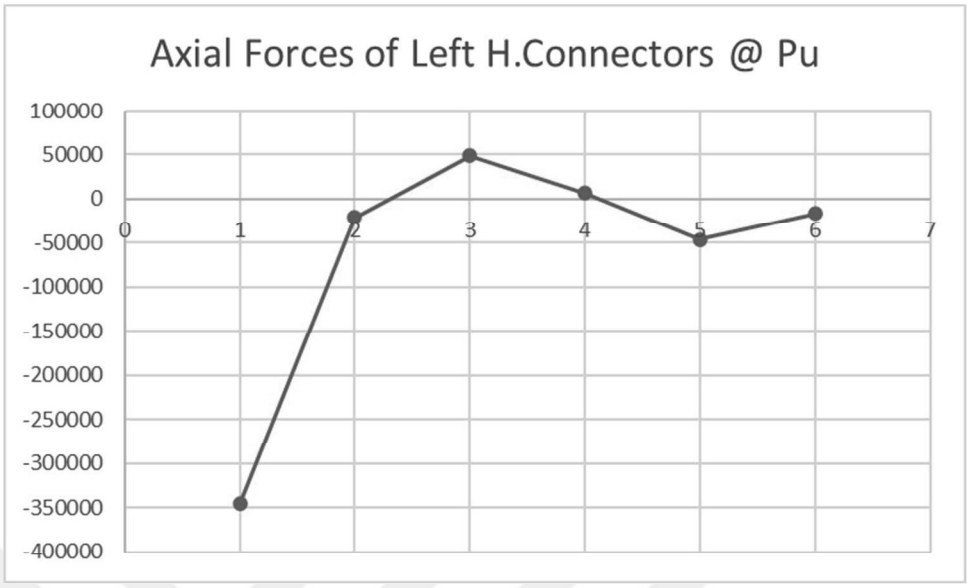
Axial Forces of Left H.Connectors @ Pu
100000
50000
0
-50000
-100000
-150000
-200000
-250000
-300000
-350000
-400000
0
1
2
3
4
5
6
7

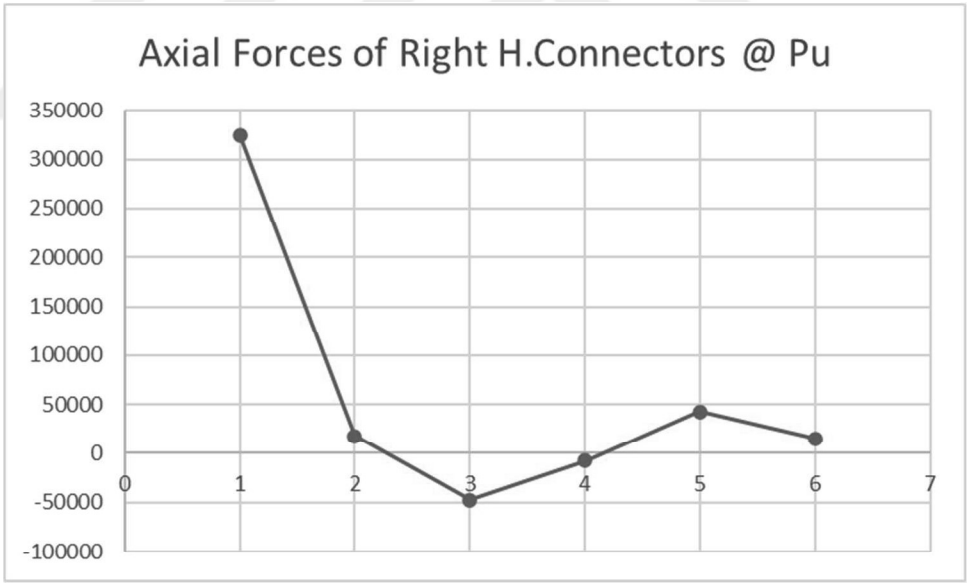
Axial Forces of Right H.Connectors @ Pu
350000
300000
250000
200000
150000
100000
50000
0
-50000
-100000
0
1
2
3
4
5
6
7

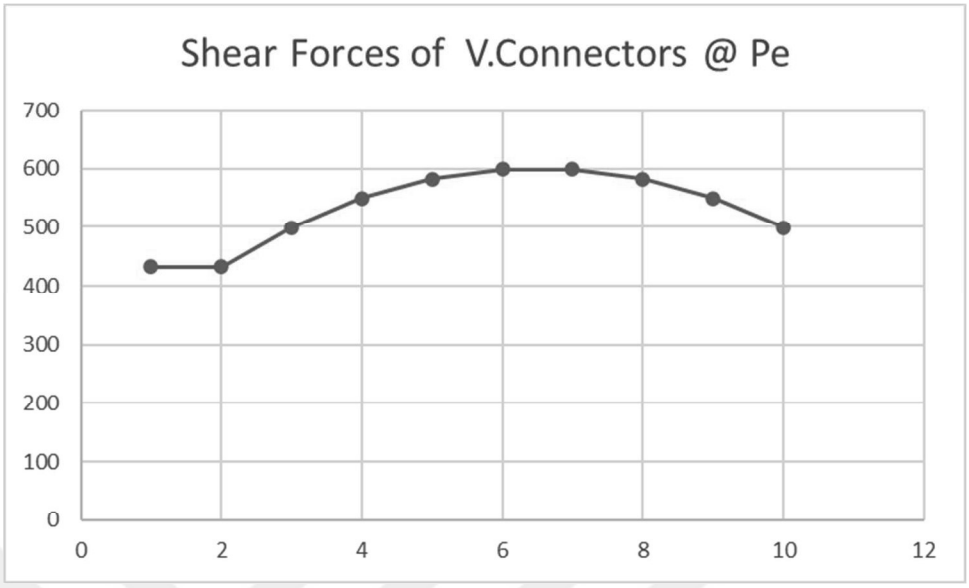
Shear Forces of V.Connectors @ Pe
700
600
500
400
300
200
100
0
0
2
4
6
8
10
12

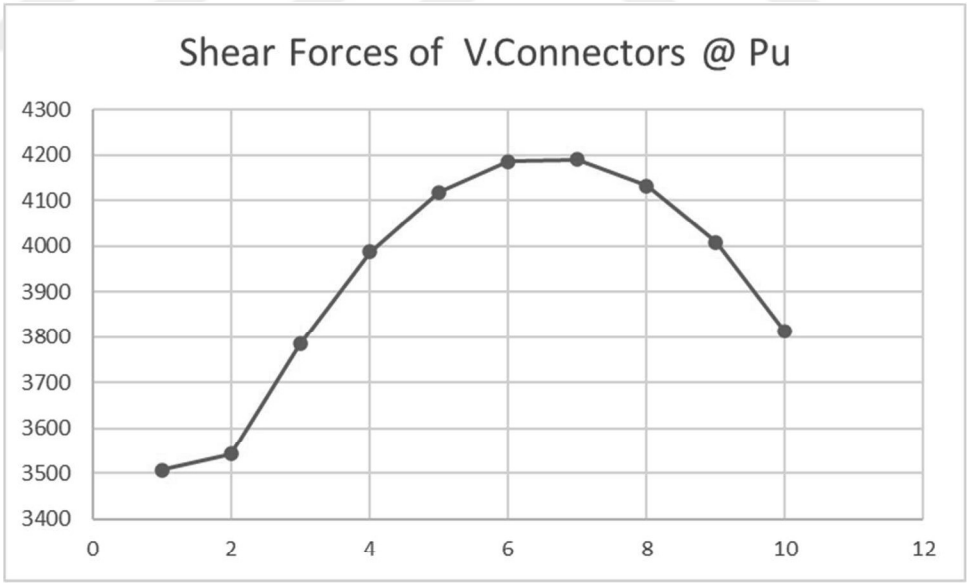
Shear Forces of V.Connectors @ Pu
4300
4200
4100
4000
3900
3800
3700
3600
3500
3400
0
2
4
6
8
10
12

5.2.1.7.3.9 SM9 Model

Internal Axial forces of the horizontal connectors and the shear forces of the horizontal connectors of the SM9 model are presented below:

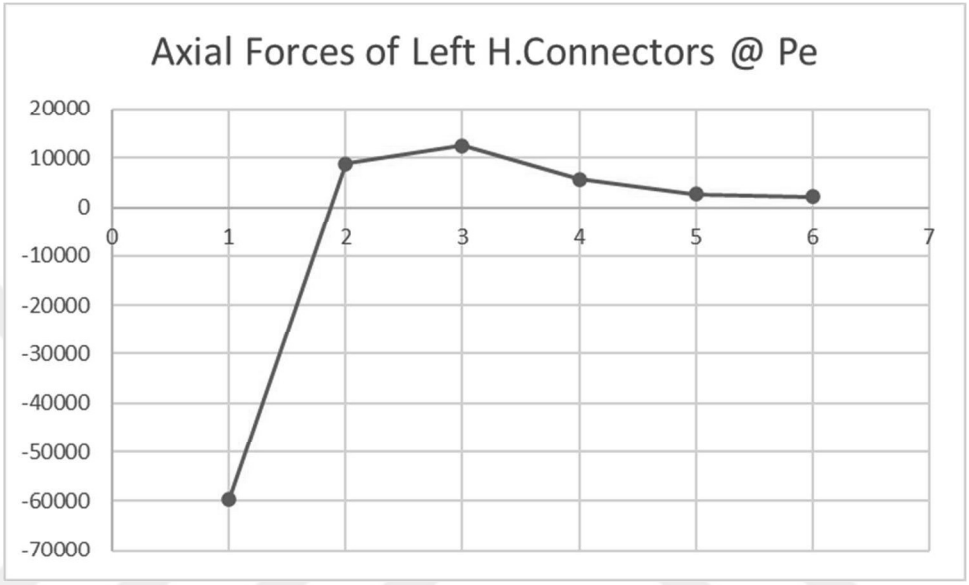

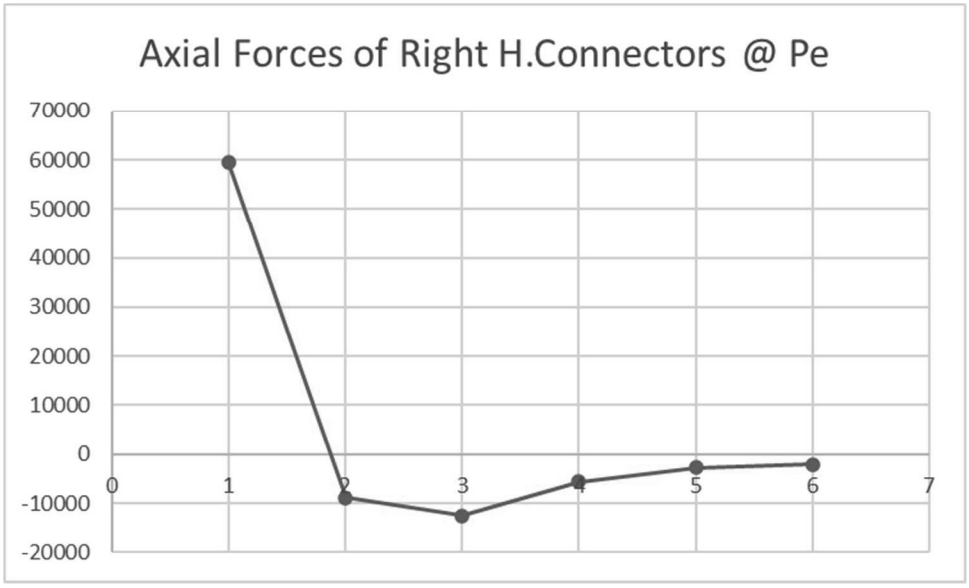

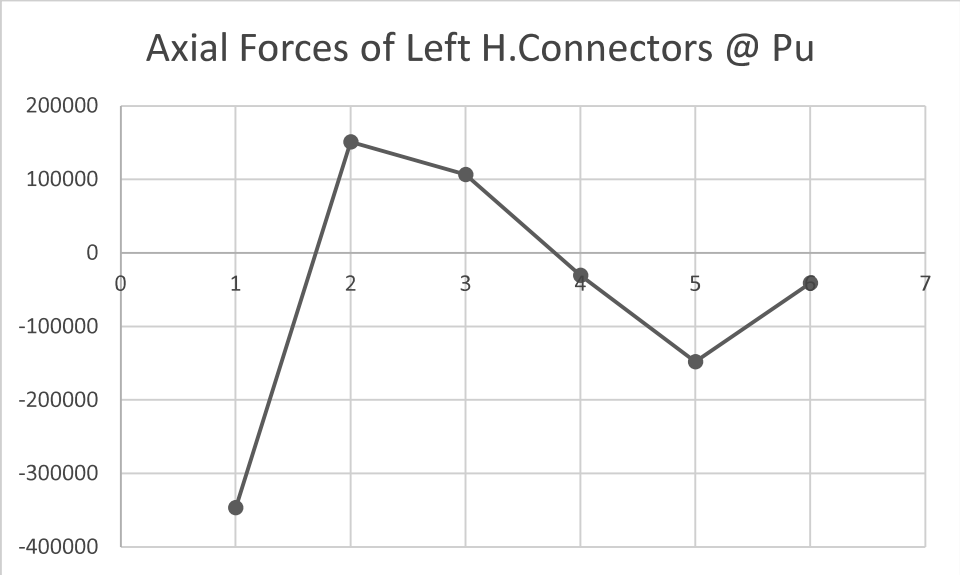
Axial Forces of Left H.Connectors @ Pu
200000
100000
0
-100000
-200000
-300000
-400000
0
1
2
3
4
5
7

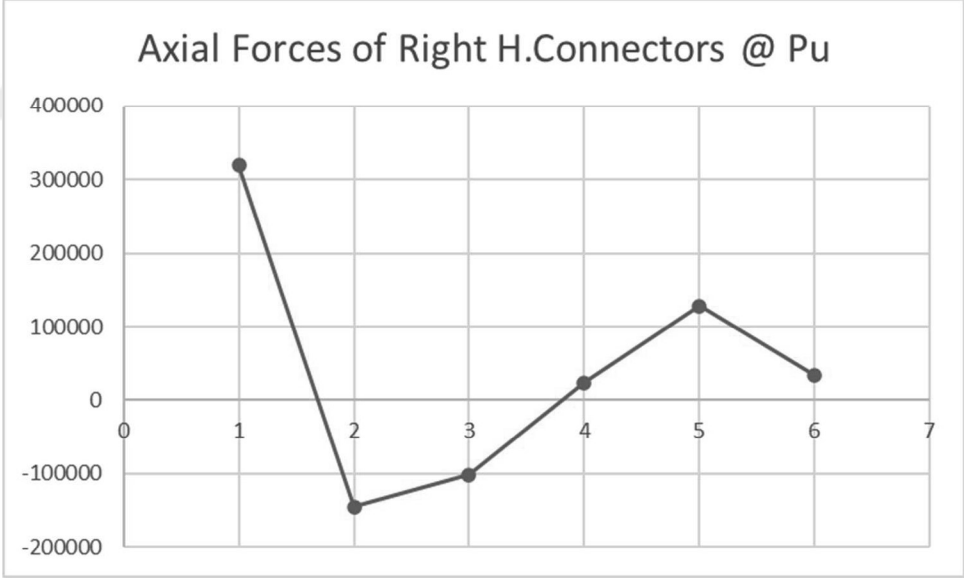
Axial Forces of Right H.Connectors @ Pu
400000
300000
200000
100000
0
-100000
-200000
0
1
2
3
4
5
6
7

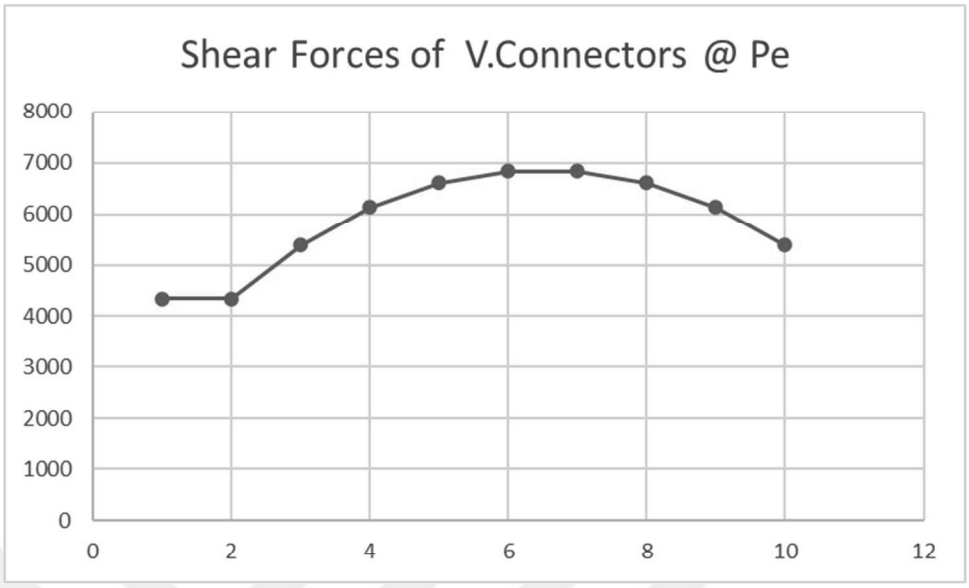
Shear Forces of V.Connectors @ Pe
8000
7000
6000
5000
4000
3000
2000
1000
0
0
2
4
6
8
10
12

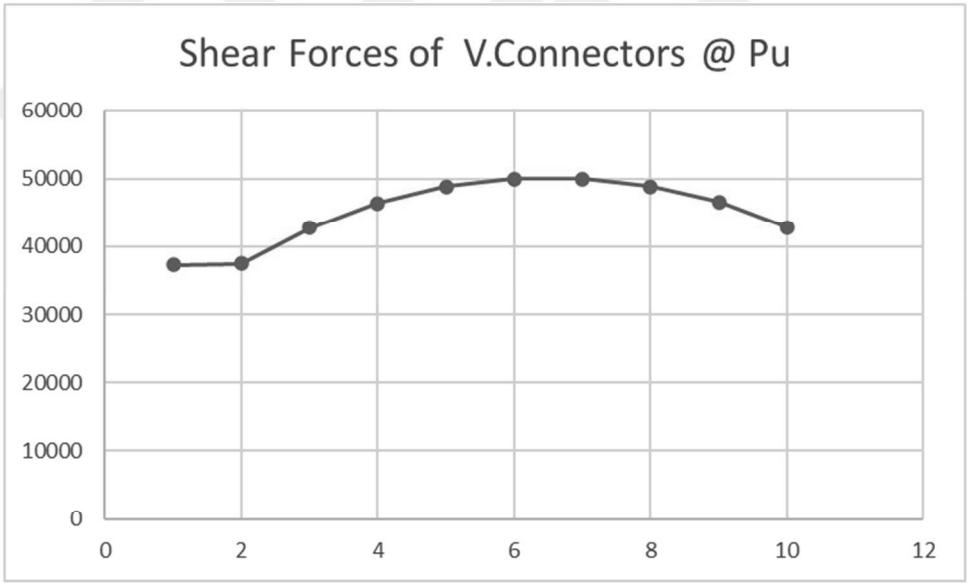
Shear Forces of V.Connectors @ Pu
60000
50000
40000
30000
20000
10000
0
0
2
4
6
8
10
12

5.2.2 Nonlinear Time History Analysis Results

In this section Nonlinear Time history analysis results of the models under selected ground motions are presented to study the energy consumption of the different element and compare the efficiency of each model.

5.3 Analysis Results' Discussion

In this section the results which were presented in previous section are compared and discussed in order to get conclusions and answers about the study questions. In the first part the results of the N.P.A are discussed and in the second part the results of the N.T.H.A are discussed.

5.3.1 Nonlinear Pushover Analysis Results' Discussion

In this section the results of N.P.A are discussed in order to come up with a conclusion about the distribution of the connectors and the retrofitting systems efficiency as well.

5.3.1.1 Efficiency of the Vertical Connectors

OM group models which have only vertical connectors are studied in this part. RC frame and connectors are kept constant and only differences are in the stiffness of the inner steel frame. The maximum load caring capacity of the both frames when they are connected with very rigid connections is 406 KN for M1 and M2 models and is 604 KN for M1 and M3 models and is 920 KN for M1 and M4 models. The results of each model will be compared to that number in order to get the ratio of the used capacities of both frames.

In the OM1 Model we can see that the Ultimate lateral load capacity is 261 KN which shows an increase of 141 percent in compare with the RC frame and is 64.28 percent of the total capacity of the frames.

In the OM2 Model we can see that the Ultimate lateral load capacity is 281 KN which shows an increase of 160 percent in compare with the RC frame and is 46.52 percent of the total capacity of the frames.

In the OM3 Model we can see that the Ultimate lateral load capacity is 295 KN which shows an increase of 173 percent in compare with the RC frame and is 32.21 percent of the total capacity of the frames.

It can be seen here that the efficiency of vertical connectors are decreasing with increasing the rigidity of the steel inner frame.

5.3.1.2 Efficiency of the Horizontal Connectors

HM group models which have only horizontal connectors are studied in this part. RC frame and connectors are kept constant and only differences are in the stiffness of the inner steel frame. The maximum load caring capacity of the both frames when they are connected with very rigid connections is 406 KN for M1 and M2 models and is 604 KN for M1 and M3 models and is 920 KN for M1 and M4 models. The results of each model will be compared to that number in order to get the ratio of the used capacities of both frames.

In the HM1 Model we can see that the Ultimate lateral load capacity is 321 KN which shows an increase of 197 percent in compare with the RC frame and is 79.06 percent of the total capacity of the frames.

In the HM2 Model we can see that the Ultimate lateral load capacity is 465 KN which shows an increase of 330 percent in compare with the RC frame and is 76.98 percent of the total capacity of the frames.

In the HM3 Model we can see that the Ultimate lateral load capacity is 604 KN which shows an increase of 460 percent in compare with the RC frame and is 65.65 percent of the total capacity of the frames.

It can be seen here that the efficiency of vertical connectors is decreasing with increasing the rigidity of the steel inner frame but in compare with the OM models, it shows that the using horizontal connectors is more efficient in transferring lateral loads from outer frame to inner frame and increasing the ultimate lateral load capacity of the models.

5.3.1.3 Efficiency of the Vertical and Horizontal Connectors simultaneously

SM group models and result can be discussed in two major parts, first part would be the comparison between models with constant inner and outer frames and changing in the diameters of the connectors and the second part would be the constant outer frame and connectors and changes in inner frame rigidity.

For the first part SM4, SM5 and SM6 models are compared as shown in bellow. The outer frame is M1 and the inner frame is M3 and the changes are in the diameter of the connectors.

In the SM4 Model we can see that the Ultimate lateral load capacity is 186 KN which shows an increase of 197 percent in compare with the RC frame and is 30.79 percent of the total capacity of the frames.

In the SM5 Model we can see that the Ultimate lateral load capacity is 489 KN which shows an increase of 330 percent in compare with the RC frame and is 80.96 percent of the total capacity of the frames.

In the SM6 Model we can see that the Ultimate lateral load capacity is 705 KN which shows an increase of 460 percent in compare with the RC frame and is 116.72 percent of the total capacity of the frames.

It can be seen here that the differences between results of three models are considerable and in these types of connections increasing the diameter of connectors from 10mm to 30mm and to 60mm, increases the ultimate lateral load capacity by 162.90 and 279.12 percent respectively and shows that the diameter of the horizontal connectors has significant effect on the general behavior of the models. Moreover, when we use very rigid connectors in these combinations, the connectors flexural rigidities became very effective and makes to reach higher loads than expected.

For the second part SM2, SM5 and SM8 models are compared as shown in bellow. The outer frame is M1 and the diameter of the connectors are kept constant and the inner frame are M2, M3 and M4.

In the SM2 Model we can see that the Ultimate lateral load capacity is 342 KN which shows an increase of 216.17 percent in compare with the RC frame and is 84.23 percent of the total capacity of the frames.

In the SM5 Model we can see that the Ultimate lateral load capacity is 489 KN which shows an increase of 352.48 percent in compare with the RC frame and is 80.96 percent of the total capacity of the frames.

In the SM8 Model we can see that the Ultimate lateral load capacity is 637 KN which shows an increase of 489.81 percent in compare with the RC frame and is 69.23 percent of the total capacity of the frames.

In this part of study, it is needed to calculate the amount of the forces which are transferred to inner frames by vertical and horizontal connectors. The table below shows that to what extend the vertical connectors transferring the load and to what extend horizontal connectors are transferring the lateral load.

Model	Pu	Ratio of Verticals (%)	Ratio of Horizontals (%)
SM1	172941	0.16	99.84
SM2	342369	8.59	91.41
SM3	589582	84.58	15.42
SM4	186542	0.14	99.86
SM5	489650	6.02	93.98
SM6	704969	90.52	9.48
SM7	207017	0.14	99.86
SM8	637742	5.18	94.82
SM9	884139	44.32	55.68

Table-

From the table it is seen that in the models with connectors with normal diameters, the most of the lateral loads are transferred to inner frame by the horizontal connectors, but in the models with very strong connectors, the vertical connectors are having more importance. But the diameters of the connectors bigger than 30 mm may not be so practical and those connectors are modeled for the study purpose only.

In order to understand the effect of connectors' distribution, after getting results from the previous part, two new models are defined and analyzed which their result are presented in table 235.

Here the transferred load ratio for these two models is presented in table below:

Model	Pu	Ratio of Verticals (%)	Ratio of Horizontals (%)
NM1	519905	11.74	88.26
NM2	484612	2.32	97.68

5.3.2 Proposing a Simplified and Generalized Procedure

In order to reach a simplified model and generalize the findings and propose a design procedure, we propose a procedure.

5.3.2.1 Unknowns of the problem and assumptions for simplified analysis

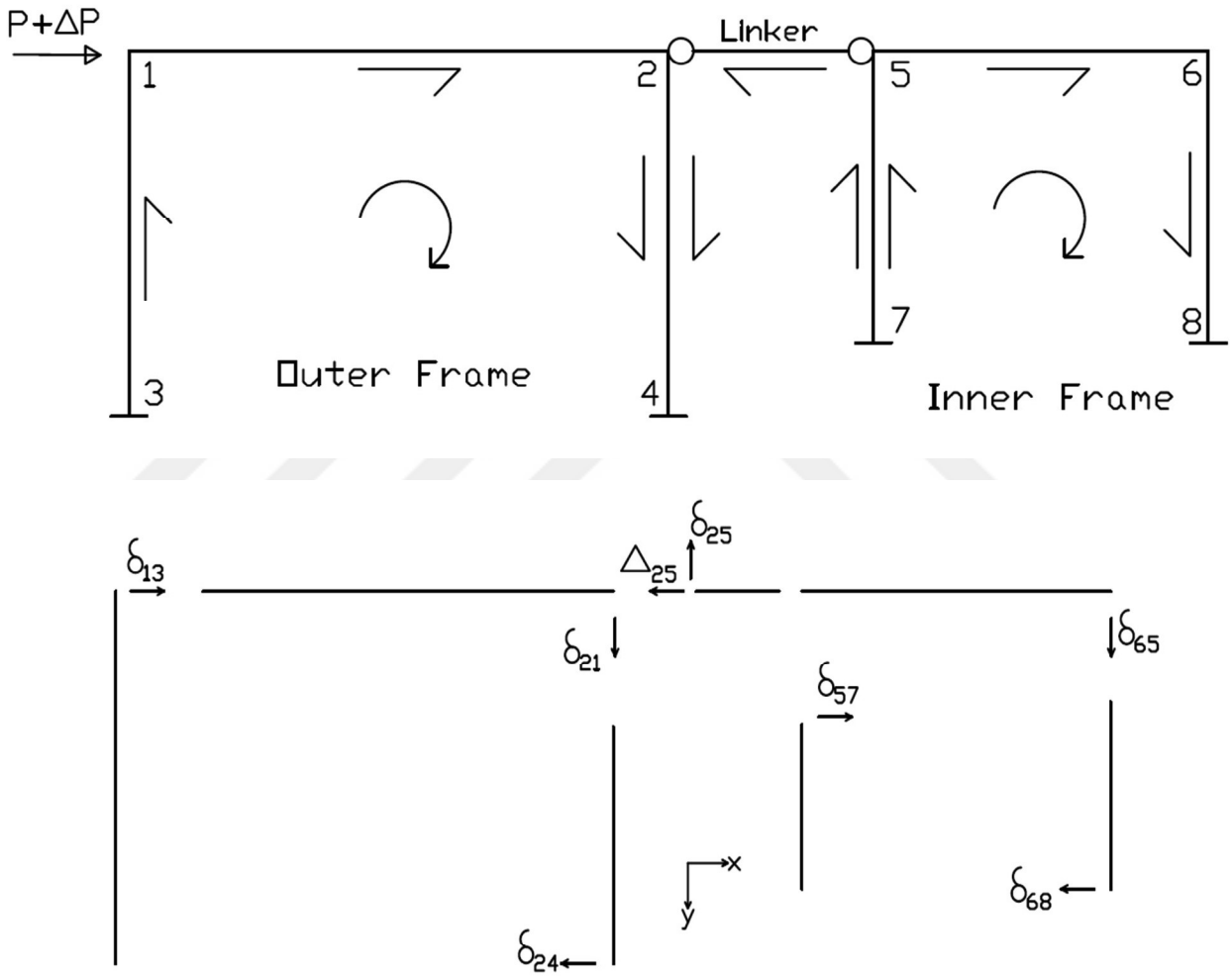

Axial deformations of prismatic members are neglected expect the linker.

Frame compatibility equations to find the independent linear end displacements:

Frame 1-2-3-4:

Lateral direction $\delta_{13} - \delta_{24} = 0$ $\delta_{13} = \delta_{24} \equiv \delta_1$

Vertical direction $\delta_{21} = 0$

Independent Linear end displacement

Frame 5-6-7-8:

Lateral direction $\delta_{57} - \delta_{68} = 0$ $\delta_{57} = \delta_{68} \equiv \delta_2$

Vertical direction $\delta_{65} = 0$

Frame 7-5-2-4

Lateral direction $-\Delta_{25} - \delta_{24} + \delta_{57} = 0$ $\Delta_{25} = \delta_{57} - \delta_{24} \equiv \delta_2 - \delta_1$

Total unknowns are node rotations θ_1 , θ_2 , θ_5 , θ_6 & δ_1 , δ_2 .

5.2.2 Proposing a general design procedure

Equilibrium equations needed to find the unknowns are as follows

$\Sigma M_1=0$, $\Sigma M_2=0$, $\Sigma M_5=0$, $\Sigma M_6=0$ and $\Sigma X_1=0$, $\Sigma X_2=0$

For the sake of simplicity one cam omit the node rotations. If that is the case then the remaining unknowns will be δ_1 & δ_2; the linear end displacements. The two lateral equilibrium equations $\Sigma X_1=0$ & $\Sigma X_2=0$ will be good enough to find them.

$\Sigma X_1=0$ $(t_{1\delta}^{13} + t_{1\delta}^{24})\delta_1 - n_{2\Delta}^{25}(\delta_2 - \delta_1) - (P+\Delta P) = 0$ (1)

$\Sigma X_2=0$ $n_{2\Delta}^{25}(\delta_2 - \delta_1) + (t_{5\delta}^{57} + t_{6\delta}^{68})\,\delta_2 = 0$ (2)

If δ_1 is chosen as the lateral story displacement of the first frame which causes the first plastic hinge and P is the load corresponds to the displacement δ_1; please read the note given at the end of this text, this will give us a chance to pick up $n_{2\Delta}^{25} = n_{5\Delta}^{25} = EF_f/L$ as the unknown of the problem.

This will be important to control the lateral force to be transferred to the inner frame. Referring to the Eqs # 1 & 2 one can obtain Eqs # 3 as is shown below:

$$n_{2\Delta}{}^{25} = n_{5\Delta}{}^{25} = \frac{(t1\delta13 + t1\delta24)\delta1 - (P+\Delta P)}{\frac{1}{(t5\delta5 + t6\delta68)}[(P+\Delta P) - (t1\delta13 + t1\delta24)\delta1] - \delta1} = EF_f / L \quad (3)$$

Where ΔP indicates the amount of lateral load increment to be carried by inner frame keeping the lateral load bared by outer frame same. The fictitious axial rigidity of linker EF_f one can easily design the shear rigidities of vertical connectors. So, choose ΔP, calculate EF_f taking L=1m and choose the amount of shear connectors, n, and calculate the individual shear rigidity simply dividing EF_f to n. One can easily adopt the procedure summarized above to the connectors in lateral directions. and/or to the cases where both vertical & lateral connectors exist at the same time.

Note #1:

- Plot the moment diagram due to unit lateral load
- Scale the lateral load which causes the first plastic hinge in the structure; 1* P
- Calculate the lateral displacement δ_1 by virtual work theorem.

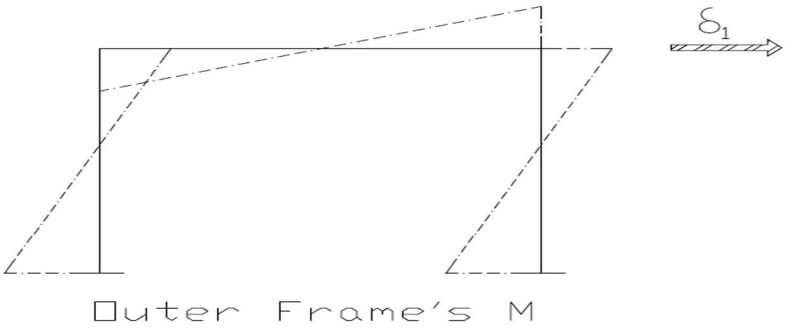

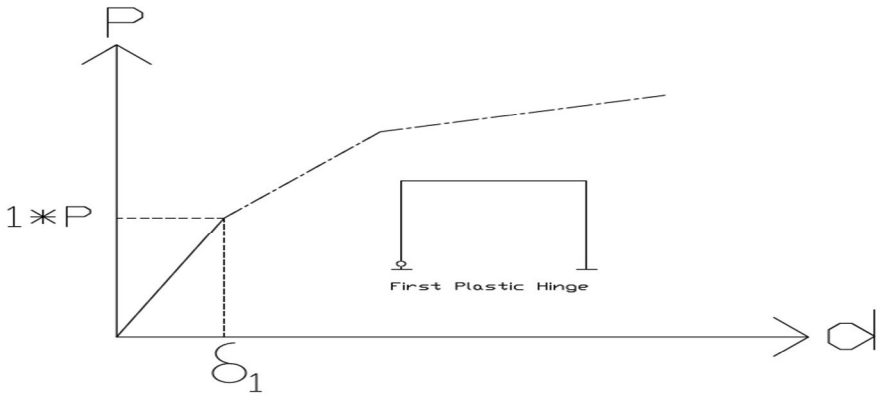

CHAPTER 6

SUMMARY, CONCLUSION AND RECOMMENDATION

6.1 Summary

This study's main objective is to study the retrofitting existing Reinforced concrete frames with an inner steel frame which are connected by different types of connectors with different diameters and different distributions. The following specific objectives were proposed;

- To study the efficiency of shear connectors in lateral and vertical directions with different shear and axial rigidities regarding ultimate lateral load capacity.
- Energy consumption capacities of connectors when the structure is subjected to code compatible real earthquakes.
- Similar studies for the different boundary conditions to study reroofing upper stories.
- Verification of the early results achieved above by multy story structural analysis.

To identify the study needs, building selection, analysis types, ground motions, and obtained result to compare the outcomes, a very detail of the literature review were conducted throughout the study. Nonlinear models were defined by assigning concentrated plasticity to the elements and nonlinear pushover analysis conducted to study the nonlinear behavior of elements and to calculate maximum lateral load carrying capacity of the models. The formation of the plastic hinges is studies and the failure modes are obtained for each model.

6.2 Conclusion

This study has investigated the strengthening and retrofitting system which allows engineers to have more and better options in the strengthening and retrofitting RC frames and based on the retrofitting goals, one can select the most suitable case. After defining 17 different models which are listed in Tables 4.1, 4.2 and 4.3 and analyzing them in nonlinear range, here we can get to conclusion for this study which are mentioned below:

- Using an inner steel frame and connecting frames with connectors is very efficient way to increase the lateral load carrying capacity of the weak RC frames.

- The amount of increasing of the lateral load carrying capacity of the RC frame depends on both the rigidities of inner frame and shear capacities and/or axial load carrying capacities and distribution of the connectors.

- The result of nonlinear pushover analysis shows that in case of using an inner steel frame with rigidity equal or lesser than the rigidity of outer frame, horizontal connectors are more efficient than vertical connectors. Moreover, the upper horizontal connectors have more contribution in the transferring lateral loads to inner frame.
- The internal forces of the vertical connectors show maximum 10 percent difference and it is concluded that all vertical connectors have almost equal participation in transferring lateral loads from outer frame to inner frame.

- The internal forces of the horizontal connectors show that more than 90 percent of the loads are transferred by two upper horizontal connectors and this study suggests that using only two horizontal connectors at the top of steel inner frame will be enough to transfer loads from outer frame to the inner frame.

- By Using the nonlinear capacities of the connectors, we see that the connectors have a 15-25 percent in the energy consumption of the models in the earthquake excitations.

6.3 Recommendation

Recommendations for prolonging studies and future work research related to the retrofitting RC frames with an inner steel frame are listed below;

- The sections used for inner steel frame are box sections and further studies can be done with different section types for the inner frame.

- The sections used for the connectors are circular sections and further studies can be done by using other types of connectors which some of them are mentioned in the chapter two of this study.

- In this study, we modeled one story one bay models which can be multi stories multi bay models in further studies to investigate the efficiency of retrofitting system in those conditions.

REFERENCES

[1] Maheri MR. Recent advances in seismic retrofit of RC frames. Asian J Civil Eng (AJCE) 2005;6(5):395–413.

[2] Sekiguchi I. Seismic strengthening of an existing steel reinforced concrete city office building in shizuoka. In: Proc. 9th world conference. Earthquake eng Tokyo-Kyoto 1988; 2:439–44.

[3] Badoux M, Jirsa O. Steel bracing of RC frames for seismic retrofitting. Struct Eng 1990;116(1):55–74.

[4] Bush TD, Jones EA, Jirsa JO. Behaviour of RC frame strengthened using structural steel bracing. Struct Eng 1991;117(4):1115–26.

[5] Nateghi-Alahi F. Seismic strengthening of eight story building using steel braces. Eng Struct 1995;17(6):455–61.

[6] Sugano S, Fujimura M. Seismic strengthening of existing reinforced concrete buildings. In: Proc7th world conference. Earthquake eng Istanbul 1980;5:449–56.

[7] Higashi Y, Endo T, Shimizu Y. Experimental studies on retrofitting of reinforced concrete structural members. In: Proc 2nd seminar on repair and retrofit of structures, Ann Arbor, Michigan, National Science Foundation; 1981:126–55.

[8] Usami H, Azuchi T, Kamiya Y, Ban H. Seismic strengthening of existing reinforced concrete buildings in Shizuoka prefecture, Japan. In: Proc 9th world conf earthquake eng, Tokyo-Kyoto 1988;2:421–6.

[9] Wylli LA, Dal Pino JA, Cohen J. Seismic upgrade preserves architecture. Modern Steel Const 1991;4:20–3.

[10] Hjelmstad KD, Foutch DA, Del Valle E, Downs RE. Forced vibration studies of an RC building retrofit with steel bracing. In: Proc 9th world conf earthquake eng, Tokyo- Kyoto 1988;2:469–74.

[11] Tagawa Y, Aoki H, Huang T, Masuda H. Experimental study of new seismic strengthening method for existing RC structures. In: Proc 10th world conf earthq eng, Rotterdam 1992:5193–8.

[12] Maheri MR, Sahebi A. Experimental investigation on the use of steel bracing in reinforced concrete frames. In: Proc 2nd int conf seism earthquake eng, Iran 1995:775–84.

[13] Maheri MR, Sahebi A. Use of steel bracing in reinforced concrete frames. Eng Struct 1997;19(12):1018–24.

[14] Tasnimi A, Masoomi A. Evaluation of response reinforced concrete frames strengthening with steel bracing. In: Proc 3rd int conf on seism earthq eng; 1999 [in Farsi].
[15] Pincheira JA, Jirsa JO. Seismic response of RC frames retrofitted with steel braces or walls. J Struct Eng 1995;121(8):1225–35.
[16] Abou-Elfath H, Ghobarah A. Behaviour of reinforced concrete frames rehabilitated with concentric steel bracing. Can J Civ Eng 2000;27:433–44.
[17] Ghobarah A, Abou-Elfath H. Rehabilitation of reinforced concrete frames using eccentric steel bracing. Eng Struct 2001;23:745–55.
[18] Maheri MR, Kousari R, Razazan M. Pushover test on steel X-braced and knee-braced RC frames. Eng Struct 2003;25:1697–705.
[19] Viswanath KG, Prakash KB, Anant D. Seismic analysis of steel braced reinforced concrete frames. Int J Civ Struct Eng 2010;1(1):114–22.
[20] Maheri MR, Akbari R. Seismic behaviour factor, R, for steel X-braced and kneebraced RC buildings. Eng Struct 2003;25:1505–13.
[21] Ghaffarzadeh H, Maheri MR. Cyclic tests on the internally braced RC frames. J Seismol Earthq Eng(JSEE) 2006;8(2):177–86.
[22] Maheri MR, Ghaffarzadeh H. Connection overstrength in steel-braced RC frames. Eng Struct 2008;30(7):1938–48.
[23] Ghaffarzadeh H, Maheri MR. Mechanical compression release device in steel bracing system for retrofitting RC frames. Earthq Eng Eng Vibrat 2006;5(1):151–8.
[24] Maheri MR, Hadjipour A. Experimental investigation and design of steel brace connection to RC frame. Eng Struct 2003;25(13):1707–14.
[25] Maheri MR, Yazdani S. Efficiency of the uniform force method in designing steel brace connection to RC frame. Construct Steel Res 2016;116:131–40.
[26] Maheri MR, Yazdani S. Seismic performance of different types of connection between steel bracing and RC frames. Iranian J Sci Tech Trans Civil Eng (IJSTC) 2016;40(4):287–96.
[27] Di Sarno L, Manfredi G. Seismic retrofitting of existing RC frames with buckling restrained braces. Improving the seismic performance of existing buildings and other structures. Soil Dyn Earthq Eng 2010;30(11):1279–97.
[28] Rahai A, Lashgari M. Seismic strengthening of nine-story RC building using concentric and buckling-restrained bracing. In: Proc 31st conf concrete struct. Singapore 2006;2:421–6.
[29] Ramin K, Maheri MR. The seismic investigation of off-diagonal steel braced RC frames.

Slovak J. Civil Eng. 2018;26(3):49–64.
[30] Ozel AE, Guneyisi EM. Effects of eccentric steel bracing systems on seismic fragility curves of mid-rise R/C buildings: a case study. Struct Safety 2011;23(1):82–95.
[31] Rahimi A, Maheri MR. The effects of retrofitting RC frames by X-bracing on the seismic performance of columns. Eng Struct 2018;173:813–30.
[32] Mazzoni S, Mckenna F, Scott MH, Fenves GL. OpenSEES command language manual [Z]. Command language manual; June 2006. http://OpenSEES.Berkeley.edu/ OPENSEES/manuals/usermanual/OpenSEES.
[33] Hsiao P, Lehman D, Roeder CH. Improved analytical model for special concentrically braced frames. J Construct Steel Res 2012;73:80–94.
[34] Gunnarsson IR. Numerical performance evaluation of braced frame systems MSc thesis Seattle: University of Washington; 2004.
[35] Kent DC, Park R. Flexural members with confined concrete. ASCE J Struct Eng 1971;97:1969–90.
[36] Menegotto M, Pinto PE. Method of analysis of cyclically loaded RC plane frames including changes in geometry and non-elastic behavior of elements under normal force and bending. Preliminary report, IABSE 1973;13:15–22.
[37] Iranian code of practice for seismic resistance design of buildings. Standard No. 2800. 4th ed; 2014.
[38] ACI Committee 318. Building code requirements for reinforced concrete (ACI 318-19) and commentary (ACI 318R-19), American Concrete Institute, Detroit, Michigan.
[39] AISC 360-16. Specification for structural steel buildings. American Institute of Steel Construction (AISC); 2016.
[40] Federal Emergency Management Agency (FEMA). Quantification of building seismic performance factors. Rep FEMA P695, Washington DC; 2009.
[41] ASCE 7-10. Minimum design loads for buildings and other structures. In: ASCE standard ASCE/SEI 7-10. American Society of Civil Engineers; 2005.
[42] Cosenza E, Del Vecchio C, Di Ludovico M, Dolce M, Moroni C, Prota A, et al. The Italian guidelines for seismic risk classification of constructions: technical principles and validation. Bull Earthq Eng 2018;16:5905–35.
[43] Paulay T, Priestley MJN. Seismic design of reinforced concrete and masonry building. USA:

John Wiley & Sons; 1992.
[44] Higazy MM, Elnashai AS, Agbadian MS. Behavior of beam-column connection under axial column tension. ASCE J Struct Eng 1988;122(5):501–11.
[45] Niroomandi A, Maheri A, Maheri MR, Mahini SS. Seismic performance of ordinary RC frames retrofitted at joints by FRP sheets. Eng Struct 2010;32(8):2326–36.
[46] Zarandi S, Maheri MR. Seismic performance of RC frames retrofitted by FRP at joints using a flange-bonded scheme. Iranian J Sci Tech Trans Civil Eng 2015;39(C1):103–23.
[47] Torabi A, Maheri MR. Seismic repair and retrofit of RC beam-column joints using stiffened steel plates. Iranian J Sci Tech Trans Civil Eng 2017;41:13–26.
[48] Javanmardi MR, Maheri MR. Anisotropic damage plasticity model for concrete and its use in plastic hinge relocation in RC frames with FRP. Structures
2017;12:212–26.

APPENDIX

SCALING OF GROUND MOTIONS

Step 1: construct target spectrum to match ground motions

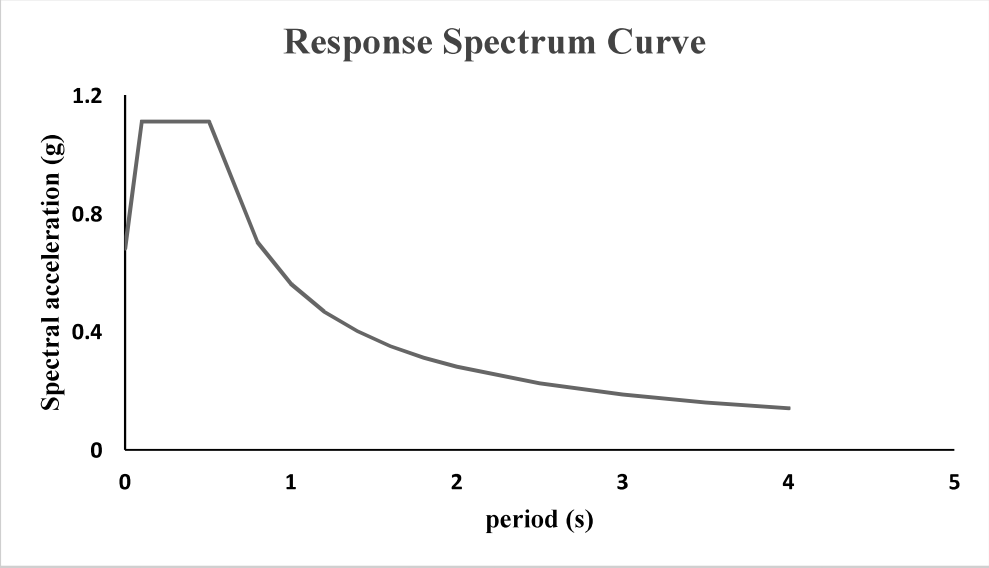

Step 2: obtain ground motion data from PEER by matching target spectrum curve

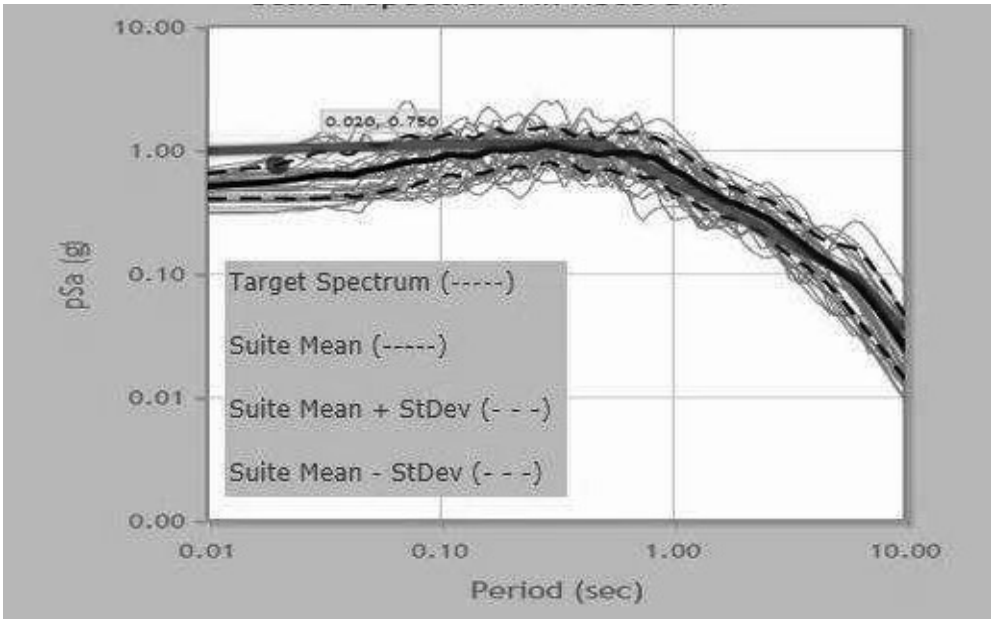

Step 3: Input the ground motion data inside siesmomatch and define target spectrum

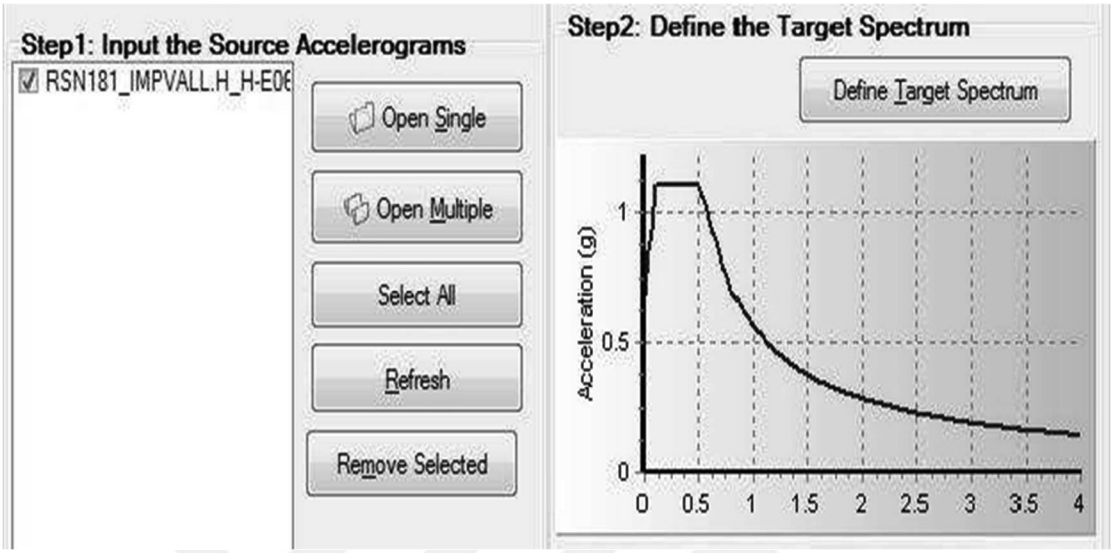

Step 4: Do matching and obtain matched response spectrum

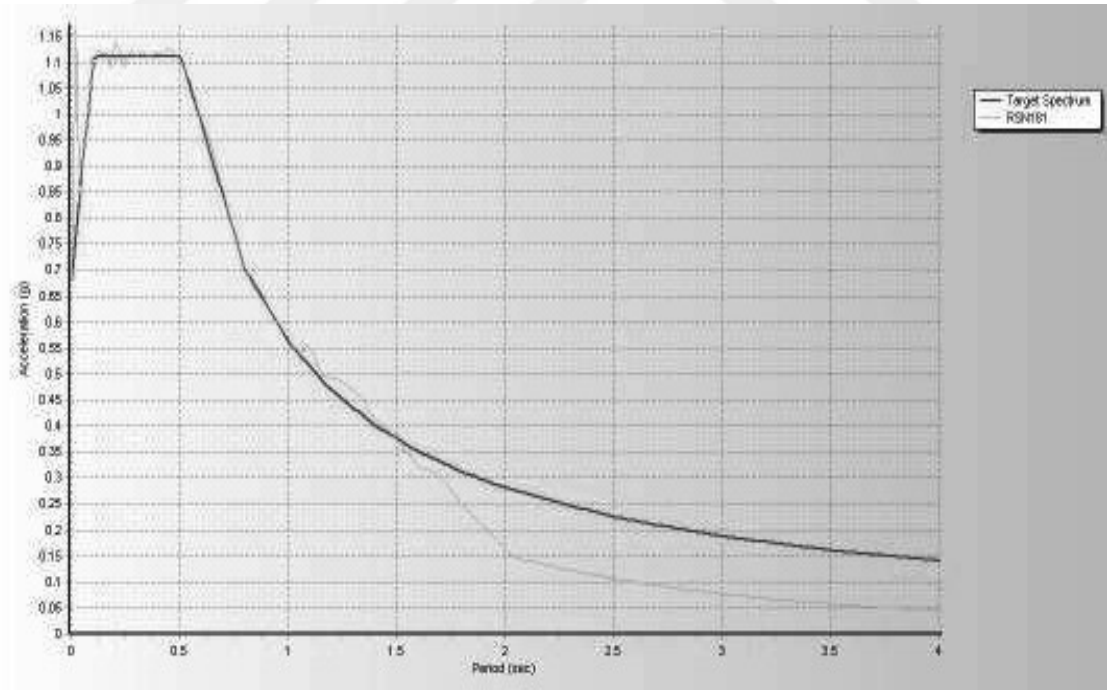

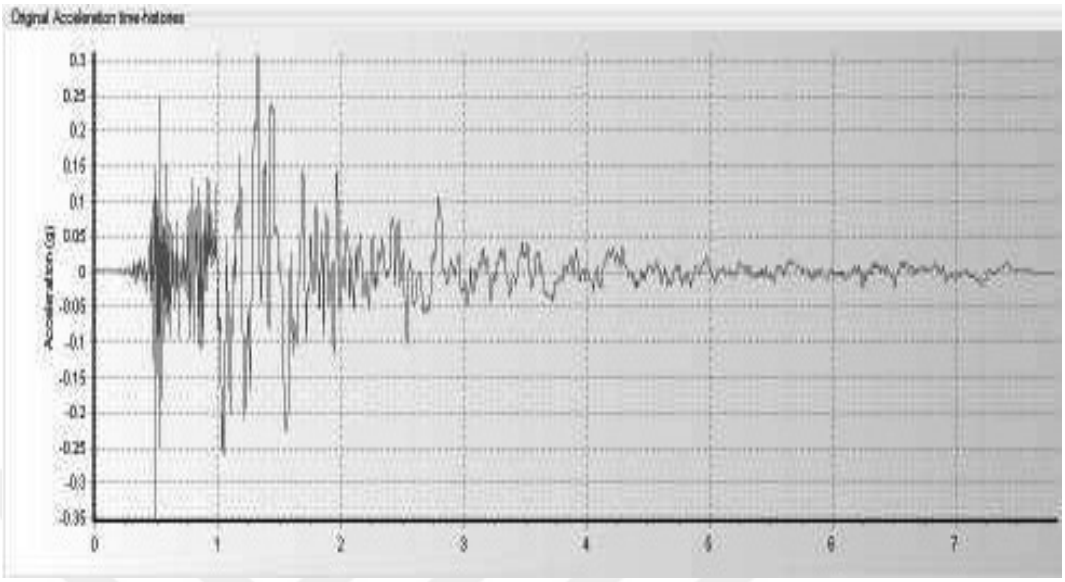

Step 5: Obtain scaled ground motion Data from seismomatch to use Nonlinear Time history Analysis inside SAP2000 software.